Chemotherapy Treatment Models: Incorporating Tumor Growth and Stochastic Cancer Staging

by

Remziye Karabekmez Kitapli

A thesis
presented to the University of Waterloo
in fulfillment of the
thesis requirement for the degree of
Doctor of Philosophy
in
Management Sciences

Waterloo, Ontario, Canada, 2021

Examining Committee Membership

The following served on the Examining Committee for this thesis. The decision of the Examining Committee is by majority vote.

External Examiner:	Dr. Mehmet U. Ayvaci Associate Professor, Naveen Jindal School of Management University of Texas
Supervisor:	Dr. Fatih Safa Erenay Associate Professor, Dept. of Management Sciences University of Waterloo
Internal Member:	Dr. Houra Mahmoudzadeh Assistant Professor, Dept. of Management Sciences University of Waterloo
Internal Member:	Dr. James H. Bookbinder Professor, Dept. of Management Sciences University of Waterloo
Internal-External Member:	Dr. Ali Elkamel Professor, Dept. of Chemical Engineering University of Waterloo

Author's Declaration

I hereby declare that I am the sole author of this thesis. This is a true copy of the thesis, including any required final revisions, as accepted by my examiners.

I understand that my thesis may be made electronically available to the public.

Abstract

Cancer is a deadly disease causing a heavy health burden worldwide throughout the recorded history. Chemotherapy is widely used to treat any type of cancer. With an enormous effort to improve cancer chemotherapy treatment strategies, a vast number of deterministic mathematical models, mostly control and compartmental models, have been developed in the literature. However, these models are criticized by clinicians for ignoring practical aspects of the disease such as stochastic staging and non-homogeneous cell growth.

This thesis focuses on extending the classical tumor-growth and chemotherapy models by incorporating stochastic stages with varying tumor growth rates. Our numerical results provide a proof of concept, showing tractability of such models and insights towards more practical modeling of chemotherapy planning problems.

The contributions of the thesis are three-fold. First, we develop a novel deterministic tumor kinetic model that can efficiently be solved to represent the deterministic case. We utilize the Gompertz equation to represent the tumor growth and a Michaelis-Menten equation to control this growth. We assume tumor growth is controlled by continuous drug delivery rates. Using data for the chemotherapy treatment of bone cancer in the literature, we find that the proposed deterministic tumor kinetic model can capture the changes in the real data set with reasonable accuracy. More importantly, this kinetic model simplifies the calculation of advanced mathematical models presented in this study.

Secondly, by adding drug toxicity and tumor reduction constraints to this tumor kinetic model, we derive an optimal control model which is solved via nonlinear programming. The introduced model finds an optimal chemotherapy treatment scheduling from low dose to high dose therapy. Extensive sensitivity analyses have been conducted to highlight the importance of the constraints limit, and the Brute-force algorithm is utilized to verify the correctness of the results for the optimal control model.

The third contribution is to extend the proposed efficient-to-solve deterministic model considering cancer staging. More advanced stages are associated with higher cancer growth rates. The stage progression occurs at each phase of the treatment with a probability based on the current tumor size (i.e., the larger tumor size is associated with a higher growth rate). The inclusion of cancer stages requires a more complex control mechanism specifying chemotherapy based on both the current tumor size and cancer stage to minimize the expected final tumor size. We construct a non-linear programming formulation for the proposed stochastic chemotherapy planning problem. This can also be solved using a reasonable and practical number of stages and treatment phases. We show that the resulting stochastic model provides more reasonable solutions compared to deterministic

models and practical rules of thumb. Some of the latter may provide infeasible solutions when the stochastic nature of the problem is ignored. The stochastic model effectively balances the need to quickly reduce tumor size, while sparing a sufficient level of toxicity for later in case of a future cancer staging. By proposing the stochastic model, we decrease the probability of stage jumps from 35% to 26% while the deterministic solution is tested in the stochastic environment. The effects of model parameters and transition probability function on the model results are studied with sensitivity analyses.

Finally, we propose a modified Simulated Annealing model for the chemotherapy scheduling problem to examine the structure of the proposed models. The results for both models are presented and explained in detail.

Acknowledgements

"Praise is to Allah (c.c.), Lord of Universes, who gave me the blessings to complete my Ph.D."

This work would not have been possible without the cooperation and the help of several individuals who contributed in different ways for the preparation and completion of this study.

First, I would like to express my gratitude to my supervisor, Prof.F.Safa Erenay, for his support, patience and encouragement throughout my study.

Secondly, I would like to thank my advisory committee members: Prof.James H. Bookbinder, Prof.Houra Mahmoudzadeh, Prof.Ali Elkamel, and Prof.Mehmet U. Ayvaci for their critical evaluation of my thesis and their helpful advice.

Thirdly, I would like to express my thanks to all my colleagues at the University of Waterloo for their support and friendship during my study, especially to Aliaa Alnaggar and Hanan Alattas. Hanan surely is the greatest officemate that I have had over the years. Aliaa was quite helpful, understanding, and encouraging for all the discussions we have made while I was writing this thesis. I cannot thank her enough for her patient, wisdom, and time. Also, I would like to thank to Nada Ghoddier, Muna Al Ateibi, Alizeh Zaman, Saedeh Araghi, and Sydea Anum Umar. I enjoyed taking courses with them and learned a lot through our friendly discussion on topics in Operations Research and Data Analytics. All of them were always there for me when I needed assistance in my either academic or personal lives, and have made my Ph.D. journey a memorable & endurable one.

Moreover, I offer my regards to a very small but precious group of Turkish friends in Waterloo Region for their prayers and confidence in my success.

Last but not least, I am truly and gratefully indebted financial, educational and administrative support of the University of Waterloo, Faculty of Engineering, and Management Sciences Department in this work.

Finally, I wish to express my appreciation and admiration to my beloved parents, Mehmet and Gökçe Karabekmez, and my sisters, Merve, Rabia, Tuba, for their endless support and ongoing love. Being away from them is always the hardest challenge, but their faith in me is fundamental to all my successes. They all taught me to believe in hope & tenacity in life in their unique ways. Their love and encouragement are worth far more than any degree.

The most valuable and special thank goes to my well-beloved husband, Feyruz Kitapli, for all the love and support he has continually and unconditionally given to me during the

course of this work. I am blessed to have an exceptionally intelligent, supportive, patient, and comforting husband. I couldn't have made it this far without having his incredible help.

Dedication

To my adorable daughter, who teaches me the real meaning of life and reminds me to be thankful for everything in my life.

To the aspirant reader, who appreciates the given effort and will have benefits from this humble study.

Table of Contents

List of Figures

List of Tables

Chapter 1

Introduction

This thesis focuses on developing new chemotherapy treatment scheduling models for incorporating stochastic cancer staging and progression. In this introductory chapter, we present our motivation behind this research with a brief discussion about cancer and chemotherapy in Section 1.1. The principal contributions of the work presented in this thesis are then stated in Section 1.2. Lastly, the outline of the content of the following chapters comes in Section 1.3.

1.1 Motivation

Cancer is a complex disease defined by the uncontrolled growth of abnormal cells due to genetic changes [Hassanpour and Dehghani, 2017]. Despite intensive investigations by both clinicians and scientists in trying to determine its underlying causes and eliminate them, cancer is still one of the most common and deadly chronic conditions affecting the world's population. According to the American Cancer Society, in 2021, nearly $1,898,160$ new cancer cases are expected to be diagnosed, and approximately $608,570$ people are expected to die due to cancer in the U.S. [Siegel et al., 2021]. That makes cancer the second most common cause of death in the US. Similarly, the Canadian Cancer Society reported $225,800$ cancer cases in 2020 [Brenner et al., 2020]. About 1 in 4 Canadians are expected to die from cancer, and nearly 1 in 2 Canadians will develop cancer in their lifetime [CCS, 2019]. Furthermore, an estimated 21.6 million new cancer cases are expected worldwide by 2030 [Bray and Soerjomataram, 2015].

The selection of appropriate treatment (e.g., treatment type & schedule, drug & dose

selection, etc.) may vary, depending on the cancer type and stage as well as the physical health and characteristics of a patient. Clinically, the main known treatments to cure cancer or control its growth are surgery, radiation therapy, immunotherapy, and chemotherapy. Among these, chemotherapy is broadly used as the main technique to both completely eradicate the disease and facilitate effective delivery, along with other treatment methods as described in Figure 1.1.

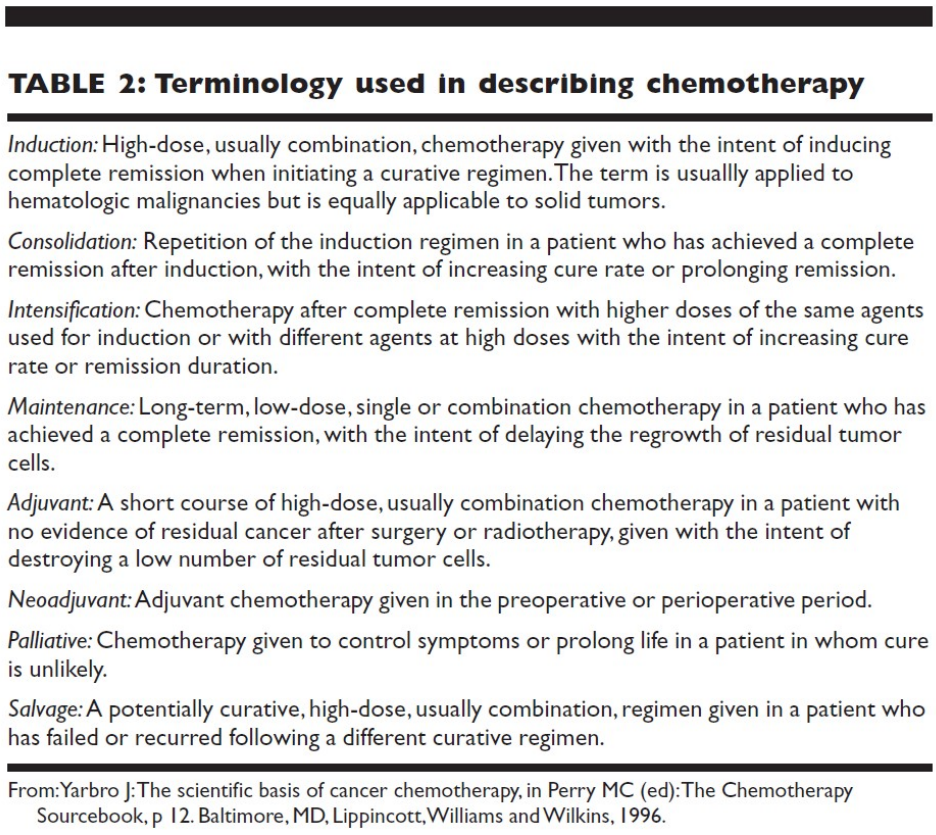

TABLE 2: Terminology used in describing chemotherapy

Induction: High-dose, usually combination, chemotherapy given with the intent of inducing complete remission when initiating a curative regimen. The term is usuallly applied to hematologic malignancies but is equally applicable to solid tumors.

Consolidation: Repetition of the induction regimen in a patient who has achieved a complete remission after induction, with the intent of increasing cure rate or prolonging remission.

Intensification: Chemotherapy after complete remission with higher doses of the same agents used for induction or with different agents at high doses with the intent of increasing cure rate or remission duration.

Maintenance: Long-term, low-dose, single or combination chemotherapy in a patient who has achieved a complete remission, with the intent of delaying the regrowth of residual tumor cells.

Adjuvant: A short course of high-dose, usually combination chemotherapy in a patient with no evidence of residual cancer after surgery or radiotherapy, given with the intent of destroying a low number of residual tumor cells.

Neoadjuvant: Adjuvant chemotherapy given in the preoperative or perioperative period.

Palliative: Chemotherapy given to control symptoms or prolong life in a patient in whom cure is unlikely.

Salvage: A potentially curative, high-dose, usually combination, regimen given in a patient who has failed or recurred following a different curative regimen.

From: Yarbro J: The scientific basis of cancer chemotherapy, in Perry MC (ed): The Chemotherapy Sourcebook, p 12. Baltimore, MD, Lippincott, Williams and Wilkins, 1996.

Figure 1.1: **Adapted from [Page and Takimoto, 2004]**

Chemotherapy is a systemic cancer-killing technique and applied to control the growth of cancerous cells by injecting an agent designed to attack cancer cells [Palumbo et al., 2013]. However, chemotherapy works as a double-edged sword since chemotherapeutic agents entering the bloodstream not only annihilate cancerous cells but also destroy healthy cells [Lundqvist et al., 2015]. Thus, it is quite important to balance the treatment efficacy and the toxic side effects when administering chemotherapy.

Drug toxicity is an important challenge to address for chemotherapy treatment since nearly all effective chemotherapeutic agents have the potential to produce toxicity even at the usual therapeutic doses [Plenderleith, 1990]. Drug toxicity adversely affects human health when excessively used since the drug accumulates in the bloodstream and causes fatal complications due to the drug's side effects [O'Brien et al., 2006]. That limits the usage of chemotherapy [Helleday, 2017]. Thus, the administration of chemotherapy requires accommodation between tumor cell population reduction and toxicity.

The stage of cancer, or the extent of cancer, is another important factor for a successful chemotherapy plan [Gress et al., 2017]. The cancer stage indicates how large a cancer lesion is and how far it has spread. Higher-stage cancers are associated with faster lesion growth [Liotta, 1984], decreased drug effectiveness [Maeda and Khatami, 2018] that requires aggressive treatment [Chabner and Longo, 2019], and increased mortality [Guan, 2015, McPhail et al., 2015]. For instance, most cancer-related deaths (more than 90%) are the result of the progressive growth of metastases that show resistance to conventional therapies [Langley and Fidler, 2007]. Therefore, the monitoring of growth factors and investigating new therapeutic targets for metastasis cells may make controlling metastasis possible [Arvelo et al., 2016].

To put it succinctly, developing an effective chemotherapy plan is essential to overcome these challenges. The current strategy in clinical practice relies on the clinical experiments carried out during or after the drug development process. Although clinical trials provide insights and efficient chemotherapy schedules, they are expensive and require long-trial time to experiment with humans and animals, as testing requires many combinations. Furthermore, clinical oncologists have not had a comprehensive model to propose as a framework for understanding, organizing, and applying their data, despite a large amount of biological and clinical data and studies published about cancer every year [Gatenby and Maini, 2003]. To tackle these obstacles, mathematical models can be an excellent tool for confirming and evaluating different biological assumptions, with less expensive and safe trials (with no immediate threat to humans).

1.2 Objectives and Contributions

The main objectives of this thesis are to:

- present a proof of concept research on the incorporation of the tumor kinetics and stochastic cancer staging into the study of chemotherapy treatment optimization.

- open a new avenue in the literature by combining control and stochastic models while tracking the tumor size and toxicity under stochastic stage jumps.

To attain these objectives, an effort has been made to extend existing chemotherapy treatment scheduling models for dynamic drug delivery of a single & cell-cycle independent drug in this dissertation. Unlike the existing literature, the effect of stochastic cancer staging on cancer progression is incorporated into the treatment decisions in our model. Our goal is to minimize tumor cell populations at the end of treatment, under a set of constraints on drug toxicity and targeted treatment effectiveness. The proposed research achieves this through the following contributions:

i. A novel "Deterministic Tumor Kinetic Model" is proposed by synthesizing two classical deterministic models. This new tumor kinetic model relies on simplifying the constraints on tumor growth as a function of drug delivery rate, rather than of drug accumulation on the body. We reveal the results of the validation exploiting real bone cancer cases from the literature. This new model has a great contribution to simplifying the solution of advanced chemotherapy treatment scheduling models that are discussed in later chapters.

ii. The proposed tumor kinetic equation is utilized to reformulate the chemotherapy treatment scheduling problem as a "Nonlinear Optimal Control Model (OCM)", based on the existing model in the literature [Martin, 1992]. The model is presented for a single cancer stage under the constraints on drug concentration for treatment cycles, cumulative toxicity for the whole treatment horizon, and targeted cancer cell reduction in each treatment point. The main objective of the OCM is to minimize the final tumor size (i.e. number of cancer cells) by optimizing the drug delivery rate at fixed time intervals. Our results indicate the optimal drug delivery schedule should start from a low dose to an increased dose towards the end. Additionally, we conduct numerous sensitivity analyses to highlight the different optimal drug delivery regimes when the constraint limits are changed.

iii. We extend the proposed OCM into a "Nonlinear Stochastic Optimization (NSO) Model" by defining probabilistic transitions to higher cancer stages during the treatment. This extension forces the model to make different inter-related treatment decisions at distinct cancer stages, and to minimize the expected final tumor population. We also consider the situation in which the schedule found in OCM has been applied to a patient having the probability of stage jump during the treatment, and compare it to the case that the schedule has been obtained in the presence of

probabilistic stage jump. The results of this contribution reveal that the optimal solution found in the latter can save at least 8% of cancer patients that do not have any stage jump throughout the treatment. This indicates that considering stage jump is an undeniable factor in designing the drug delivery plan for patients with cancer. Furthermore, as survival depends on the tumor size, which is our main target in this thesis, considering both tumor size and stage is more realistic in terms of the clinician's perspective.

1.3 Thesis Outline

This thesis is organized as follows:

Chapter 2 is dedicated to background information on the kinetics of the tumor progression and a literature review on the cancer growth and cell-killing models. We also review the relevant literature on the deterministic, stochastic and metaheuristic design of chemotherapy-treatment scheduling.

Chapter 3 introduces a novel deterministic tumor kinetics model. We show the results of the validation, exploiting real bone cancer cases from the literature.

In Chapter 4, we propose an optimal control model that characterizes the limitations of drug usage and minimizes the number of tumor cells at the end of the treatment.

Chapter 5 defines the proposed stochastic chemotherapy treatment planning model that optimizes dynamic drug delivery rate decisions, based on tumor size and stochastic cancer stage. Two sequential optimization models and a non-linear stochastic programming formulation are developed to solve the proposed model. Results from numerical experiments are reported to illustrate patterns in the treatment plan that consider the stochastic cancer staging.

Chapter 6 introduces a metaheuristic algorithm to examine the structure of the proposed chemotherapy treatment scheduling models.

Finally, Chapter 7 provides a summary of the work, highlighting the contributions which have been achieved, and gives directions for further research.

Chapter 2

Background and Literature Review

This chapter first presents a tumor-staging concept in comprehension of the biological motivation for the proposed chemotherapy treatment scheduling problem stated in Chapter 1. A brief but indispensable overview on tumor progression and regression models is also given. The overview begins with *tumor growth models*, and in particular *Gompertzian* growth function is explained. This is then followed by the cancer chemotherapy treatment models named "chemotherapeutic induced cell-kill". Three main hypotheses are reviewed to understand their impacts on tumor progression. Afterwards, the literature review is divided into three main categories, which are the *optimal control, stochastic*, and *meta-heuristic* models to assess the status of this research on chemotherapy treatment scheduling problems.

2.1 Stages of Cancer

Staging is a way of describing to what extent a tumor progresses/spreads in the body, and which sections of the body it affects [Patel and West, 2020]. This extension is categorized in many different ways. In the American Joint Committee on Cancer (AJCC), the letters T, N, and M describes the area of cancer and the letters in the TNM system stand for tumor, nodes, metastasis [Amin et al., 2017]. Additionally, that cancer stage may be expressed as local (tumor is in the primary location), regional (tumor spreads to the lymph nodes), and metastasis (tumor disseminates to other part of the body) [Brierley et al., 2019]. This representation specifies how large the cancer is, and how far cancer has spread [Koo et al., 2020]. Furthermore, TNM's number-based staging system divide cancers into stages usually numbered from 1 to 4 in Roman numerals. Stage I implies that cancer is relatively small

and is in its primary location. Stage II means that cancer has not spread into surrounding tissue but the tumor is larger than in Stage I. In Stage II, cancer cells may have spread into lymph nodes close to the tumor. This result is cancer-type dependent. In Stage III, the cancer is usually larger. It may have started to spread into surrounding tissues, and there are cancer cells in the lymph nodes in the area. Stage IV means that cancer has spread to another body organ from where it started. This is called metastatic cancer [Compton and Greene, 2004].

2.2 Tumor Growth and Control Models

2.2.1 Tumor Growth Models

Tumor growth involves a large number of complex biological processes. These have been experimentally investigated in the biological literature in terms of providing their full mechanism [Hanahan and Weinberg, 2000], [Hanahan and Weinberg, 2011]. Likewise, with the set of all functional capabilities of tumor development, many mathematical models have ultimately been designed, over more than five decades, to understand the response of the cancer population to clinical intervention [Enderling and AJ Chaplain, 2014].

In one of the earlier studies, Vaidya and Alexandro [1982] evaluated the exponential, Gompertz, von Bertalanffy, and the logistic models. The data on the untreated primary human lung carcinoma and induced sarcoma in mice were simulated to compare the performance of given tumor growth models. Even though the logistic equation gave the best fit in the cases of seven patients, the von Bertalanffy equation was the best in seven in ten mice. The models were compared based on the percentage error in predicting the volume of a tumor.

Benzekry et al. [2014] explicitly listed well-known mathematical models in terms of the functional form of their empirical tumor growth. The listed tumor growth functions were included as exponential, exponential-linear, power-law, Gompertzian, logistic, generalized logistic, and von Bertalanffy. A quantitative analysis of these models was proposed, to be assessed against data retrieved from two in-vivo systems, which are Lewis lung carcinoma and human breast carcinoma. On the one hand, the authors found that Gompertzian and exponential-linear models provide the ideal fit for the dynamics of tumor growth in breast cancer data. On the other hand, for the lung data, Gompertzian and power-law models were among the ideal candidates. Nonetheless, since the authors did not investigate the models in terms of fundamental growth characteristics, a great number of studies are

needed to find the optimal representative tumor growth models which are required to be validated with clinical results.

In another study, Sápi et al. [2015] discussed tumor growth models regarding their complexity and modeling power in the dynamics of tumor development. Distinct from Benzekry et al. [2014], they addressed the biological functions of tumor growth (e.g., avoiding cell death, creating new vessels to reach the nutrients and oxygen) using exponential, logistic and Gompertzian equations for analyzing tumor development. It was pointed out that existing studies may not capture the dynamics of tumor progression without looking at the main characteristics of cancer growth. Hence, that research underlines the still strong need to create a mathematical model that represents the cancer dynamics; for instance, under angiogenic inhibition, which means the prevention of new vessels for tumor cells. However, since those authors reviewed only a few growth models, their outcomes cannot be reliable. There are other characteristics of tumor growth besides angiogenic inhibition to be investigated for truly understanding cancer dynamics, and the preceding analyses only evaluated a limited number of growth functions. Nevertheless, this is a valuable study showing the gap in the literature.

Finally, a quite recent study by Murphy et al. [2016] summarized the differences in predictions of tumor growth models with a cautionary example. Unlike the above-mentioned studies, here the models with and without applying chemotherapy were examined. The authors derived equations for the maximum tumor size, doubling time, and the minimum required amount of chemotherapy to suppress the tumor. Lastly, they compared their findings based on the chosen models with a sample data set. In conclusion, they highlighted that the mathematical models in cancer treatment planning need attentive consideration of the model assumptions; hence, no clear conclusion on which growth models could be employed to best represent the tumor progression was made.

Last but not least, Haustein and Schumacher [2012] developed a simple and fast computational model to describe tumor progression and metastasis formation, which is the distant stage in cancer development. They used the Gompertzian function to demonstrate tumor growth. They adapted their model to clinical breast cancer data, so that the model reveal its ability to perform systematic analyses relevant for clinical breast cancer research and treatment. Thus, the Gompertzian equation was used in the model for a specific cancer stage and led to an appropriate result. Simply, they argued that the Gompertzian equation is effective in designing optimal chemotherapy treatment while considering tumor progression. This is a novel study, combining tumor growth and the steps of an advanced tumor stage at the same time, and the outcome is promising for further investigations.

A series of these recent review/summary studies listed above indicates that more effort

and new models are required if the intricacies of tumor growth are to be understood [Gerlee, 2013], since there is no certain or best mathematical model to represent tumor growth. In other words, as Gompertz and logistic equation curves were compared and commented on by Winsor [1932], none of the tumor growth equations has any substantial advantage over the others in the range of phenomena which it will fit. All these models are proposed to describe the kinetics of the cell cycle, cell-cell interactions, the cell age distribution, and micro-environmental factors while considering the functionality of tumor development [Bajzer et al., 1996]. Among those presented tumor growth models, the Gompertzian equation is used to capture the behaviour of tumor growth in this thesis. The Gompertzian equation is efficient, and many clinical results reveal that it fits well to a given data set ([Bajzer et al., 1996],[Benzekry et al., 2014],[Ribeiro, 2017]).

2.2.1.1 Gompertzian Equation

The Gompertzian function was first introduced in 1825 as a mathematical model to study the human mortality rate [Gompertz, 1825]. Later on, it became popular to describe the growth of certain tumor cell populations, not only animal [Laird, 1965] but also human tumors [Akanuma, 1978]. Furthermore, the clinical application of the Gompertzian model was used in IgG multiple myeloma in humans, not only for the dynamics of the tumor growth but also regression using the cycle nonspecific drugs and validated against real data [Sullivan and Salmon, 1972]. More recently, a group of researchers in pharmaceutical biosciences reviewed the mixed models of tumor growth, and the way anticancer drugs affect tumor size dynamics [Ribba et al., 2014]. Results indicated that the Gompertz model is an interesting model for analyzing tumor dynamics, not only because of its simple mathematical representation in tumor growth, since it has three parameters (initial point, growth rate, and saturation threshold), but also its ability to incorporate different drug effects. Moreover, the Gompertzian equation has been also employed to explore the populations of other diverse organisms; a shortlist of such literature can be found in [Tuckwell, 2016]. Recently, the Gompertz function has been used to present the behaviour of Covid-19 pandemic spread in 11 selected countries [Ohnishi et al., 2020].

2.2.2 Tumor Control Models

In the previous section, several tumor growth models were introduced in terms of their ability in representing that growth. We illustrated that the Gompertzian equation provides a good characterization of tumor growth, and highlighted the need for more research to propose a universal tumor growth model. In this section, we review the literature on control

mechanisms for tumor progression. Based on research conducted on tumor growth models so far, several control mechanisms have been developed. We provide a few of these control mechanisms, which concern the process of killing tumor cells and present the chemotherapy treatment planning models. In other words, chemotherapeutic induced cell-kill models are introduced in terms of their designed objective to prevent tumor progression.

As has been previously reported in the literature, the design of chemotherapy treatments and dose planning is quite vital for patients, since these drugs not only kill tumor cells but also destroy normal healthy cells. Thus, when drugs are applied to either shrink or eliminate the number of cancerous cells corresponding to its diagnosed stage, it is important to consider their effectiveness in killing cancer cells, drug doses, drug types, and treatment times. Although a large number of methods are reported in the literature to address these issues, a few control functions have demonstrated that limit and eliminate tumor progression.

2.2.2.1 Tumor Growth Control Functions

Several functional forms are proposed as cancer cell-killing terms in the literature. First of all, Skipper et al. [1964] have assumed that cell kill is proportional to the tumor population, which is called the *log-kill hypothesis*. According to this hypothesis, a fixed dose of the chemotherapeutic drug eradicates the same fraction of tumor cells regardless of the size of the tumor at the time of treatment [Traina and Norton, 2011]. Namely, a fixed fraction of tumor cells is reduced by a given dose of chemotherapy [Usher, 1994]. However, Norton et al. [1976] have shown that this hypothesis failed to be consistent with some clinical results for Hodgkin's disease and acute lymphoblast leukemia. Thus, Norton and Simon proposed another hypothesis, called the *Norton-Simon hypothesis*, that the rate of killed cells in response to treatment is directly proportional to the growth rate at the time of treatment ([Norton et al., 1976], [Simon and Norton, 2006], [Traina and Norton, 2017]). Finally, Holford and Sheiner [1981] introduced another hypothesis named E_{max}. According to this hypothesis, cell-kill is proportional to a *saturable* function of a tumor mass. This hypothesis is stated, based on the fact that some chemotherapeutic drugs must be metabolized by an enzyme before being activated, in the form of Michaelis-Menten kinetics. This reaction is saturable because of the fixed amount of enzyme.

In summary, three different cell-killing models are introduced based on their proportions of the tumor population, tumor growth rate, and tumor mass, respectively. These three cell-kill models have all been used in the literature. We elaborate on some studies which used all three of those models and compared their impact & performance. Panetta and Fister [2003] used optimal control techniques to study these three models and found that

the log-kill model requires fewer drugs, compared to the Norton-Simon model to reduce an equivalent amount of cancer over the same treatment interval. The other study combined several growth models with these three different cell-kill hypotheses to predict the optimal sequencing of chemotherapeutic and surgical treatments in the context of ovarian cancer [Kohandel et al., 2006]. In another study, Moradi et al. [2013] used these three mathematical cell-kill models within an optimal control theory context and aimed to minimize the drug usage while reducing the tumor volume with three various control strategies. The authors examined their control strategies by exploiting these three hypotheses. Several combined results are extensively outlined in the paper, and all three hypotheses affected the outcomes practically equally.

2.2.2.2 Michaelis-Menten Kinetics

In our problem, we are mostly interested in the pharmaceutical application of the above hypotheses, which are composed of pharmacokinetic (PK - "what body does to the drug") and pharmacodynamic (PD - "what drug does to the body") effects of the drug on the system. Among them, the E_{max} model is widely used in its simplest version, known as the Michaelis-Menten model, that we focus on in this research. Michaelis-Menten models study an enzymatic reaction which is of great use in pharmacology, biology, and medical research [Wong et al., 2004]. Optimal designs for the Michaelis-Menten model have been studied by Swan and Vincent [1977], Boer et al. [2000], Dette and Biedermann [2003], among many others.

The simplest form of Michaelis-Menten encountered most frequently in biology is the familiar enzyme kinetic function:

$$y = \frac{ax}{b+x}; \forall x \in [0, x_0] \tag{2.1}$$

where y is the reaction velocity, a is the maximum velocity of this reaction, x is the concentration of a substrate, and b is the half-saturation constant, the value of x, where y is half-maximal [Wong et al., 2004].

This Michaelis-Menten equation accounts for original enzymatic dynamics and interprets how reaction rates depend on the concentration of enzyme and substrate. Fig. 2.1 demonstrates the saturation curve for an enyzme-reaction.

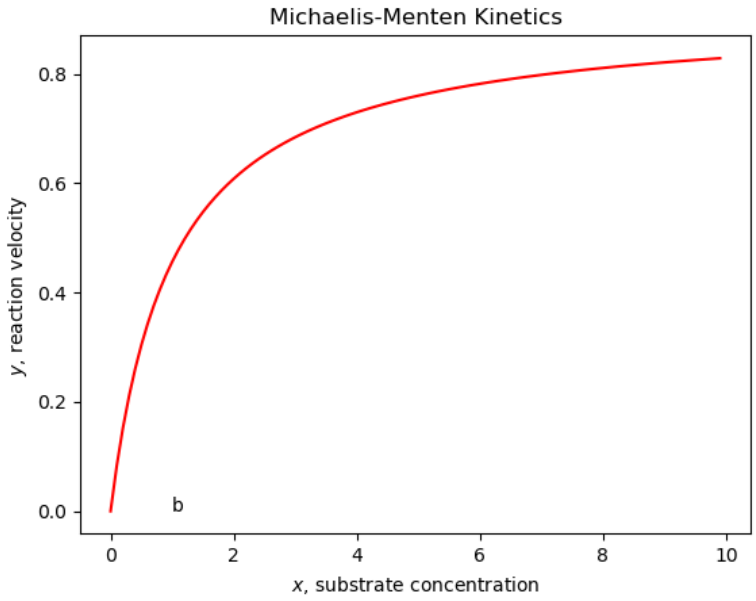

Figure 2.1: **Michaelis-Menten Saturation Curve for an Enzyme Reaction.**

2.3 Optimal Control Models in Cancer Chemotherapy Treatment Design

Optimal control theory, which plays an important role in designing engineering systems, is a branch of continuous-time and continuous-state mathematical optimization used in deriving control policies for optimizing system performance. In addition to engineering, optimal control theory has many applications in biology, economics, ecology, finance, management, and medicine [La Torre et al., 2015]. The formulation of an optimal control problem demands

i. a mathematical model of the process to be controlled

ii. a statement of physical restrictions to control the process, and a performance criterion (objective function) that specifies that model's purpose [Kirk, 2004].

The optimal control models (OCMs) have been extensively used in the problem of chemotherapy treatment planning. Many mathematical models have been developed to

devise an optimal chemotherapy plan that determines the dosages of the drugs administered to cancer patients. These OCMs are extensively reviewed in the literature by Swan [1990], Shi et al. [2014], Sbeity [2015], Moore [2018], and Rojas and Belmonte-Beitia [2018].

Swan [1990] reviewed the interaction of optimal control theory with chemotherapy in three broad areas: miscellaneous growth kinetic models, cell cycle models, and the classification of other models which do not directly relate to tumor growth kinetics, but they could be employed if wanted. This review is worth mentioning as it provides a comprehensive view of the earlier attempts on chemotherapy drug scheduling models. The most of the later studies have used the modeling blocks defined in these earlier works.

Shi et al. [2014] summarized the mathematical models focused on the optimal design of chemotherapy treatment. They organized the paper in terms of modeling methods e.g., optimal control model & others, and then classified optimal control models concerning their solution approach. Within each category, they reviewed the existing models in terms of the key design factors in the model such as objective function, tumor cell types, number of a drug in designing chemotherapy such as the number of cancerous cells, toxicity, and resistance. By discussing the solution techniques, they questioned the models' effectiveness to reduce the costs/harms of chemotherapy and/or maximize the associated benefits. Finally, they concluded limitations of existing researches due to lack of clinical relevance of the models, and so provides several suggestions to overcome these obstacles. However, the paper does not specifically provide key tumor growth or control expression for each reviewed study.

Sbeity [2015] conducted a comprehensive summary of covering papers in the cancer chemotherapy treatment planning literature. The focus of the paper was on the methodology, and the mathematical models were grouped such as nonlinear differential equations, compartment models, and hybrid models. Different than Shi et al. [2014], this paper provided mathematical equations with their defined parameters and assumptions which helps the readers to detect the differences in the approaches. Their objectives in the review were to discuss the limitations of the existing theoretical research and provide several directions to improve research in optimizing chemotherapy treatment planning using clinical data.

Moore [2018] focused on the OCM's application to diseases and therapies, particularly the optimization of combination treatments. The author initially provided an overview of OCM that starts with the historical development of optimal control (OC) and is followed by the basic theory of OC. Leukeima was as an illustration of the purpose of the model, and the author provided references for more complex cases. It is a well-written paper by sharing a personal anecdote to grasp the readers' attention, especially biopharma community, on the importance of OCM for optimizing drug regimens.

Rojas and Belmonte-Beitia [2018] provided a survey paper for a series of problems of OCM (only the systems of differential equations) applied to cancer treatments. Initially, cell-cycle-specific compartmental models for cancer chemotherapy have been analyzed. Then, optimal solutions for the low-grade glioma were studied. The dynamics of cancer cell populations were considered with a 2-compartment model with sensitive and resistant populations. Finally, they have studied antiangiogenetic treatments to highlight the tumor microenvironment. They concluded by emphasizing the need for mathematical models to implement their understanding and develop new optimal treatment strategies.

With these above review papers, it is observed that there exists a vast literature of OCMs that are applied to cancer chemotherapy treatment dating back to the 1970s and 1980s with the fundamental work by Eisen [1979] and Swan [1988] (and their references) and continued throughout the 1990s. Swan and Vincent [1977] is the pioneer for modeling the chemotherapy process as an OCM based on the Gompertzian model. This study constructs the foundation of our ultimate stochastic optimization model. More details are provided in Chapter 3.

Then, this chemotherapy treatment design problem is enriched gradually over the years by focusing to minimize the number of tumor cells along with many aspects considering drug toxicity ([Murray, 1990], [Zhu et al., 2018], [Devia and Giordano, 2019]), drug resistance ([Martin, 1992], [Martin and Teo, 1993], [Costa et al., 1995], [Swierniak et al., 2005], [Mansoori et al., 2017]), the cell-cycle specific drug regimen ([Panetta and Fister, 2000], [Swierniak et al., 2003], [Dua et al., 2008]), multi-drug ([Weiss and Nowak-Sliwinska, 2017]), and building multi-objective OCM ([Alam et al., 2013a]) in the development of mathematical models. Cancer chemotherapy treatment scheduling problem regenerates a wide range of classification based on research studied not only on how to design the model but also the solution approach ([Schaettler and Ledzewicz, 2014], [Schättler and Ledzewicz, 2015]).

These mentioned papers consider cancer at one site. However, there are some recent studies that consider, for example, the evolution of metastases population as an OCM for designing a chemotherapy schedule [Benzekry, 2017]. The idea of that thesis is similar to this present work; however, our model introduces a new stochastic mathematical model to the literature in Chapter 5 by providing a dynamic programming mechanism.

Drug resistance is a substantial obstacle to achieving success in chemotherapy treatment. Drug resistance occurs when cancer cells stop reacting to the injected or infused drug(s). In other terms, drug resistance is the reduction of the medication's effectiveness to the disease, and depends on several factors [Housman et al., 2014]. Initially, tumor cells were thought of as a group of homogeneous cells, and treatment was aimed to kill as many cells as possible to eradicate the disease. However, over time, it has been understood that

tumor cells have a heterogenic feature [Heppner, 1984]. Therefore, while the treatment focused on the most dominant cell group, drugs used to target that group might not have any impact on some sub-group known as "chemotherapeutic resistance cells" [Gottesman, 2002]. Thus, drug resistance may cause a decrease in the efficacy of the ongoing treatment and lead to an invasion of cancer metastases [Mansoori et al., 2017]. Since drug resistance can cause failure in chemotherapy treatment [Housman et al., 2014], Coldman and Goldie [1983] developed a model to investigate the drug resistance of cancer cells. It has been shown that an increasing population of cancer cells triggers drug-resistant cells. Thus, Martin et al. [1990] and Martin [1992] added a constraint to the model. This prevents the intermediate tumor size from becoming extremely large by eliminating the drug resistance effect. In this thesis, we control the drug resistance in the same way as in Martin [1992], by taking a continuous state constraint that allows the model to monitor the tumor cell count throughout the treatment.

Methods for solving the OCMs represents another direction in the literature. The numerical method proposed by Goh and Teo [1988] was used by Martin [1992] to find an optimal schedule of chemotherapy drugs with the inclusion of drug toxicity constraints. This methodology is implemented to solve the simplified OCM in Chapter 4. In the literature, there are other mathematical methods to solve the OCMs in chemotherapy treatment scheduling. These include Newton's method [Martin et al., 1992b], the Pontryagin Maximum Principle [Panetta, 1998], iterative algorithms [Pereira et al., 1995], nonlinear programming [d'Onofrio et al., 2009], and a deterministic oscillatory search algorithm [Archana et al., 2018].

Nevertheless, different simulation techniques have been recently developed to optimize the dose schedule of chemotherapy in cancer treatment [Simbawa, 2017], specifically in colon cancer [Cockrell and Axelrod, 2019] and non-small lung cancer [Kozłowska et al., 2020].

To sum up, for a comprehensive review on chemotherapy models and control of chemotherapy, along with the control of other cancer modalities, the reader is kindly directed to a recent study by Padmanabhan et al. [2021].

2.4 Stochastic Models in Cancer Chemotherapy Treatment Design

Current control models (mostly stated in Section 2.3) for chemotherapy treatment planning consider the decision process at the beginning of chemotherapy and then calculate the

optimal design for the whole period [Shi et al., 2014]. On the one hand, this approach still specifies the optimal dynamic controls, as the effect of the drug delivery decisions is deterministic. On the other hand, a biological system has a complex nature that prevents a completely deterministic description by a set of mathematical functions. Therefore, various stochastic descriptions of the biological processes need to be utilized until the true nature of their behavior can be thoroughly understood [Padgett and Tsokos, 1970].

From various aspects, stochastic chemotherapy models have been studied extensively over the years to describe some random behavior of a biological system: tumor growth ([Albano and Giorno, 2006], [Rosenkranz, 1985], [Lisei and Julitz, 2008]), drug resistance ([Coldman and Goldie, 1986], [Komarova, 2006]), and cancer metastasis [Frei et al., 2018].

Since drug resistance is one of the main causes of failure in the treatment of cancer, a few papers addressed this issue probabilistically as well. As pioneers of developing stochastic models of drug resistance, Coldman and Goldie [1983] analysed tumor size as a stochastic process to develop treatment plans maximizing the probability of having no resistant cells. In a later study, they modeled the presence of drug-resistant mutants using a stochastic model to design an effective chemotherapy plan [Coldman and Goldie, 1986]. Moreover, Coldman and Murray [2000] designed a model to maximize the probability of successfully treating cancer & the probability of no toxicity and solved it by sequential quadratic programming. Komarova [2006] formulated a stochastic model for multi-drug resistance and investigated the dependence of treatment outcomes on the initial tumor load, mutation rates, and the turnover rate of cancerous cells. In these studies, the birth-death process was taken into account while designing the model.

Some other studies captured the randomness in tumor growth in time by defining the growth using stochastic differential equations (SDEs). For instance, Lisei and Julitz [2008] modeled tumor growth using SDEs with multiplicative noise terms causing random variations on the growth functions. They showed the existence of the solution when the control term is written as a differential inclusion problem. Rao and Rao [2006] studied cancer cell growth as a two-stage stochastic model. It was assumed that the growth of a pre-malignant cell (normal cells), mutation (start of cancer), loss of pre-malignant, and the birth of malignant cells are random and follow Poisson processes with different parameters. Then, Rao et al. [2014] extended this study on tumor growth by considering stochastic optimization models for cancer chemotherapy treatment planning. Multi-objective stochastic optimization problems were designed to minimize, first, the expected intensity of cancer-causing cells, either in the mutant or malignant stage, and second, the stay time of cancer-causing cells during the time of treatment by considering the cells at both mutant and malignant stages, respectively. Simply put, this paper studied the trade-off between drug vacation (which can be ineffective to control the growth of cancer) and the drug administration

period (regular amount of the same drug with small quantities cause drug resistance) by utilizing a two-stage stochastic model for cancer growth during chemotherapy treatment.

In another perception, Padi et al. [2010] studied stochastic models for optimal drug administration in cancer chemotherapy. They considered the problem of determining the optimal threshold limits on the drug administration period and the length of that period, while monitoring chemotherapy treatments. They developed stochastic models for tumor size during the presence & absence of drugs by utilizing difference-differential equations (delay differential equation).

In contrast to the extensive work examining tumor growth and regression, relatively few models have been proposed to describe metastasis. Pinho et al. [2002] modeled a system of five differential equations and one functional differential equation for cancer treatment by chemotherapy where there is a metastasis from a primary to a secondary site by the cancer cells. Newton et al. [2012] designed a stochastic Markov chain model for metastatic progression for primary lung cancer. Through an iterative numerical search, the model simulates and quantifies disease progression pathways and timescales of progression from the lung position to other sites. Frei et al. [2018] introduced and analyzed a branching stochastic process with a settlement that has been applied to metastatic cancer growth. However, these studies neglect the chemotherapeutic effect on tumor progression. Moreover, there are other studies with Markov models considering the early stage of cancer and the effect of cancer therapy at each stage in terms of survival [Boher et al., 1999], [Büyükdamgaci-Alogan et al., 2008]. Other studies on modeling metastatic growth include Benzekry [2012], Hartung et al. [2014], and **?**.

MDPs are powerful analytical tools for finding optimal solutions to sequential and stochastic decision problems. With an MDP, standard Markov models are generalized in which a decision process is embedded, and multiple decisions are made over time [Alagoz et al., 2010]. In recent studies presented in Table 2.1, MDPs receive great attention in the problem of chemotherapy treatment planning. The need of utilizing MDPs are emphasized by Shi et al. [2014], since Markov decision processes (MDPs) may help to overcome the gaps between theoretical research and clinical application by allowing to include stochastic features in a pure optimization problem. For comprehensive coverage of MDPs, Puterman [1990] and Bertsekas [2000] can be referred. Furthermore, some other applications of MDPs in medical decision making can be found in the studies of Schaefer et al. [2005], Ayvaci et al. [2012], Erenay et al. [2014], Steimle and Denton [2017], Scheller-Wolf [2018].

Table 2.1: Recent MDP Papers in Chemotherapy Treatment Design

Paper	Model/Method	Objectives	Features	Stochastic Components
Bazrafshan and Lotfi [2020]	Markov decision process model/value iteration	max.patient survival, min drug toxicity, and chemo costs	multi-drug, sequential treatment, details on drug dosage, new drug combinations	Uniform distribution of the toxicity shifts in treatment period
Maass and Kim [2020]	Markov decision process/backward induction	optimize multi-modality treatment	degree of tumor progression and normal tissue side effect, different categories of treatment modalities based on the characteristics of repeatability, tumor reduction and risk to normal tissue	states are conditionally independent
Imani et al. [2020]	Markov decision process/value iteration	maximizing quality-adjusted life years (QALYs), expected cost of the intervention, treatment.	multi-objective, data-driven decision making	Historical data is used to estimate state-action transition dynamics in breast cancer

2.5 Metaheuristic Models in Cancer Chemotherapy Treatment Design

Most optimization problems are highly nonlinear and are subject to various complex constraints [Yang, 2011]. Therefore, finding an optimal solution to such optimization problems with an exact algorithm may be computationally challenging, and often impractical. Thus, approximate algorithms and heuristics/metaheuristics are needed for solving large-scale models due to a high-dimensional search space [Neapolitan and Naimipour, 1997].

"Meta" means "higher level" and "heuristic" means "to discover" in Greek [Lazar, 2002]. Heuristics are techniques that are mostly problem specific to find good (near-) optimal solutions in a reasonable computational cost to guarantee neither feasibility nor optimality [Russell and Norvig, 1995]. However, metaheuristic are problem-independent that can be applied to a broad range of problems. Metaheuristic algorithms have an advantage in both their effectiveness and general applicability over heuristics [Ólafsson, 2006]. Metaheuristics are designed to address many optimization problems where exact methods have failed to produce efficient solutions within reasonable time limits [Ólafsson, 2006].

The detailed classification of metaheuristic algorithms, along with their advantages and disadvantages, has been extensively reviewed by Beheshti and Shamsuddin [2013]. In another recent review, Hussain et al. [2019] performed a comprehensive picture of metaheuristic research to highlight potential open questions and critical issues raised in the literature. The other comprehensive review has been conducted by Abdel-Basset et al. [2018] and Gautam et al. [2019]

A metaheuristic algorithm has been utilized for over a decade to solve the problem of optimal chemotherapy treatment planning. A summary of the studies before 2010 that consider solving the optimal chemotherapy treatment planning problem by heuristic algorithms can be found in Shi et al. [2014], while the more recent applications in this category are listed in Table 2.2.

Among the recently developed heuristics, Alam et al. [2013a] proposed a model of chemotherapy drug(s) scheduling for cell-cycle specific cancer treatment They managed the cell-cycle-specific tumor growth by using a control model, where a close loop control model with a multi-objective Genetic Algorithm (MOGA) has been utilized to search for suitable drug concentrations at the tumor site. The model considered the trade-off between the number of proliferating cells at the end of the treatment, and average drug toxicity over the treatment. The results slightly outperformed the authors' previously published practical swarm algorithm (PSO) [Alam et al., 2010]. Later, the authors developed another cancer chemotherapy treatment model to optimize drug doses and treatment intervals for reducing the final number of cancer cells under the constraints of maximum allowable drug concentration, toxicity, cumulative drug concentration, and tumor size constraints [Alam et al., 2013b]. In that study, the authors aimed to improve the practicality of the resulting treatment policies by considering treatment schemes with i) variable intervals and variable doses (VIVD), ii) fixed intervals and variable doses (FIVD), and iii) periodic dose (PD). They emphasized the importance of FIVD and PD schemes due to their characteristic of "periodicity" and ease of implementation along with friendliness to patients.

Agur et al. [2006] has studied the problem of adapting heuristics to optimize chemotherapy scheduling to present attainable treatment options by aiming to cure the patient as quickly as possible. The possible schedules were tested by three local search-based heuristics to observe a solution that can locally optimize the objective function. Simulated annealing (SA) were outperformed over threshold acceptance (TA) and old bachelor acceptance (OBA) in terms of computational effort. Wang et al. [2018] addressed the problem of combination chemotherapy with dose adjustment. A mono-chemotherapy model with two cell-cycle phase-specific chemotherapeutic drugs has been constructed as an extension to Agur et al. [2006] that has considered one drug administered at a fixed dose. A memetic algorithm (ME) was designed by utilizing the advantages of evolutionary algorithms and

local search heuristics to solve the problem. The results demonstrated that combination chemotherapy was superior to a single-drug treatment plan. Later, Wang et al. [2019] proposed optimization of cell cycle-specific combination chemotherapy in the presence of drug resistance by combining the cell cycle mechanism of Agur et al. [2006] with the multiple drugs and drug resistance mechanisms of Tse et al. [2007]. Based on the numerical results, they advocated more flexible drug regimens compared to the clinical chemotherapy regimens in terms of the treatment cycle to minimize not only the number of tumor cells, but also the post-treatment chemotherapy-induced toxicity.

Heydarpoor et al. [2020] designed a multi-objective optimization model to minimize both the cancerous cell density and drug dose and solved it with Particle Swarm Optimization (PSO) and Genetic Algorithm (GA). Their tumor model was combining the works of De Pillis and Radunskaya [2003] and Salamci and Banks [2010], i.e., phase-spaced nonlinear tumor growth under an immune response & chemotherapy according to a state dependent Riccati equation. Their results illustrated that the PSO method has outperformed GA and emphasized that both have been developed to gain a proper understanding of medical supervision to a cancer patient.

Table 2.2: Summary of Recent Metaheuristic Models in Chemotherapy Treatment Design

Paper	Model/Method	Objectives	Features
Alam et al. [2013a]	close-loop control model solved by GA	minimize the proliferating cells at the end of the treatment and drug toxicity over the whole period of treatment	multi-objective, cell-cycle specific
Alam et al. [2013b]	GA	minimize the tumor volume	single drug, single objective, no cell-cycle specific
Wang et al. [2018]	Heuristic/combined population-based evolutionary search and neighbourhood-based strategies	maximum efficacy while minimizing the toxicity	multi-drug dose varying chemotherapy, cell-cycle specific
Wang et al. [2019]	Heuristic/Memetic Algorithm with an advanced local search	minimize the quantity of tumor cells and post-treatment drug toxicity	cell cycle specificity of drugs, multi-drug, drug resistance
Heydarpoor et al. [2020]	GA & PSO	minimize cancerous cells and approved drug amount	immune response

2.6 Conclusions

In this chapter, we reviewed tumor growth & control models and hypotheses on cancer chemotherapy models to identify which models we are interested in to define the proposed tumor kinetic model in Chapter 3. Also, the literature review on OCMs in cancer chemotherapy design is fully presented by focusing especially on the review papers. Based on the studies that review papers indicated in Section 2.3, the proposed OCMs in the literature do not take into account tumor progression through its stage while designing mathematical models. They instead assume that the tumor growth rate is constant for each type of cancer cell. However, the modeling design was taken an advanced stage where the first optimal control model was designed by Swan and Vincent [1977] considering the multi-drug, multi-objective, drug resistance, cell-cycle specific features in the design of chemotherapy treatment schedule.

Nonetheless, there exists a considerable body of literature on modeling the growth of cancer with stochastic assumptions. However, to the best of our knowledge, no existing work in the literature models the possibility of stochastic cancer staging while a patient is under treatment. To fill this gap, this thesis provides a mathematical model capturing stochastic jump while designing a chemotherapy plan and propose a metaheuristic approach to solve the proposed model.

Most existing models on the chemotherapy treatment planning problem use deterministic dynamic control and a compartmental model with system states defined as the number of cancer cells in the body. However, these models are not regarded well and criticized by clinicians as they tend to ignore some important aspects like cancer staging and heterogeneity in growth rate over time. To propose an alternative approach, we extend a well-known deterministic control model of Martin [1992] for optimizing chemotherapy treatment plans/schedules and incorporate stochastic cancer staging in that model. Therefore, this work attempts to present a proof of concept research on the incorporation of tumor kinetics and stochastic cancer staging into the study of chemotherapy optimization. We explore to open a new avenue into the literature by combining control and stochastic models, to keep track of tumor size and toxicity under stochastic stage jumps.

Although cancer chemotherapy has been studied stochastically over the years as seen in Section 2.4, the research in designing chemotherapy considering the possibility of stage jump, while the patient is under the treatment, has received no attention in the literature. Therefore, this study addresses the need for a new mathematical model for cancer chemotherapy that incorporates stochastic cancer staging into the optimization model while minimizing the number of tumor cells at the end of the treatment. To properly address

this problem, sequential decision approaches and a metaheuristic algorithm are proposed in this thesis.

The insights reported in this thesis are unique contributions, because studies in the literature do not consider the probability of tumor stage jump while minimizing the number of tumor cells at the end of the treatment. We position our work combination of studies in the literature, and yet differentiate our work from them because this thesis: 1) develops a new simplified tumor kinetic model 2) presents an analytical model to determine the optimal chemotherapy treatment schedule 3) proposes stochastic optimization 4) implements Simulated Annealing (SA) algorithm for the solution of the proposed stochastic optimization model. As indicated in the research of Agur et al. [2006] and Villasana and Ochoa [2004], SA is a great candidate to solve a given optimal control problem with simplicity and efficacy.

In this context, this thesis provides a new model on the problem of the chemotherapy treatment schedule. Our modeling approach provides a new direction to the literature for developing the optimal drug delivery plan by considering the dynamic factor of tumor growth incorporating probabilistic tumor stage jump. Although our modeling framework is basic, considering mainly drug toxicity & indirectly drug resistance in the failure of chemotherapy treatment, it can be extended to a more realistic dynamic problem. However, even as it is, it provides valuable insights about the optimal drug delivery schedule of chemotherapy treatment.

Chapter 3

Tumor Kinetic Model

This chapter starts with a summary of mathematical models for tumor growth and control. Then, to reduce the computational difficulty for the numerical simulation, optimization and stochastic models which will be discussed in other chapters, we propose a simplified tumor kinetic model. We achieve this by the assumption of a controlled, constant drug delivery rate and the validated approximation of drug concentration. Finally, using a real data set given in the literature, we calibrate parameters for the simplified tumor kinetic model and summarize the results which demonstrate the agreement of the model with the real data. We conclude this chapter with a discussion that utilizes the proposed model as a building block for nonlinear and stochastic optimization models in the later chapters.

3.1 General Tumor Kinetic Model

3.1.1 Tumor Growth Equation

In general, untreated tumor cells are assumed to follow a Gompertzian type of growth pattern (see details in Subsubsection 2.2.1.1), and initially at time $t = 0$ the size of the tumor is $N(0) = N_0$. In the Gompertz function, the growth rate decays as the tumor population increases. The general mathematical formulation of the Gompertzian function for tumor growth can be modeled by the first-order differential equation

$$\frac{dN(t)}{dt} = -\lambda N(t) ln \left[\frac{N(t)}{\theta}\right], \tag{3.1}$$

where $N(t)$ represents the total cancer cell population at time t, λ is the intrinsic growth rate and θ is the asymptotic maximum tumor population (also known as carrying capacity) that can be reached with the available resources when λ is positive [Sullivan and Salmon, 1972]. The solution of the growth function is

$$N(t) = \theta exp\left\{\ln\left[\frac{N_0}{\theta}\right] exp(-\lambda t)\right\}, \tag{3.2}$$

where N_0 is the initial tumor population at the starting observation time. Particularly, $N(t) = N_0$ as $t = 0$ and $N(t) = \theta$ as $t \to \infty$ are the equilibrium solutions to the Gompertzian equation ([Laird, 1964], [Laird, 1965]). Thus, the growth is at the slowest points both at the start and at the end of the planning horizon as shown in Fig. 3.1. In general, the Gompertzian function has a sigmoid shape, as the tumor initially grows because of the availability of nutrients and oxygen, and gradually decelerates until the tumor reaches its maximum value.

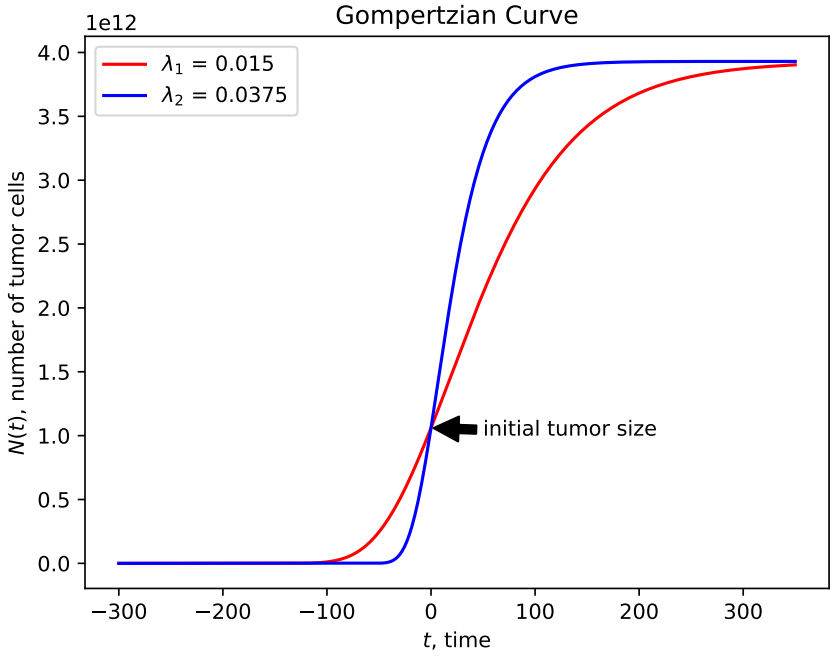

Figure 3.1: **Gompertz Curves under Different Growth Rates, λ.**

3.1.2 Tumor Growth Control under Treatment

The effect of a chemotherapeutic drug on tumor population size (i.e., the number of cancer cells) is captured in several ways, including a special case of E_{max} type of cell-kill model in the literature (see Subsubsection 2.2.2.1 for the other types of models). This specific type of E_{max} cell-kill model is called a Michaelis-Menten type of saturation term, which was first introduced by Himmelstein and Bischoff [1973]. This hypothesis assumes that the cell-kill is proportional to a saturable function of a tumor mass with the following equation:

$$\frac{k_1 v(t)}{k_2 + v(t)}. \tag{3.3}$$

Eq. (3.3) is called *Michaelis-Menten* equation (see details in Subsubsection 2.2.2.2). Here, $v(t)$ denotes the concentration of the anti-cancer drug, and k_1 & k_2 are positive constants. Specifically, k_1 represents the maximum reaction rate reached by the system; whereas, k_2 shows the substrate concentration when the reaction rate is half of the maximum reaction rate [Michaelis and Menten, 2007].

3.1.3 Tumor Kinetic Model

Many studies used this type of rate of loss term, i.e. Eq. (3.3), in their tumor kinetics model to control tumor growth by a chemotherapy agent during the treatment. The resulting tumor growth function under treatment is as follows:

$$\frac{dN(t)}{dt} = -\lambda N(t) ln\left[\frac{N(t)}{\theta}\right] - \frac{k_1 v(t)}{k_2 + v(t)} N(t), \quad N(0) = N_0 \tag{3.4}$$

which describes the net growth of a tumor cell population.

The tumor kinetic model under treatment depends on the drug concentration, which can be modeled in several ways. One of the most common and classical mathematical representations of anti-neoplastic drug concentration after the drug administration is the one proposed by Bellman [1983] as illustrated in Fig. 3.2:

$$\frac{dv(t)}{dt} = u(t) - \gamma v(t), \quad v(0) = v_0 \tag{3.5}$$

where γ is a constant rate of drug concentration decay. The concentration of the drug is assumed to decay exponentially by a fraction $\gamma v(t)$ over the time $d(t)$. Before administration, the drug concentration $v(t)$ is assumed v_0, which is often taken as 0. Furthermore, $u(t)$, the drug delivery rate, refers to the amount of the drug delivered to the cancer site during the treatment time.

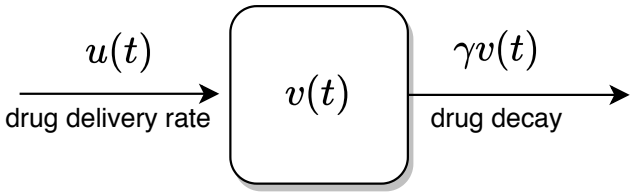

Figure 3.2: **A Visual Representation of Drug Concentration Change in Cancer Site.**

3.2 Proposed Tumor Kinetic Model

We assume continuous drug delivery with a constant rate during the treatment duration. This leads to a simplified approximation of the drug concentration in Eq. (3.5) and the resulting tumor kinetics model under cancer treatment. This approximation reduces the computational difficulty when the number of decision variables is increased in both *OCM* and *NSO* model, which will be discussed in the following chapters.

3.2.1 Constant and Continuous Drug Delivery Rate

Assumption 3.2.1 *Tumor growth is controlled with a constant and continuous drug delivery between each treatment period.*

Assumption 3.2.1 implies that drug concentration stabilizes and converges to a linear function of the drug delivery rate. Therefore, considering constant drug delivery rate at treatment points helps maintain the tractability of the mathematical model, and may be a reasonable assumption for particular types of anti-cancer agents & cancer types such as glioma in the brain and spinal cord. For instance, a continuous daily regimen of a specific chemotherapeutic agent (temozolomide) against gliomas was well tolerated for periods up to 6 or 7 weeks [Brock et al., 1998]. Thanks to the recent innovations in wearable health technologies, the feasibility of continuous drug delivery improves [Iqbal et al., 2021]. Many recent papers advocate the use of continuous treatment to better combat the tumors [Abdulrashid et al., 2019]. It is noted that this assumption, $u(t) = u$, will be later relaxed to continuous and constant drug delivery at each treatment period in the decision horizon (i.e., delivery rates vary from period to period). However, the replacement of $v(t)$ by the drug delivery rate, $u(t)$, will remain the same for the rest of the thesis.

3.2.2 Approximation of Drug Concentration

Assumption 3.2.2 *We assume that $u(t)$, drug delivery rate, to be constant at predefined decision horizon as $u(t) = u$.*

The solution of $v(t)$ in Eq. (3.5) [details in Appendix B] when $u(t) = u$ for the whole treatment time is as follows:

$$v(t) = (1 - e^{-\gamma t})\frac{u}{\gamma}. \tag{3.6}$$

As t increases, $v(t)$ converges to $\frac{u}{\gamma}$. If γ is sufficiently large, $v(t)$ may converge to $\frac{u}{\gamma}$. Thus, $v(t)$ in the second component of the kinetics model in Eq. (3.6) can be approximated to $\frac{u}{\gamma}$ with minimal error.

To conclude, Eq. (3.3) is widely used and validated in earlier studies. In this thesis, we demonstrate that when u is continuous and γ is large enough, we can rewrite Eq. (3.3) as

$$\frac{k_1 u}{\gamma k_2 + u}. \tag{3.7}$$

Therefore, Eq. (3.3) and Eq. (3.7) are equivalent under the given assumptions. Thus, our approximated Michaelis-Menten kinetic is valid.

3.2.3 Other Assumptions

Combinations of drug agents rather than a single agent are proposed to create more efficient treatment plans in terms of reducing drug resistance [Murray, 1997]. However, we assume a single drug agent administered the cancer site (which could be a static combination of multiple drugs), since integrating time-specific effects of different drugs makes the model harder to solve. Using a single drug administration, we also eliminate several additional assumptions and parameters related to the effects of other drugs in the model. To consider the maximum cumulative effect on the tumor population, it is reasonable to combine the effects of each drug for the cell evolution in a particular phase [Swierniak et al., 2005].

Every cell has cycles that result in the replication of cells. The cell cycle is usually divided into 5 phases which are $G0$, a phase where cells remain resting; $G1$, the first growth phase; S, a phase when DNA is replicated; $G2$, the second growth phase; M, mitosis phase. The injected drug can interfere with any of these division stages. Thus, considering the modeling of cell-cycle specific drug administration is important since the fraction of killed

cells depends on the growth fraction of tumor cells [Panetta and Fister, 2003]. However, since our primary goal here is creating a simple deterministic model incorporating tumor growths and the effects of the drug for killing the cancer cell, we assume the model is composed of a non-cycle-specific drug.

3.2.4 Numerical Validation

Fig. 3.3 displays the change of the drug concentration during a single treatment time cycle. According to the graph, the drug concentration reaches its maximum value in a comparably short time relative to the treatment time intervals, say, $\Delta t = 28$ days and remains stable even for different drug decay constants. In pharmacokinetics, this phenomenon is called steady-state concentration. Steady-state concentration describes dynamic equilibrium when the amount of a drug being absorbed is the same amount eliminated from the cancer site when the drug is given continuously ([Gupta, 2016], [Wadhwa and Cascella, 2020], [Parkway, 2020]). Since the change of drug concentration is constant, $dv(t)/dt = 0$. That leads to $u = \gamma v(t)$.

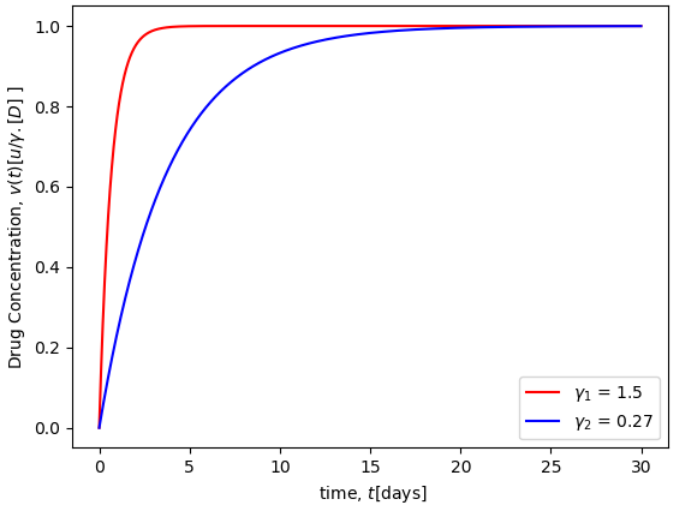

Figure 3.3: **Drug Concentration Change under Different Drug Decay Parameters, γ.**

3.2.5 Simplified Tumor Kinetic Model

Here, we give the complete tumor growth and control model which includes the simplified and approximated control term under the assumption of controlled constant & continuous drug delivery rate.

As seen in Fig. 3.3, the drug concentration function, $v(t)$, can be approximated as a step-function if γ is sufficiently large, i.e., we can validate the approximation $v(t) = u/\gamma$. Therefore, the tumor growth change in Eq. (3.4) can be rewritten as

$$\frac{dN(t)}{dt} = -\lambda N(t) ln \left[\frac{N(t)}{\theta}\right] - \frac{k_1 u}{\gamma k_2 + u} N(t). \tag{3.8}$$

Ultimately, Eq. (3.8) is considered as "*The Proposed Tumor Kinetic Model*" and includes our assumption that tumor growth is controlled by the drug delivery rate.

Its solution is given as

$$N(t) = \theta exp \left\{ \frac{\lambda(\gamma k_2 + u) \ln\left[\frac{N_0}{\theta}\right] - (e^{\lambda t} - 1) u k_1}{\lambda e^{\lambda t}(\gamma k_2 + u)} \right\}. \tag{3.9}$$

3.2.6 Nondimensionalizing of the Proposed Tumor Kinetic Model

The mathematical model generally keeps track of system states representing physical quantities measured by units. Dealing with these units while solving the model may be cumbersome. Hence, non-dimensionalization helps partially or fully remove units from their physical quantities by substituting them with new variables. Moreover, Eq. (3.8) is a nonlinear first order differential equation. Therefore, defining a nondimensional cancer population term allows us to convert Eq. (3.8) into a separable differential equation.

We define the nondimensional cancer population as

$$y(t) = \ln \left[\frac{N(t)}{\theta}\right]. \tag{3.10}$$

Thus, $N(t)$ in terms of $y(t)$ can be written as

$$N(t) = \theta e^{y(t)}. \tag{3.11}$$

Then, by taking the derivative of both sides with respect to t, we reach

$$\dot{N}(t) = \theta e^{y(t)} \dot{y}(t). \tag{3.12}$$

Substituting Eq. (3.11) and Eq. (3.12) into Eq. (3.8), we obtain the following differential equation:

$$\dot{y}(t) = -\lambda y(t) - \left[\frac{k_1 u}{\gamma k_2 + u}\right], \tag{3.13}$$

which defines the "*Nondimensional Tumor Kinetic Model*". Furthermore, using Eq. (3.9) in Eq. (3.10), the solution of Eq. (3.13) is calculated as

$$y(t) = -\frac{1}{\lambda}\left(\frac{k_1 u}{\gamma k_2 + u}\right) + \left[y(t_0) + \frac{1}{\lambda}\left(\frac{k_1 u}{\gamma k_2 + u}\right)\right] e^{-\lambda t}. \tag{3.14}$$

In an alternative way, Eq. (3.13) can be solved using an integrating factor, whose details are provided in Appendix A, with its solution.

3.3 Computational Results

In this section, we numerically solve Eq. (3.14) by using the initial tumor size. Parameters and their notations used in the implementation of the proposed model and its validation are listed in Table 3.1.

3.3.1 MCP Program with Real Data Set

Medical data for a cohort of bone cancer patients who are under treatment with three cytotoxic agents, which are melphalan, cyclophosphamide, and prednisone program (MCP), are reported in Swan and Vincent [1977]. This data set consists of the number of tumor cells depending on the time of chemotherapy treatment and is presented in Table 3.2 with four typical cases of a chemotherapy treatment program. According to the MCP program, the chemotherapy treatment schedule is designed as follows:

(i.) On day 1:

   a. Orally, a certain dosage of melphalan is given. Afterwards, it is repeated for the next three days,

Table 3.1: The Descriptions, Values and Sources of the Parameters Used in the Tumor Kinetic Model

Parameter	Description	Value	Unit	Source
N_0	Initial tumor population	presented in Table 3.2	cells	Swan and Vincent [1977]
θ	Asymptotic maximum tumor population	$3.9313 * 10^{12}$	cells	Swan and Vincent [1977]
λ	A positive tumor growth rate constant	0.015	$1/t$	Swan and Vincent [1977]
γ	A positive constant decay of drug concentration	1.5	$1/t$	Swan and Vincent [1977]
$u(t)$	Drug delivery rate at the cancer site	calibrated by assumption	$[D]/t$	calibrated
$v(t)$	Drug concentration at the cancer site	time dependent	$[D]$	-
k_1	Reaction rate constant	presented in Table 3.2	$1/t$	calibrated
k_2	Substrate concentration at $\frac{k_1}{2}$	a relative constant	$[D]$	-
Δt	A single treatment time cycle	28	t	Swan and Vincent [1977]

[D] is the unit of drug concentration/ mass of drug delivered to a cancer site.

b. Intravenously, a certain dosage of cyclophosphamide is given,

c. Orally, a certain dosage of prednisone is given. Then, it is repeated for the next three days.

(ii.) About a month later, the above schedule is repeated with a reduced dose, and it will continue in the same way until the treatment schedule is completed.

3.3.2 Evaluation of Parameters

Based on the standard MCP program given in Table 3.2, Swan and Vincent [1977] assumed that the administered drug(s) is given to a desirable concentration k_2 in every time interval Δt. Different than our assumption, they assumed that the drug has an instantaneous effect on the cancer site when it is first applied. Then, depending on the drug decay constant, drug concentration will decrease after some time. Since we control tumor growth with a constant drug delivery rate, the drug delivery rate $u = \frac{k_2}{\Delta t}$ is constant for the treatment horizons so that drug concentration levels can be kept at a certain value throughout the treatment. Thus, the total drug dose is equal to that of Swan and Vincent [1977]. Therefore, the

Table 3.2: Data Set Taken from Bone Cancer Patients Based on MCP Chemotherapy Treatment Schedule

Patient A				
Time (day)	Δt	Tumor cells, N (x 10^{12})	y	k_1
0	0	1.297	-1.109	
25	25	0.383	-2.329	3.232
71	46	0.108	-3.595	3.141
155	84	0.0985	-3.687	2.402
159	4	0.0956	-3.717	2.710
182	23	0.0945	-3.728	2.422
189	7	0.0940	-3.733	2.437
Patient B				
Time (day)	Δt	Tumor cells, N (x 10^{12})	y	k_1
0	0	2.70	-0.375	
19	19	1.92	-0.717	1.129
29	10	1.77	-0.798	0.839
47	18	1.49	-0.970	0.984
68	21	1.68	-0.850	0.339
103	35	1.63	-0.880	0.596
138	35	1.58	-0.912	0.617
178	40	1.33	-1.08	0.835
Patient C				
Time (day)	Δt	Tumor cells, N (x 10^{12})	y	k_1
0	0	1.53	-0.944	
39	39	0.597	-1.885	1.979
66	27	0.556	-1.956	1.353
94	28	0.336	-2.460	2.210
122	28	0.355	-2.405	1.483
150	28	0.271	-2.675	2.059
Patient D				
Time (day)	Δt	Tumor cells, N (x 10^{12})	y	k_1
0	0	1.06	-1.311	
29	29	1.08	-1.292	0.811
61	32	0.955	-1.415	1.041
89	28	0.973	-1.396	0.877
110	21	1.01	-1.359	0.812
138	28	0.937	-1.434	1.018

solution of the tumor kinetic model in Eq. (3.14) from t_{i-1} to t_i, for $i = 1, 2, \cdots, n$, where n is the number of treatment cycles, can be rewritten as

$$y(t_i) = -\frac{1}{\lambda}\left(\frac{k_1}{\gamma\Delta t + 1}\right) + \left[y(t_{i-1}) + \frac{1}{\lambda}\left(\frac{k_1}{\gamma\Delta t + 1}\right)\right] e^{-\lambda\Delta t}. \tag{3.15}$$

Moreover, if we consider the time interval $[t_{i-1}, t_i]$, we can find constant quantity k_1 in this specified time interval with respect to $y(t_{i-1})$ and $y(t_i)$ as:

$$k_1(t_i) = \lambda(\gamma\Delta t + 1)\left[\frac{y(t_i)e^{\lambda\Delta t} - y(t_{i-1})}{1 - e^{\lambda\Delta t}}\right]. \tag{3.16}$$

The values of quantities in the right-hand side of Eq. (3.16) are known from Table 3.2. Therefore, the value of k_1 is obtained using these values and presented in the same table. It has been observed that the drug reaction rate parameter k_1 varies for each time interval and it changes for each patient.

The average value of k_1, denoted as $\overline{k_1}$, in each patient is necessary for the evaluation of the model that calculates the number of nondimensional tumor populations in Eq. (3.15). Thus, we calculate the average drug effectiveness parameter, $\overline{k_1}$, in Eq. (3.16) and display it in Table 3.3 for each patient. It is important to note that the higher value of $\overline{k_1}$ is preferable.

Table 3.3: Comparison of the Average of Drug Effectiveness Parameter

	Average of Drug Effectiveness Quantity ($\overline{k_1}$)
Patient A	2.724
Patient B	0.763
Patient C	1.817
Patient D	0.912

3.3.3 Calibration Results

We present our model results in Fig. 3.4 that compare the tumor growth trajectories of the four patients given real data sets in Table 3.2 and Swan and Vincent [1977]. Plots illustrate that our model's tumor growth trajectories have an adequate agreement with the actual

data compared to Swan and Vincent [1977]. This is an indicator that the assumptions which we have made and parameters that we have used for the development of the model are reasonable. The reason we care about the alignment of model results to the real data set is both models and the real data represent the same tumor growth under the same treatment. Therefore, the outcomes of these two models are comparable to each other, and their compliance with the real data indicates the accuracy of their representation of tumor growth. As the proposed model produces similar trajectories to both the real data and the existing model, we concur that the proposed model provides a reasonable representation of tumor growth and will be used as a foundation for the rest of the model & its extensions proposed in later chapters.

3.3.4 Accuracy Check

Another way to check the validity of a model is to compare the root mean square error (RMSE) of each model to the particular patient trajectories in the given data set. Table 3.4 shows the comparison for the RMSE of our model and Swan and Vincent [1977] model. The results present that the RMSE of our proposed model is comparable to that of their model, even though our model develops a simpler tumor dynamic model. The easier evaluation of our model becomes notably useful when we match our tumor growth model with the more realistic drug concentration constraints to find the optimal chemotherapy plan in the next chapter.

Table 3.4: Error Calculation

	Performance Measure	
	RMSE(Proposed Model)	**RMSE(Swan and Vincent [1977])**
Patient A	0.3233	1.1460
Patient B	0.12539	0.07984
Patient C	0.14927	0.19056
Patient D	0.03538	0.03575

3.4 Conclusions

In this chapter, we study the Gompertzian equation to present tumor growth and employ an approximation of the Michaelis-Menten kinetics equation, with available bone cancer

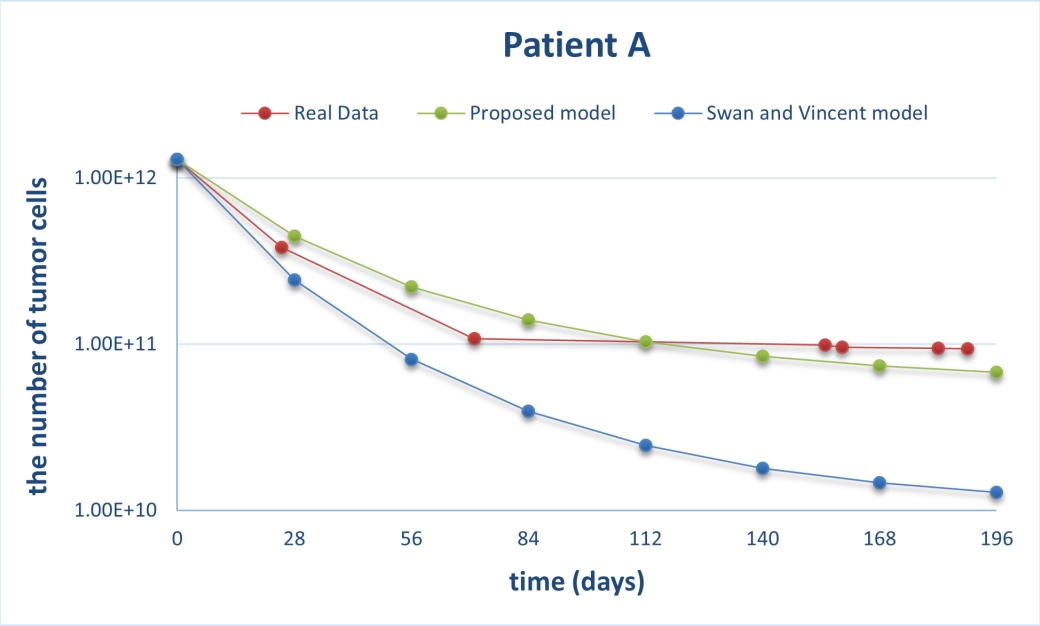
Patient A
Real Data
Proposed model
Swan and Vincent model
the number of tumor cells
1.00E+12
1.00E+11
1.00E+10
0
28
56
84
112
140
168
196
time (days)

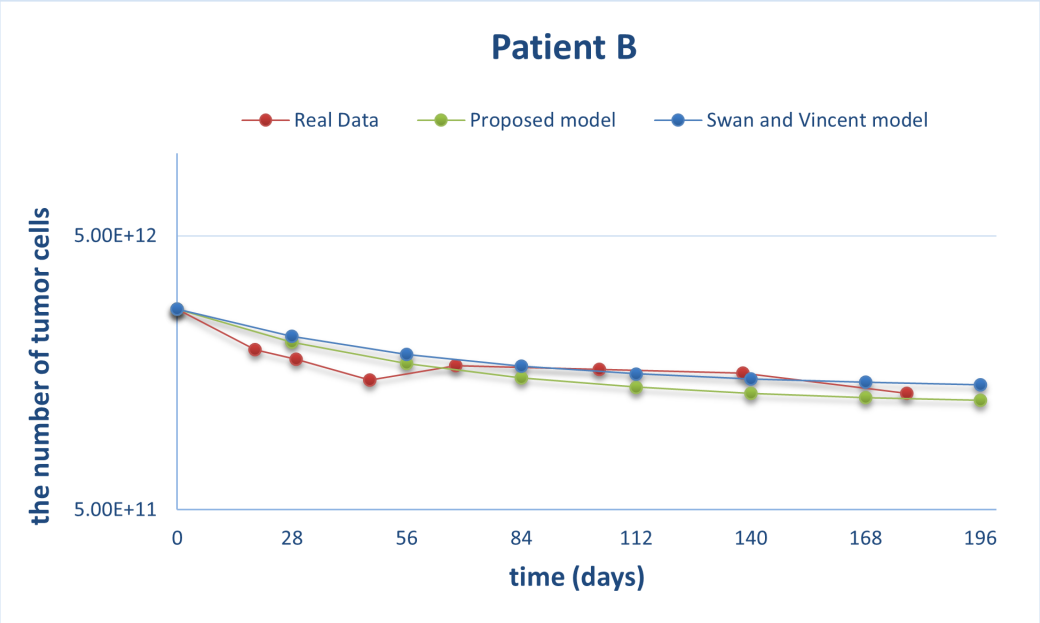
Patient B
Real Data
Proposed model
Swan and Vincent model
the number of tumor cells
5.00E+12
5.00E+11
0
28
56
84
112
140
168
196
time (days)

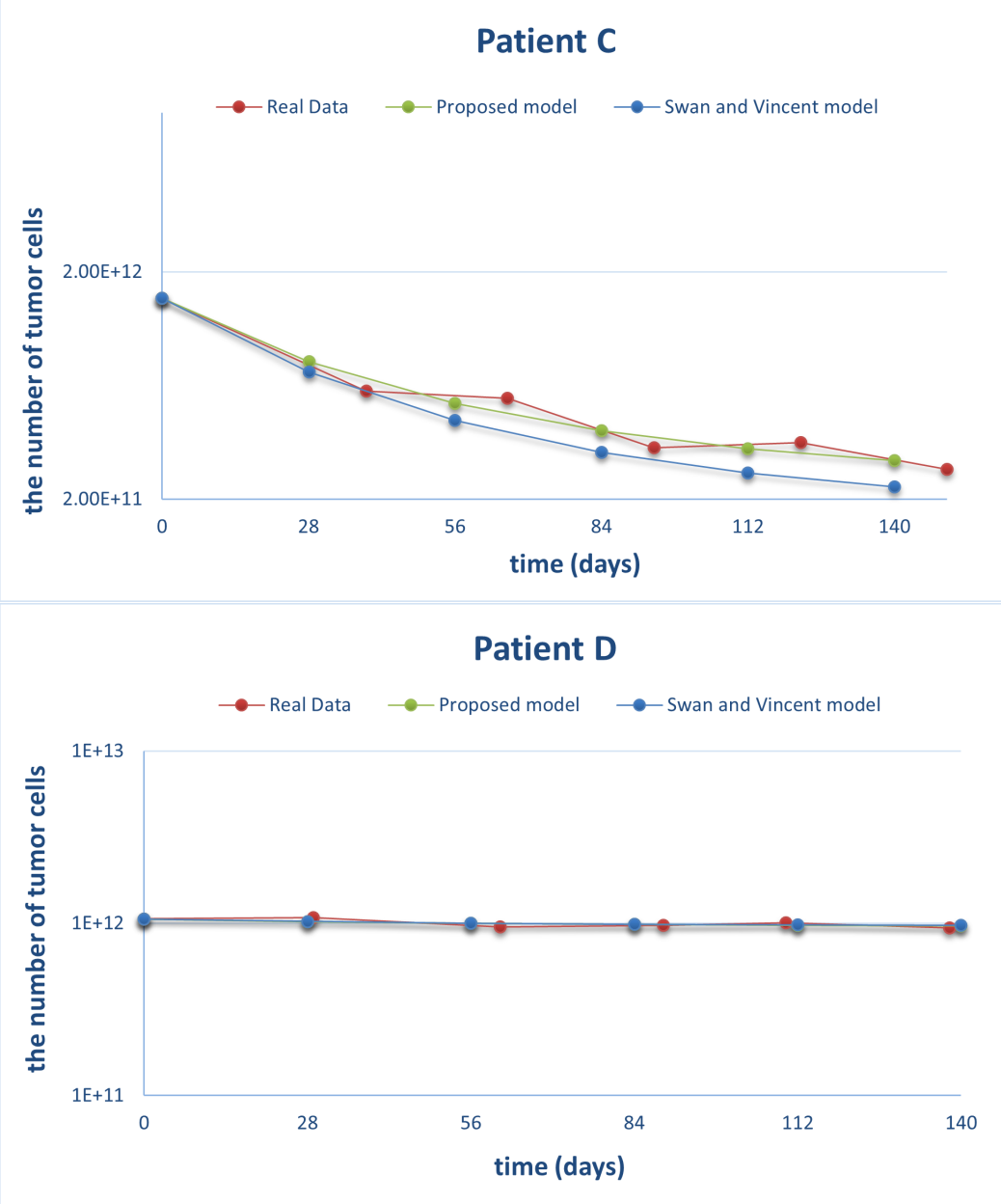

Figure 3.4: **Comparison of the Real Data with the Results of the Proposed Model and Swan and Vincent [1977] Model.**

patients' data, to control tumor growth by injecting cancer agent(s). We propose a simplified and effective tumor kinetic function, assuming the constant drug delivery rate controls tumor growth. We demonstrate that the current model is successful in mimicking the real data set published in the literature, and numerical results are presented to highlight the alignment of the proposed kinetic model with the real data set. Also, the performance measures are compared between the proposed and the published study, and show a good fit for the well-accepted tumor kinetic model.

Furthermore, our findings align with Remesh [2013] that daily scheduling (when the pharmacokinetic parameters are considered) can be applied alternatively in a more effective manner. Moreover, continuous drug therapy [University of Washington, 2021] can prevent the tumor resistance to the chemotherapy, since cyclic chemotherapy has the disadvantage that the residual tumor cells which are resistant to the chemotherapy can remain [Remesh, 2013].

To conclude, the proposed tumor kinetic model can be useful within a complex mathematical model. We observed that it well captures the changes of a given real data set with reasonable accuracy. However, since the data is not sufficient enough for a realistic analysis though provides a numerical experimental setting to test the idea, we consider our results as a hypothetical analysis. Most importantly, by taking the drug delivery rate continuously constant during the treatment time plan, the drug concentration is approximated as a step-function of the drug delivery rate. This new deterministic model is necessary to lay the foundation for the stochastic cancer staging control model we present in this thesis.

Chapter 4

Optimal Control Model (OCM) for Chemotherapy Treatment Planning

This chapter presents an *Optimal Control Model (OCM)* for cancer chemotherapy treatment plan. In Chapter 3, we designed a new simplified tumor kinetic model [Eq. (3.8)] for a given time-independent (i.e., stationary) drug delivery rate. We calibrated the proposed model using a data set from the literature, and numerically validated the model by comparing it with real data from the literature. Now, we extend this tumor kinetic model by employing optimal control theory to find an optimal non-stationary drug schedule under drug toxicity and tumor reduction constraints.

4.1 Problem Description and Formulation

Chemotherapy is one of the main treatment modalities for cancer patients to kill cancer cells using drugs that are administered through veins or taken orally. However, the chemotherapeutic agent not only kills tumor cells but also destroys normal cells. To tackle this problem, many mathematical models have been developed and an extensive literature review on cancer chemotherapy treatment plans was presented in Chapter 2. In this chapter, the problem of chemotherapy treatment planning is modeled as an *OCM*. Specifically, the model is developed by considering the non-cycle specific and single drug features.

The model presented below constitutes a nonlinear problem for finding the optimal drug delivery rates.

Objective

$$\underset{u(t)}{\text{minimize}} \quad J[u(t)] = N(T) \tag{4.1}$$

Constraints

$$\frac{dN(t)}{dt} = -\lambda N(t) ln\left[\frac{N(t)}{\theta}\right] - \frac{k_1 u(t)}{\gamma k_2 + u(t)} N(t), \quad N(0) = N_0 \tag{4.2}$$

$$N(\xi_{j+1}) \leq \eta N(\xi_j), \quad j = 0, 1, 2, \cdots, M \tag{4.3}$$

$$0 \leq v(t) \leq v_{max}, \quad \forall t \in [0, T] \tag{4.4}$$

$$\int_0^T v(t)dt \leq v_{cum}. \tag{4.5}$$

Decision variable

$u(t) \in \mathbb{R}^n$	drug delivery rate function

State variable

$N(t) \in \mathbb{R}^n$	the population of tumor cells at time t

Parameters

T	terminal time
$[0, T]$	time horizon for the system
λ	tumor growth rate
θ	maximum tumor size at the cancer site
k_1	drug effectiveness parameter
k_2	drug concentration at the half of $\frac{k_1}{2}$
N_0	initial tumor size
$N(\xi_j)$	the number of tumor cells at the check point $j = 0, 1, ..., M$
M	treatment check points for the reduction constraint
η	the minimum fractional reduction constant in the tumor size
v_{max}	maximum allowable toxicity at any time t
v_{cum}	maximum cumulative toxicity throughout the treatment
v_0	initial drug concentration at the cancer site

In the model, the treatment planning horizon is $[0, T]$, which is divided into n equally-distanced-periods referring the treatment cycles. The function of these treatment cycles will be clarified in Section 4.2.

Eq. (4.1), objective of the model, minimizes the number of tumor cells at the end of the chemotherapy treatment horizon under the drug delivery rates, $u(t)$. This objective function is controlled by several constraints which are further explained below. Several studies, such as Martin [1992], proposed models to minimize $N(T)$ under similar constraints but for different control mechanisms.

Eq. (4.2) represents the tumor growth dynamic that has a direct impact on the size of tumor cells at any time during the treatment, as extensively explained in Chapter 3.

Studies reveal that drug resistant cells may appear when the tumor population increases [Goldie and Coldman, 1979]. Therefore, one of the main goals in chemotherapy treatment is to keep the tumor size decreasing throughout the treatment duration, while achieving the maximal reduction in tumor burden at the end of planning horizon. In this context, Eq. (4.3) aims to prevent drug resistance by forcing the model to decrease the tumor size at, or faster than, a given rate within predefined time intervals, i.e., $[\xi_j, \xi_{j+1}]$. More specifically, Eq. (4.3) requires the model to reduce the tumor size at least by $(1-\eta)100\%$ (i.e. $\eta \in [0,1]$) between ξ_j and ξ_{j+1} for $j = 0, 1, \cdots, M$; where $\xi_j = j$, and $M = T/\Delta t$ refers to the total number of tumor growth checkpoints set in every Δt unit time.

Another goal for a successful chemotherapy regimen is to minimize the toxic side effects, since chemotherapeutic drugs are toxic not only to cancer cells, but also to normal healthy cells. Since these toxic agents may cause some serious side effects, constraints Eq. (4.4) and Eq. (4.5) ensure that the drug toxicity is kept under control. Constraint Eq. (4.4) enforces that the toxicity at any time $t \in [0, T]$ does not pass the limit a patient can tolerate, i.e., v_{max}. Constraint Eq. (4.5) limits the cumulative drug concentration over the whole treatment horizon to a positive threshold v_{cum}.

4.2 Solution Approach

Section 4.1 presents a nonlinear optimal control problem, which is usually very complex to solve using analytical techniques when $u(t)$ is a continuous variable in t. Although allowing $u(t)$ to vary in t (e.g., continuous control) would achieve better performance, it is not very practical as treatment decisions are usually assessed periodically. For example, drug administration or dosing decisions are periodically made and reviewed (e.g., every month). Moreover, periodically adjusted decisions would provide a more tractable model. Therefore, we convert this optimal control problem into an optimal parameter selection problem using a numerical method called the "control parametrization technique" ([Li et al., 2006], [Lin et al., 2013]). The control parametrization approach is introduced by Goh

and Teo [1988] to solve general optimal control problems. With this technique, piecewise constant functions are administered to define the set of a possible sequence of control variables at the predefined switching points. The height of piecewise constant functions is considered as the decision variables named as control variables. This technique is commonly used in the chemotherapy treatment planning literature [Dua et al., 2008] and is considered a fine approximation to the continuous control case.

The control variable, $u(t)$, is defined with n different σ values for n different time intervals. We assume that the drug delivery rate, $u(t)$, is constant for each treatment cycle. Then, the control variable $u(t)$ is described with the constant value $\vec{\sigma}$

$$u(t) = \vec{\sigma} = \frac{k_2}{\Delta t}(\sigma_1, \sigma_2, ..., \sigma_n) \in \mathbb{R}^n \tag{4.6}$$

where each $\sigma_i, i = 1, 2, ..., n$, represents the height of the piecewise continuous functions. Thus, $u(t)$ is defined as follows:

$$u(t) = \vec{\sigma} = \begin{cases} \frac{k_2}{\Delta t}\sigma_1, & 0 = t_0 \leq t < t_1 \\ \frac{k_2}{\Delta t}\sigma_2, & t_1 \leq t < t_2 \\ \vdots & \\ \frac{k_2}{\Delta t}\sigma_n, & t_{n-1} \leq t \leq t_n = T \end{cases} \tag{4.7}$$

where $t_0 = 0$ and $t_n = T$ are the initial and final time points, respectively. These t_i's are defined as the switching times in the formulation as $t_j = j\frac{T}{n}$ for $j = 0, 1, 2, ..., n$ where $n = \frac{T}{\Delta t}$ is the number of treatment cycles.

4.2.1 Nondimensionalization of the OCM

As mentioned in the previous chapter, the tumor dynamic equation Eq. (4.2) is a nonlinear differential equation and consequently, constraint Eq. (4.3) is a nonlinear function. Thus, defining a nondimensional cancer population term allows us to convert this nonlinear function into a separable differential equation that can be solved easily. Subsequently, the nonlinear function will be unitless after the transformation. Recall that:

$$y(t) = \ln\left[\frac{N(t)}{\theta}\right] \tag{4.8}$$

Therefore, the *OCM* can be rewritten in terms of the nondimensional scale as:

$$\underset{\sigma_i, i=1,\dots,n}{\text{minimize}} \quad J(\vec{\sigma}) = y(T), \tag{4.9}$$

$$\text{subject to} \quad y(t_i) = -\frac{1}{\lambda}\left[\frac{k_1\sigma_i}{\gamma\Delta t + \sigma_i}\right] + \left[y(t_{i-1}) + \frac{1}{\lambda}\left(\frac{k_1\sigma_i}{\gamma\Delta t + \sigma_i}\right)\right] e^{-\lambda\Delta t} \tag{4.10}$$

$$y(\xi_{j+1}) - y(\xi_j) \leq \ln(\eta), \qquad j = 0, 1, 2, \cdots, M \tag{4.11}$$

$$0 \leq \frac{k_2}{\gamma\Delta t}\sigma_i \leq v_{max}, \qquad i = 1, 2, ..., n \tag{4.12}$$

$$0 \leq \frac{k_2}{\gamma}\sum_{i=1}^{n}\sigma_i \leq v_{cum}, \qquad i = 1, 2, ..., n \tag{4.13}$$

where $\vec{\sigma}$, defined in Eq. (4.7), is the decision variable vector and $y(t); \forall t \in [0, T]$, is the nondimensional state variable. We refer to this optimization model as "*Nondimensional Optimal Control Model (NOCM)*".

Eq. (4.9) is the objective function of *NOCM* that minimizes the nondimensional tumor cells where T is the final treatment time under piecewise vector $\vec{\sigma} \in \mathbb{R}^n$. After nondimensionalizing, constraint Eq. (4.10) is the solution of the differential equation in Eq. (4.2) from t_{i-1} to t_i for $i = 1, 2, \cdots, n$, where $t_n = T$ is the final treatment time. This is the structural equation that has also defines the objective function. Constraints Eq. (4.11), Eq. (4.12) and Eq. (4.13) present the nondimensional tumor reduction, the maximum drug toxicity in each cycle and the cumulative drug toxicity for the whole treatment, respectively.

To conclude, if we use Eq. (3.3) in Eq. (4.1), Eq. (4.4) and Eq. (4.5), we may not be able to derive the exact integration of these functions, and get the simplified equations from the integrations as in Eq. (4.9), Eq. (4.12) and Eq. (4.13). Therefore, the system of [Eq. (4.1) – Eq. (4.5)] and [Eq. (4.9) – Eq. (4.13)] are equivalent when $v(t) = \frac{u(t)}{\gamma}$. Due to the simplification we made in Chapter 3, which is controlling the tumor growth by the drug delivery rate, $u(t)$, instead of the drug concentration, $v(t)$, the representation of the former model is simplified and becomes easy to solve after verifying this replacement.

4.3 Results and Discussions

The *NOCM* is implemented on *Maple 2018* optimization software to derive the optimal drug delivery rate for chemotherapy treatment with $n = 7$ periods and computational

experiments were carried out on a workstation with the following specifications: AMD Ryzen 7 4700U with Radeon Graphics, 2.00 GHz, and 16GB of RAM. *Maple* solves the model with an *NLPSolve* command which follows the sequential quadratic programming (SQP) approach. SQP method is available for a constrained nonlinear program and uses derivatives automatically computed by *Maple*. The computational difficulty of the OCM is reduced since the functions in the model are simplified thanks to the proposed tumor kinetic model and easily taken derivatives. Therefore, the solution time is ignorable to report in standard problem sizes. However, we state the computational time of the OCM for larger problem instances. In addition, global optimality of the solutions founded by *Maple* is verified by the software.

In *NOCM*, $u(t)$ is defined with control variables $\sigma_i, i = 1, 2, ..., n$, for certain time intervals in which $u(t)$ is constant in every specified time interval. The duration of treatment is assumed to last for $T = 196$ days and the drug is given every 4 weeks ($\Delta t = 28$).

In Chapter 3, we presented parameters $\lambda, \gamma, \theta, N_0$ in Table 3.1 that have been used to develop the tumor kinetic equation. In addition to these parameters, Table 4.1 displays the parameters used in the *NOCM*. The *NOCM* is initially solved by the introduced data values in Table 3.1 & Table 4.1 and then we present the results for $N(t)$ using the transformation in Eq. (3.10).

Table 4.1: Additional Parameters for the NOCM

Parameter	**Description**	**Value**	**Unit**	**Source**
T	Final treatment time	196	days	[Swan and Vincent, 1977]
η	The minimum fractional reduction in tumor size	0.5	-	[Martin et al., 1990]
k_2	Desirable drug concentration	50	$[D]$	calibrated
v_{max}	Maximum drug concentration	k_2	$[D]$	[Martin et al., 1990]
v_{cum}	Cumulative drug toxicity	$\frac{k_2 T}{3.5}$	$[D].days$	calibrated

The way of calculation k_1 was discussed in Chapter 3 and its average value for each patient was also presented in the same chapter in Table 3.3. For initial numerical testing, we take $k_1 = 0.912$ which has been calculated as the drug effectiveness quantity of Patient D.

The minimum fractional reduction in tumor size is set to 50% every four weeks [Martin, 1992]. Thus, η is 0.5. With the number ($M = \frac{T}{\Delta t}$) of main checkpoints, this constraint

is checked at $\xi_j = j\frac{T}{M}, j = 0, 1, 2, \cdots, M$, characteristic times. Hence, in each treatment point, the tumor population reduction has been checked whether at least 50% tumor size reduction constraint has been met from the previous treatment point.

k_2 is a relative parameter and does not affect the optimal solution. To match the values used in the literature for v_{max} and v_{cum}, we choose k_2 as 50. Therefore, the toxicity limits are set as $v_{max} = 50[D]$ and $v_{cum} = 2.8 * 10^3[D].days$, respectively. $[D]$ is the unit of drug concentration. It is important to note that this numerical settings is inspired by the problem instances clinically and empirically derived by the works of Swan and Vincent [1977] and Martin et al. [1992b]. Moreover, similar numerical settings are commomly employed in various modeling exercise in the literature [Tse et al., 2007].

4.3.1 Drug Delivery Rate Schedule and Tumor Size Change

Fig. 4.1a presents the optimal drug delivery rates based on the limits of the given constraints, and Fig. 4.1b illustrates the corresponding number of tumor cells change by time.

Since we force the tumor size to decrease by 50% in the next period, tumor cells decrease constantly even when the optimal drug delivery rate is low at the beginning of the treatment. Then, the drug rate increases in the middle of the treatment. At the end of treatment, the optimal drug delivery rate reaches its maximum level.

In the first four treatment cycles, the drug delivery rate is determined by the tumor reduction constraint which forces a 50% decrease in the tumor population. Then, for the remaining treatment intervals, the maximum available drug is applied to minimize the number of tumor cells. Intuitively, we expect that the majority of drug delivery rate should have been given at the last treatment point, i.e. t_7. However, for minimizing the final tumor size, increasing the dose at t_5 by a unit that causes more than 50% tumor reduction produces a better outcome than holding the amount of the dose at the end.

Fig. 4.2 illustrates the change in drug concentration functions that correspond to the controls of the optimal control variables. Since the drug delivery rate is relatively low in the first four months of the treatment compared to that of the remaining treatment intervals as shown in Fig. 4.1a, the drug toxicity at the cancer site is also low and increases toward the end of the treatment.

4.3.2 Verification of the Result with Brute-Force Search for OCM

In this section, we utilize the Brute-Force search or Exhaustive search to the problem of *OCM* by enumerating all possible solutions and controls when each candidate meets the

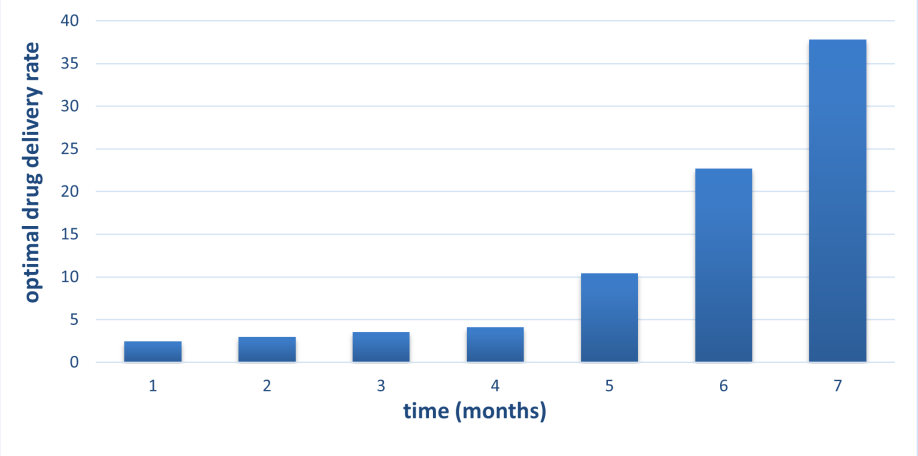

(a)

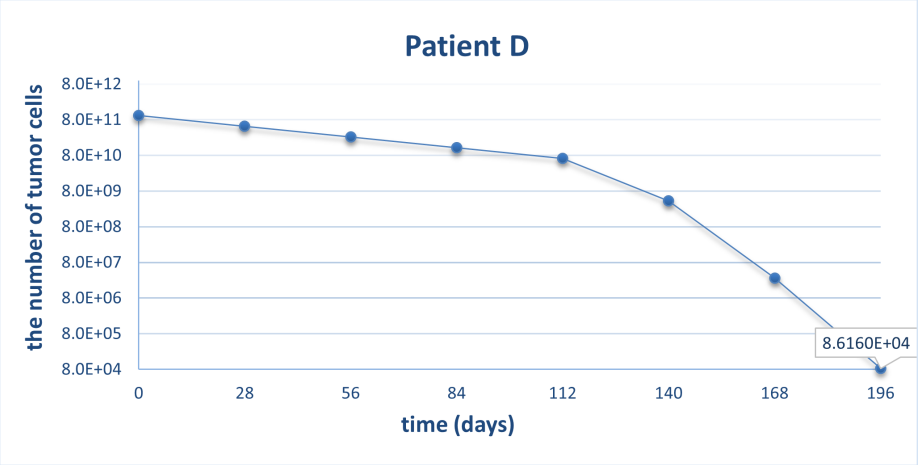

(b)

Figure 4.1: a) **Optimal Drug Delivery Rate and** b) **Tumor Size Change when** $v_{max} = 50[D], v_{cum} = 2.8 * 10^3[D]days$**, Reduction** $= 50\%$**.**

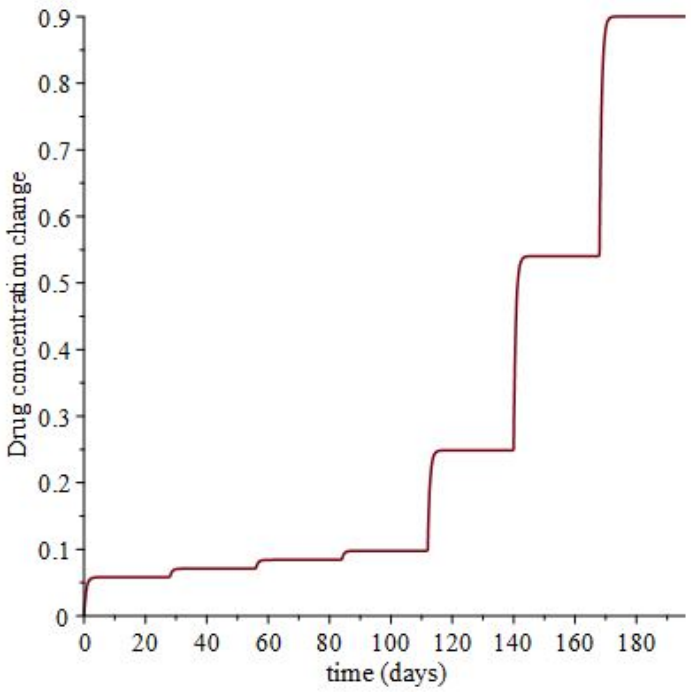

Figure 4.2: **Drug Concentration-Time Curve Following Administration of the Controls of Fig. 4.1a.**

constraints of the problem. With this search, we test systematically all possible candidates for the control variable in the model to find the minimum number of tumor size. This technique consists of checking if an assigned value of the decision variable is feasible and guarantees to find the minimal value of the state variable, $N(t)$. The result of this method has been used to make a comparison with results from *OCM*.

Algorithm 1 iterates over the whole decision variables, $\sigma_i, i = 1, ..., n$, from ϵ to v_{max} by ϵ, step size. $v_{max} = 42$ and $v_{cum} = 84$ are taken so that the results can be comparable with the proposed *OCM*. Those below steps verbally explains the flow of the Algorithm 1.

Step 1 Initialize σ_i and assign the current state as $N_0 =$ finaltumor

Step 2 If $totalv_{cum}$ is less than or equal to v_{cum}, we calculate N_i otherwise go back to **Step 1**.

Step 3 If Eq. (4.3) holds, then checks if $N_n <$ finaltumor, σ_i^* becomes the best value and updates the current state from N_0 to N_n otherwise store the current state as an incumbent.

Step 4 If Eq. (4.3) does not hold, go to **Step 1**.

Step 5 Repeat the above steps until $\sigma_i = v_{max}$.

While **Step 2** meets the total cumulative drug constraint in the *OCM*, **Step 3** checks the 50% reduction in the tumor size in the next iteration. In general, Algorithm 1 is computationally complex, since it counts for all $\sigma_i, i = 1, ..., n$ values up to v_{max} starting from ϵ and requires days to execute it in some instances when ϵ has even slightly decreased. Table 4.2 demonstrates the number of trials and corresponding run-time for the algorithm at different step sizes. It is observed that for $\epsilon = 14$, the algorithm has infeasible solutions. When $\epsilon = 1$, execution time is estimated as 9 days. Therefore, the algorithm has been interrupted and no solution has been produced.

4.3.2.1 Improvised Step 2 in Brute-Force Search

Algorithm 1 is easy to implement and typically provides a solution to the problem if the feasible region is nonempty. However, when the number of candidate solutions increases, the computational time significantly increases. To mitigate the computational cost, total drug cumulative can be taken as equal to the drug cumulative limit as $totalv_{cum} = v_{cum}$ which is different than **Step 2** in Algorithm 1, since the cumulative drug is less than

ALGORITHM 1: Brute-Force Search

Input : σ_i , decision variables
v_{max} , upper bound to the decision variables
v_{cum} , limit to summation of decision variables
ϵ , step size

Output : σ_i^* , best control variables
$N(T)$, finaltumor size // i=1,...,n

finaltumor $\leftarrow N_0$
feasible $\leftarrow 0$
infeasible $\leftarrow 0$

/* starts the iteration */

for $\sigma_i \leftarrow \epsilon$ **to** v_{max} *by* ϵ **do**
  while $\sigma_i \leq v_{max}$ **do**
    $totalv_{cum} \leftarrow \frac{k_2}{\gamma} \sum_{i=1}^{n} \sigma_i$ // defines the cumulative drug delivery rate
    if $totalv_{cum} \leq v_{cum}$ **then**
      // checks the cumulative drug delivery rate limit
      while $i \leq n$ **do**
        repeat
          calculate N_i in Eq. (4.2) // calculates all N_i until $i = n$
        until $N_n \leftarrow N_i$
        if $N_{i+1} \leq \eta N_i$ **then**
          // checks tumor reduction limit
          if $N_n <$ *finaltumor* **then**
            finaltumor $\leftarrow N_n$
            σ_i^* // gives the best solution
            feasible $\leftarrow$ feasible + 1
          else
            finaltumor $\leftarrow$ finaltumor
            σ_i // gives the feasible solution
            feasible $\leftarrow$ feasible + 1
        else
          infeasible $\leftarrow$ infeasible + 1
    else
      infeasible $\leftarrow$ infeasible+1
  // completes the iteration when $\sigma_i = v_{max}$

the number of trials = $(\frac{v_{max}-\epsilon}{\epsilon} + 1)^n$ // n=7
estimated run-time = the number of trials/base time from the previous solution

Table 4.2: Results for Brute-Force Search

Step Size (ϵ)	$N(T)$	**The Number of Trials**	**Run Time** (min)	**The Number of Calculations**
14	-	2187	0.035	-
7	$4.04E+05$	279936	0.05	792
6	$3.88E+05$	823543	0.077	3425
3	$1.54E+05$	105413504	6.11	1160016
2	$1.41E+05$	1801088541	112	26164368
1	stopped the operation	230539333248	13000 (estimated)	-

v_{cum} does not satisfy the optimality condition, and more than v_{cum} violates the feasibility (totally allowed drug dose during the whole treatment). With this modification, run time and the number of calculations for different step size in the algorithm decreases notably though the solution of $N(T)$ and the number of trials will remain the same as in Table 4.2 and they are omitted to present in Table 4.3 except the final tumor size at $\epsilon = 1$. As shown in Table 4.3, the result approaches the optimal solution found in *Maple* while step size, ϵ, is decreasing. However, to avoid computational inefficiency, we terminate the algorithm when $\epsilon = 1$, since the search direction is clearly shown to its direction to the optimal solution. With this technique, we indicate that Maple has found, or has come very close to, the global minimum in the present model.

Table 4.3: Improved Performance Measure in Algorithm 1

Step Size (ϵ)	$N(T)$	**Run Time** (sec)	**The Number of Calculations**
14		1.980	0
7		2.716	462
6		3.907	1709
3		266.551	283998
2		4500.450	4225068
1	$1.13E+05$	484980	345972432

4.3.2.2 Narrowing Grid Brute-Force Search for OCM

To mitigate time inefficiency of Algorithm 1, we develop another solution approach that narrows the search space while finding the minimum tumor size at the end of the treatment in the feasible region. The algorithm has been implemented in the following manner:

Different than Algorithm 1, this approach requires a defined range for decision variables, $\sigma_i, i = 1, ..., n$, based on the previous solution sets so that we can conduct the faster iterations. We test the results for various step size and present the outcomes in Table 4.4. When $\epsilon = 1$, the run time in Table 4.3 has decreased notably with this heuristic design.

Table 4.4: Accelerated Performance Measure in Algorithm 1

Step Size (ϵ)	$N(T)$	**Run Time** (sec)	**The Number of Calculations**
1	$1.13E+05$	1.952	13056
0.5	$9.42E+04$	6.465	20047
0.25	$9.07E+04$	102.16	205345
0.1	$8.84E+04$	4.8	859
0.05	$8.66E+04$	3.053	6843

Fig. 4.3 presents the convergence of the algorithm to the optimal solution that has been obtained by *Maple*.

4.3.3 Increased Number of Control Variables

We now provide an increased number of control variables to the problem of *OCM* so that we can test the effect of continuous drug delivery dose on the final tumor size. Depending on the type of administration strategy, we propose two different options on the tumor reduction constraint. In the original problem, we could find an optimal solution the meets the half-size tumor reduction criteria in every four week treatment. When we increase the number of decision variables, either we keep the half-size reduction in every month, or we offer the continuous reduction by adjusting the tumor reduction constraint to the control variables. For instance, when $n = 14$, the tumor reduction constraint checks if the tumor size reduces by $\sqrt{2}$ instead of 0.5 in every two weeks. It is important to note that with this continuous tumor reduction adjustment while increasing the control variables, we add a new constraint to the model.

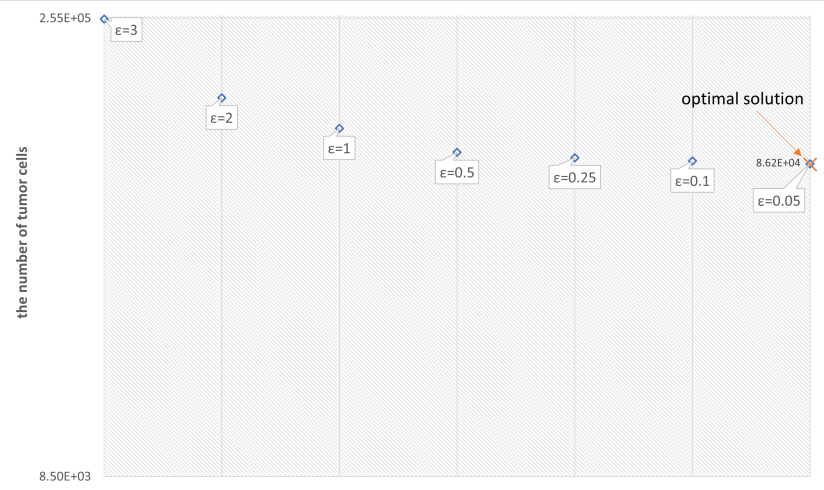

Figure 4.3: **The Convergence of Modified Brute-Force Search to the Solution of *OCM*.**

Table 4.5 and Table 4.6 provide the number of final tumor cells in the population, for different sizes of control variables. As the size of the control variables increases, the final tumor cells decrease but eventually converge to $7.1740E{+}04$ and $7.7460E{+}04$, respectively. Compared to the solution of $n = 7$, the result is not quite significant and not practical due to time-inefficiency that increases exponentially. Thus, an increased number of control variables will not have much effect on the final tumor population for the presented model. Moreover, increasing the decision variables further than weekly or daily is not clinically reasonable.

Final tumor size in Table 4.6 is slightly higher than Table 4.5 and requires more time to produce the result; even though, Table 4.6 provides the continuous tumor size reduction throughout the treatment.

4.3.4 Sensitivity Analysis on Tumor Reduction and Cumulative Toxicity Limits

The proposed *NOCM* is parameter-dependent. Therefore, we can obtain different results by changing the limits of the constraints. For example, we can relax the tumor reduction constraint to 90% by keeping the other two constraint limits constant. this means that tumor size is forced to decrease at a minimum of 10% for the next period. Since the total cumulative drug constraint will restrain to use of more drugs, drug delivery is initially given

Table 4.5: Tumor Cell Population After 7 Months of Therapy Using the Optimal Solutions to the Problem of NOCM while Maintaining the Monthly Tumor Reduction Criteria. n represents the Number of Control Variables.

n	$N(T)$	**Run-Time** (seconds)
7	$8.6160E+04$	1.454
14	$7.4740E+04$	1.475
28	$7.2470E+04$	1.513
56	$7.1920E+04$	1.542
112	$7.1780E+04$	1.678
224	$7.1750E+04$	2.206
448	$7.1740E+04$	4.714
896	$7.1740E+04$	18.686

Table 4.6: Tumor Cell Population After 7 Months of Therapy Using the Optimal Solutions to the Problem of NOCM while Maintaining the Continuous Tumor Reduction Criteria. n represents the Number of Control Variables.

n	$N(T)$	**Run-Time** (seconds)
7	$8.6160E+04$	1.454
14	$7.9380E+04$	1.471
28	$7.7940E+04$	1.450
56	$7.7580E+04$	1.872
112	$7.7490E+04$	3.367
224	$7.7470E+04$	13.304
448	$7.7460E+04$	91.962
896	$7.7460E+04$	1486.441 ($\sim 25min$)

in smaller doses than the previous scenario in Fig. 4.1a, and steeply increase towards the end, as seen in Fig. 4.4a. This happens because we relax the tumor size reduction limit for the subsequent periods, so the model keeps the bulk of drugs at the end of the treatment. When we look at the tumor change equation in Fig. 4.4b, we can interpret that patients can be exposed to more tumor cells for most of the treatment period which might not be ideal.

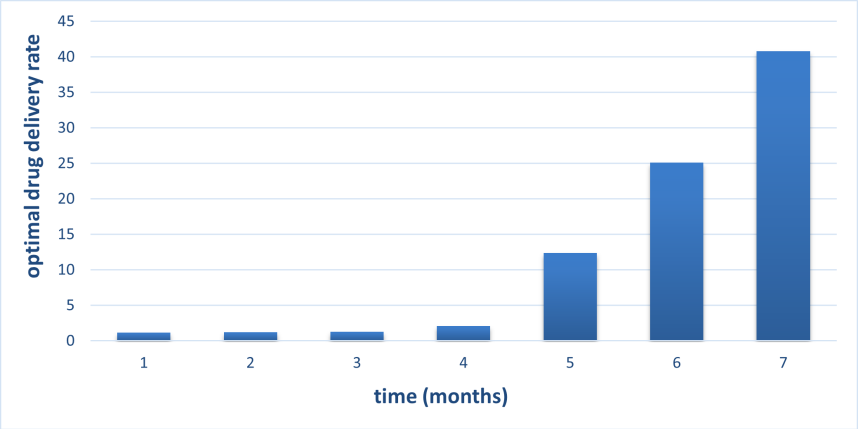

(a)

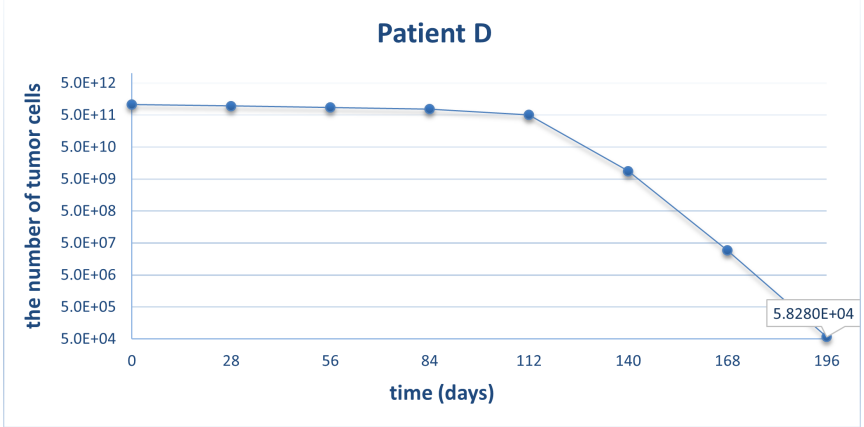

(b)

Figure 4.4: **a) Optimal Drug Delivery Rate and b) Tumor Size Change when Reduction = 90%.**

To see the effect of tumor reduction constraint on the treatment schedule, the tumor reduction constraint has been extracted from the model. Therefore, the first three months

are scheduled with no drug and the drug delivery rate gradually increases towards the end of the treatment as seen in Fig. 4.5a. Consequently, Fig. 4.5b represents the corresponding tumor size to the scheduled drug delivery rate based on the maximum and cumulative drug dose constraints. This result is not realistic for a given treatment period since tumor will increase for the first three months of the treatment. The result would make more sense if we consider for 4-months treatment schedule. On the other hand, for a given problem setting, if the drug was given in the first 4 month of the treatment, tumor will increase again, and this increase will end up a higher point than the final tumor size has been found by the model.

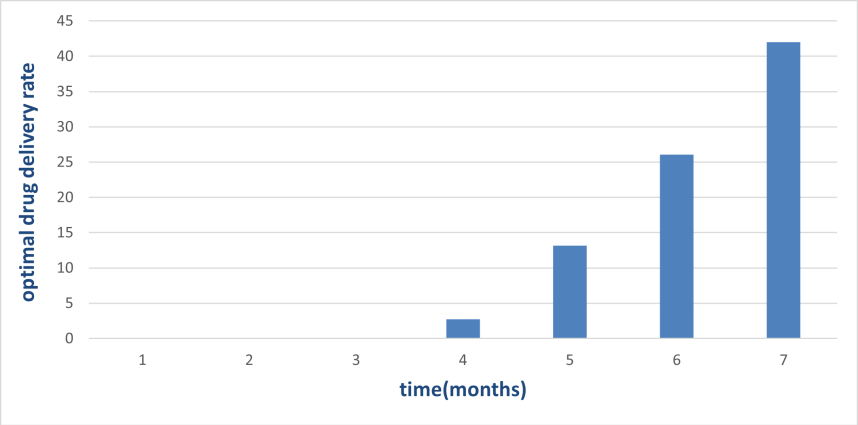

(a)

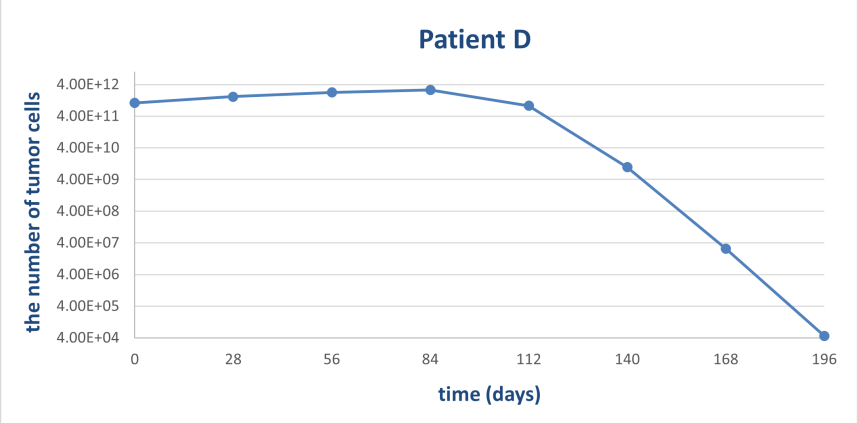

(b)

Figure 4.5: a) **Optimal Drug Delivery Rate and** b) **Tumor Size Change when Reduction Constraint is omitted.**

To observe the effect of cumulative drug toxicity limit on drug delivery plan and tumor size change, we double the cumulative drug toxicity compared to the first scenario. Increased toxicity level will allow using more drugs even in the initial periods of the treatment as seen in Fig. 4.6a. Eventually, it results in decreasing the number of tumor cell populations at the end of the treatment drastically shown in Fig. 4.6b. Although it appears rational considering our objective to minimize tumor cell population at the end of the treatment, we do not know the clinical effects of this increased toxicity level in a patient's general health.

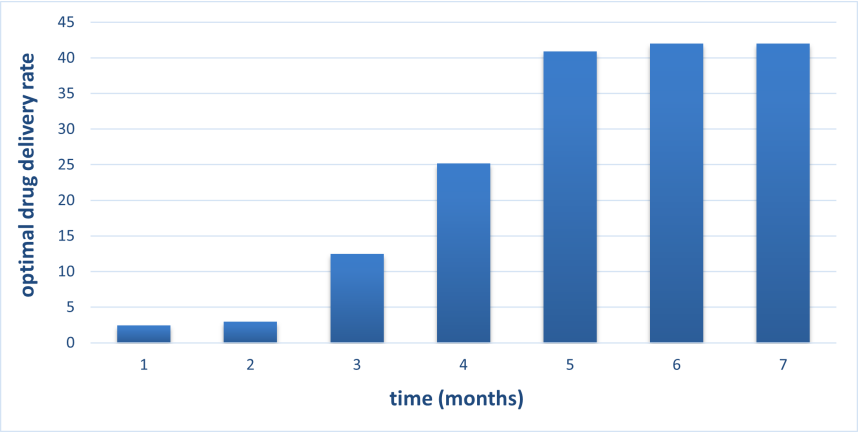

(a)

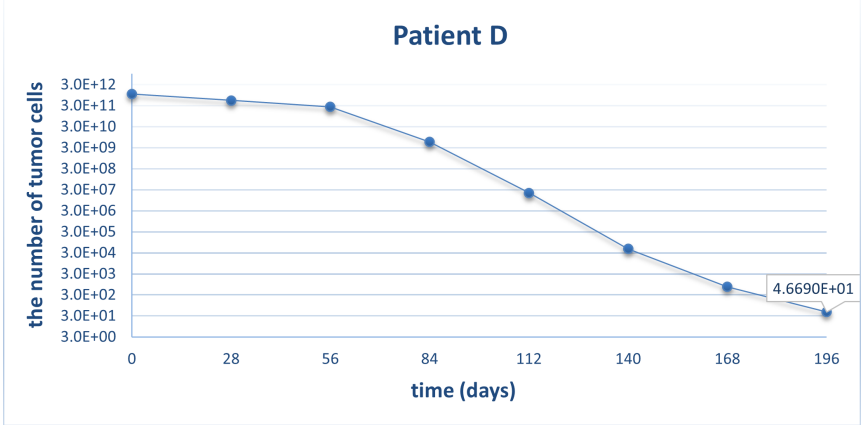

(b)

Figure 4.6: a) **Optimal Drug Delivery Rate and** b) **Tumor Size Change when** $v_{cum} = 5.6 * 10^3[D]days$**.**

The above figures should be taken as an example of the real chemotherapy treatment schedule rather than the universal result, since the shape of the curve depends on method-specific parameter values and the type and size of the scheduling problem. That means we might obtain different results with the different configurations on the system.

4.4 Conclusions

In this chapter, we present a nonlinear optimization problem to study the effects of the proposed tumor kinetic model in Chapter 3. The major focus of this chapter was to provide an extension to the tumor kinetic function for identifying the optimal chemotherapy schedule in the presence of drug toxicity and tumor size reduction constraints. We construct a drug delivery rate schedule by utilizing an *OCM* for cancer chemotherapy with a single agent to minimize the final tumor size.

The proposed system balances out delivering the drug dose and minimizing tumor population over the entire treatment time. Although a large amount of drug can be given to minimize the number of tumor cells initially, the drug is delivered slowly to ensure 50% reduction in each treatment point. In our study, even though our main target is to reduce the final tumor size at the end of the treatment (which is quite important), focusing solely on this target may not be realistic. Therefore, this study can be extended as a multi-objective optimization problem. For example, maximizing immune/normal cells or minimizing drug usage can be added to the proposed model.

By employing *OCM*, we show the defined tumor kinetic model minimizes the number of tumor cells along with other constraints in the design of an efficient drug schedule. Hence, we show that the most effective way to reduce the number of tumor cells is to keep the initial drug administration minimal, and then follow it by high-intensity therapy towards the end of the treatment cycles. This is because of Michaelis-Menten's kinetics. We know that when the number of tumor cells is high, it is easy to kill them initially. However, if we give the bulk of the drug from the beginning of the treatment, then it is going to be hard to destroy the tumor cells at the end of the treatment, since the number of tumor cells is low, and that means they will grow faster. Therefore, in our problem, the drug delivery rate is increasing gradually by satisfying the toxicity and reduction constraints. Similar results were proposed in the literature. Martin et al. [1992a] proposed the same scheduling plan as starting low dose and increased the dose towards to end. Moreover, Dua et al. [2008] presented the same result for the frequency of the drug by holding the dose the same. Thus, knowing the theoretically optimal solutions also becomes of practical interest. Although our findings are not used as a common practice to cure the cancer, there are

studies to challenge the conventional therapies (maximum tolerated dose [Benzekry and Hahnfeldt, 2013], metronomic therapy [Simsek et al., 2019], and adaptive therapy [Gatenby et al., 2009]) such as varying dose [Foo et al., 2012], and upfront low [He et al., 2020] or increasing dose [Gray et al., 2019] chemotherapy with the combination of immunotherapy.

Another limitation to discuss here is that if we rerun the model with a cancer size equal to the final tumor size of the optimal solution, and apply no cancer drug, the tumor may grow to a larger size given enough time. This may sound problematic about the appropriateness of the optimal solution as an endpoint of the treatment. However, the final tumor size we found in the optimal solution indicates similar final tumor sizes with the existing OCMs in the literature [Martin, 1992]. Also, the optimized model solution is a million times smaller than the initial size. Therefore, it is reasonable to assume that a tumor reduced to the size in the optimal solution would not grow back in reality. Nevertheless, we can add a constraint that $N(T) < k$, where k is a very small number. However, given enough toxicity tolerance limits, this constraint could be unnecessary or redundant.

To conclude, we demonstrate that with the proposed kinetic model, the deterministic optimization model can be solved more resource-efficiently and mitigate the computational time in larger instances. To verify the correctness of the proposed model, the algorithm of Brute-Force and its modified versions have been developed, and the results have demonstrated the correctness of the proposed model. Sensitivity analyses have also been conducted on drug toxicity and tumor reduction constraint limits to analyze their impacts on the solution. Since the classical systems are presented with hard constraints, we continue with the tradition and do not consider room for the violation of these constraints.

Chapter 5

Nonlinear Stochastic Optimization (NSO) Model for Chemotherapy Treatment Planning

In this chapter, we develop a stochastic optimization model for optimal drug delivery rate in cancer chemotherapy treatment. We provide an extension to the deterministic growth case in which stochastic cancer staging has been integrated into the controlled tumor growth mechanism discussed in Chapter 4. We address the problem of cancer staging at any given treatment time under a chemotherapy treatment schedule. To examine the problem, we study a sequential stochastic scheduling problem that allocates drug rates with deterministic values to sequentially upcoming treatment time points so that it can minimize the expected total number of tumor populations. Then, we develop the *Nonlinear Stochastic Optimization Model (NSO)* by considering the probability of stage jump as a function of decision variables. Moreover, we develop a Brute-Force search algorithm to verify the solution of the model. The main purpose of this chapter is to provide insight into the effect of stochastic cancer staging on chemotherapy design.

5.1 Problem Description and Formulation

The growth of metastatic tumor cells in internal organs is usually too tiny to be detected while the primary tumor is being treated [Liotta, 1984]. Since the growth of tumor cells is random, deterministic models may not capture all the necessary dynamics to identify

the decision under the presence of uncertainty while designing the optimal chemotherapy treatment plan. In our defined model, we consider randomness for the growth of tumor cells in an upper stage during each treatment time. Once cancer probabilistically moves to an upper stage, tumor growth increases at a faster rate since tumors far away from their origin frequently multiply and increase in number with time [Baba and Câtoi, 2007].

Fig. 5.1 demonstrates the mortality percentage for bladder cancer stages. As can be seen in the table, a patient in the metastasis stage has a higher risk to die. To reduce this risk rate, we propose an alternative mechanism by considering the probability of cancer stage jump during the chemotherapy treatment. If this probability is taken into account earlier, cancer stage jump to the higher staging can be prevented, so that the mortality rate can be mitigated with this proposed mechanism. However, considering this stage jump while designing a chemotherapy treatment turns the problem into a more complex dynamic structure and increases the complexity of the solution domain. To tackle the problem, we initially implement the effect of probabilistic staging in the model for a given policy, to prove the necessity of this implementation for drug delivery design while treating cancer patients. Afterwards, a new stochastic optimization model is presented later in the chapter.

Clinical State (CS)	TNM Staging	Incidence	Prevalence	Annual Mortality Hazard (%)
Localized	Stage 0a	36,837	397,461	6.8
Localized in situ	Stage 0is	3,856	26,505	6.3
Locally Advanced	Stage I	18,942	161,214	7.6
MIBC	Stage II/III	13,744	97,712	12.2
mUC	Stage IV	7,079	36,495	41.5
Total	---	**80,458**	**719,387**	**9.4**

Note: MIBC-muscle invasive bladder cancer; TNM: Tumor, Nodes, Metastasis

Figure 5.1: **The Mortality Percentage for Bladder Cancer Stages [Fleming et al., 2020].**

5.2 Methodology

We introduce a new mathematical model for a chemotherapy treatment plan that considers stage jump probability. When a patient arrives to get treated, the proposed stochastic optimization model considers replanning the drug delivery rate schedule for the rest of the treatment, as if a stage jump might occur any time after the first admission. With this approach, we present a trajectory for each treatment time. Table 5.1 provides notations that are used throughout this chapter.

Table 5.1: List of Notations

Notation	Description
$i \in \mathbb{I} \equiv \{1, .., n\}$	The index of treatment time point
$j \in \mathbb{J} \equiv \{1, .., n\}$	The index of stage jump probabilities at the corresponding time intervals during the treatment
n	The number of treatment times
S_R, S_M	The possible stage for a tumor: regional or metastases stages, respectively
t_i	The treatment time
$N^j(t_i)$	The number of tumor sizes in each time point i, under j different scenarios
$E[N(t_i)]$	Expected tumor size at time point i
p_i	probability of stage jump at each time point i
ps_j	Probability of j different scenarios
μ_s	The weight of the probability p_i
T	Final treatment point

The main assumptions of the proposed model are listed in the following:

Assumption 5.2.1 *The drug effectiveness parameter k_1 is constant for different stages of cancer.*

Assumption 5.2.2 *Only a one-time stage jump is taken into account throughout the treatment horizon, i.e. the tumor either jumps from a regional stage S_R to a metastases stage S_M or stays in the regional stage, S_R.*

Assumption 5.2.3 $p_0 = 0$, *which means we neglect the probability of the stage jump at t_0.*

Assumption 5.2.4 *Regardless of which cancer stage a patient is in, the tumor follows the Gompertzian type of growth function.*

Assumption 5.2.5 *We omit the probability of stage jumps at t_n.*

Cancer Staging and Probabilistic Model for A Stage Jump

We divide the total treatment duration into n treatment cycles, as in Section 4.2, and we take the decision variable $u(t)$ as a piecewise function in Eq. (4.7). In each time epoch $t_i, i \in 0, 1, ..., n$, the treatment plan is specified as $\sigma_1, ..., \sigma_n$. At the end of each epoch, we assume the cancer stage changes based on the size of a tumor. The probability that the tumor stage changes in epoch i, under the chemotherapy treatment plan, is equal to p_i given as follows:

$$p_i = \mu_s \left(\frac{\frac{N(t_{i-1})+N(t_i)}{2}}{\theta} \right), \quad i = 1, 2, ..., n \tag{5.1}$$

where $N(t_i)$ represents tumor population at given epoch t_i, θ is maximum tumor size in any tumor stage. μ_s is the linear weight of each cancer cell to the stage transition. With p_i, n scenarios are defined as the tumor might jump to S_M from S_R at t_i. That means the sample space of this problem when $n = 7$ is $p_1, ..., p_7$.

At this point, we can also define the probability of these scenarios occurring as $ps_j, j = 1, ..., n$ that we explicitly require in the later sections. For instance, ps_3 means the tumor has not jumped to an upper stage at t_1 or t_2 but at t_3. In the following, we present the likelihood of stage transition throughout the treatment horizon:

$$ps_j = \begin{cases} p_j \prod_{k=0}^{j-1} (1 - p_k), & j < n \\ \prod_{k=0}^{j-1} (1 - p_k), & j = n \end{cases} \tag{5.2}$$

i.e. when $n = 7$

$$
\begin{aligned}
ps_1 &= p_1 \\
ps_2 &= p_2(1-p_1) \\
ps_3 &= p_3(1-p_2)(1-p_1) \\
ps_4 &= p_4(1-p_3)(1-p_2)(1-p_1) \\
ps_5 &= p_5(1-p_4)(1-p_3)(1-p_2)(1-p_1) \\
ps_6 &= p_6(1-p_5)(1-p_4)(1-p_3)(1-p_2)(1-p_1) \\
ps_7 &= (1-p_6)(1-p_5)(1-p_4)(1-p_3)(1-p_2)(1-p_1)
\end{aligned}
$$

The cumulative probability of different scenarios is:

$$ps_j = \sum_{j=1}^{n} = 1$$

Calculating Expected Tumor Size

Using the probability of stage jump at each point and the corresponding tumor size, we calculate the expected tumor size at each treatment point.

$$E[N(t_i)] = \sum_{j=0}^{i-1} \left[p_j \prod_{k=1}^{j-1} (1-p_k) \right] N^j(t_i) + \left[\prod_{k=0}^{i-1} (1-p_k) \right] N^i(t_i), i = 1, ..., n \tag{5.3}$$

where $N^j(t_i)$ is tumor size at time i when stage jump occurs at time j. This equation indicates that the stage jump either occurs at any time until that treatment point $t_{i-1}, i = 1, 2, ..., n$, or there will be no jump until t_i. Appendix D provides an explicit form of Eq. (5.3). Finally, Eq. (5.4) is defined to provide the value of the growth rate for regional (λ_R) and metastases (λ_M) stages of cancer, respectively.

$$\overline{\lambda} = \begin{cases} \lambda_R & j \leq i \\ \lambda_M & otherwise \end{cases} \tag{5.4}$$

5.2.1 Myopic Policy Based on Observed Cancer Stage

In this section, the outline of the stochastic solution approaches is presented. To calculate the expected cancer cell population at the end of the treatment under the probabilistic staging, we first employ a myopic policy. The myopic policy is the most elementary policy, i.e. that considers it a single criterion. The idea behind this approach optimizes the average immediate reward/cost, now; however, it does not consider any stochastic feature of decisions in the future [Powell, 2007]. For the design of a treatment scheduling, clinicians produce treatment plans based on the current stage of a cancer. In this study, we only consider the probability of stage jump at each treatment time, and do not include any other probabilistic feature for the rest of the treatment times. This policy reflects the observation based policy.

Policy I - Sequential Optimization through Observation

In this approach, we sequentially consider the probability of stage jump at each time t_i. Until the jump point, the optimal drug delivery rate(s) calculated in Chapter 4 is taken. We assume that the tumor might jump to an upper stage at t_i and grow faster. Then, the sets of new optimal drug delivery rates are calculated based on the newly updated λ. For instance, a cancer patient at the regional stage, S_R, with a tumor growth rate λ_R has taken the chemotherapy at t_0. Therefore, we take σ_1 from the OCM and calculate the rest of the decision variables considering that stochastic jump might happen at t_1. If the tumor goes to an upper stage, S_M (i.e. cancer being metastasis), at t_1, the rest of the control variables $[\sigma_2, ..., \sigma_n]$ are solved using [Eq. (4.9) – Eq. (4.13)] with a given σ_1 and λ_M. Then, until the end of the final treatment point, we solve the problem iteratively considering the possibility of stage jump in each treatment period. An algorithm for this approach is presented in Algorithm 2.

Fig. 5.2 shows a visual representation of the algorithm. This diagram illustrates how sequential optimization works under the given optimal policy. t_i represents treatment time points. λ_R and λ_M present the tumor growth rates for regional and metastases stages, respectively. The values of $\sigma_i, i = 1, 2, ..., n$, come from [Eq. (4.9) – Eq. (4.13)] and superscripts $(1, 2, ..., n-1)$ of σ_i indicate at which time point the tumor stage jump happens.

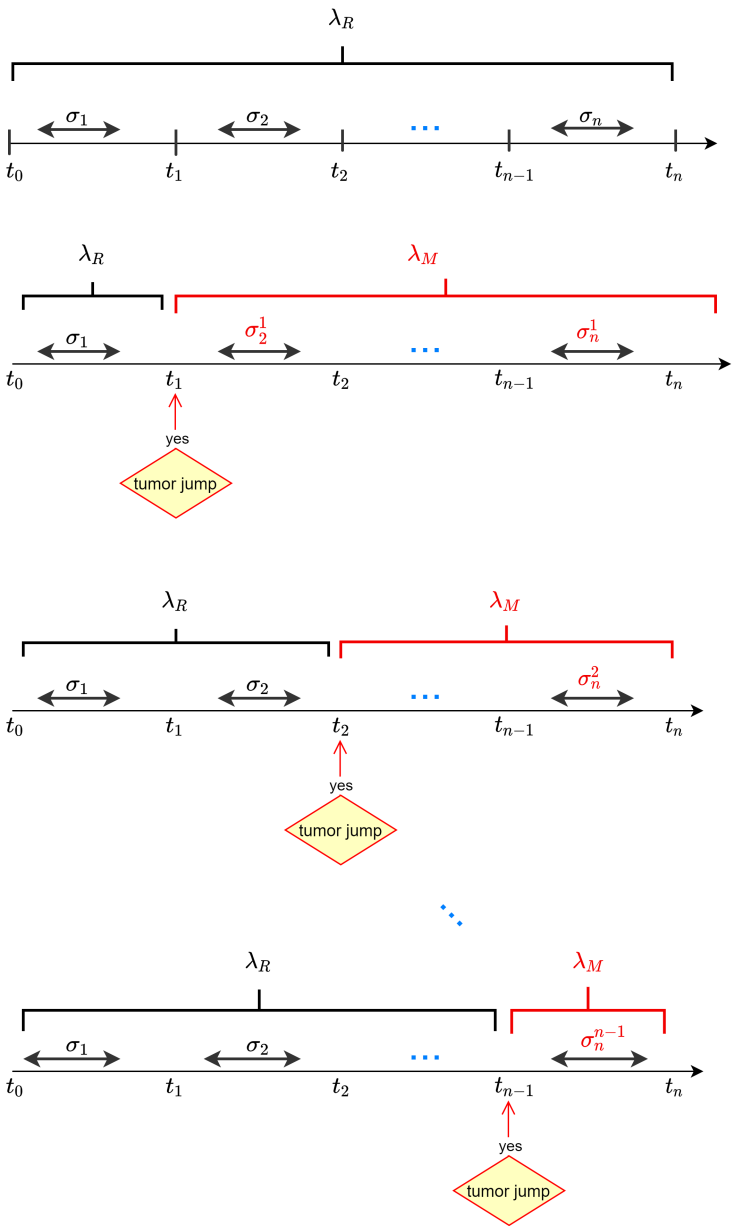

Figure 5.2: **A Visual Representation of Policy I.**

ALGORITHM 2: Stage Jump through Observation

Data: $\sigma_i, i = 1, ..., n$, decision variables
$\lambda \in \{\lambda_R, \lambda_M\}$
$\mathbb{S} \in \{S_R, S_M\}$
Result: new drug delivery schedule

if $\mathbb{S} = S_M$ *at any time* t **then**
  change $\lambda_M \leftarrow \lambda_R$
  take $[\sigma_1, ..., \sigma_{i-1}]$ from the solution of [Eq. (4.9) – Eq. (4.13)]
  compute the rest of decision variable: $[\sigma_i, \sigma_{i+1}, ..., \sigma_n]$
else
  do nothing

Policy II - Sequential Optimization by Accepting Stage Progression at the Beginning of the Treatment

This approach is the generalization of the previous approach. Similar to Section 5.2.1, the probability of a stage jump is sequentially taken into account. However, we conduct the optimization while considering the stage jump ahead of time. That is before initializing the treatment, the stage jump is taken into account. For example, if a tumor jumps at t_1, we solve the problem [Eq. (4.9) – Eq. (4.13)] by taking the growth rate as λ_R up to t_1, and as λ_M after t_1, to find optimal drug delivery rates considering the probability of a stage jump at t_1. Then, we follow the same steps for each treatment point. This approach is summarized in Algorithm 3.

ALGORITHM 3: Stage Jump Ahead of Time

Data: $\sigma_i, i = 1, ..., n$, decision variables
$\lambda \in \{\lambda_R, \lambda_M\}$
$\mathbb{S} \in \{S_R, S_M\}$
Result: new drug delivery schedule

if $\mathbb{S} = S_R$ *at* $t = t_i, i = 1, ..., n$ // consider no jump yet
then
  calculate $[\sigma_1,...,\sigma_k], k = 1, ..., i \longleftarrow (\lambda = \lambda_R)$ // solving [Eq. (4.9)-Eq. (4.13)] for λ_R
else
  // consider the jump at the time i
  calculate $[\sigma_{k+1}, ..., \sigma_n], k = i, ..., n \longleftarrow (\lambda = \lambda_M)$ // solving [Eq. (4.9)-Eq. (4.13)] for λ_M

Fig. 5.3 shows a visual representation of the algorithm. In constrast to Policy I, we solve the model of [Eq. (4.9) – Eq. (4.13)] for λ_R up to the jump point and for λ_M after the jump point. Therefore, the superscripts $(1, 2, ..., n-1)$ of σ_i indicate at which time point the tumor stage jump happens. The optimal drug delivery rate can thus be calculated with λ_R up to the jump point and λ_M after the jump point. In plain language, the optimal drug delivery rates are calculated with the probability of tumor jump considered ahead of time.

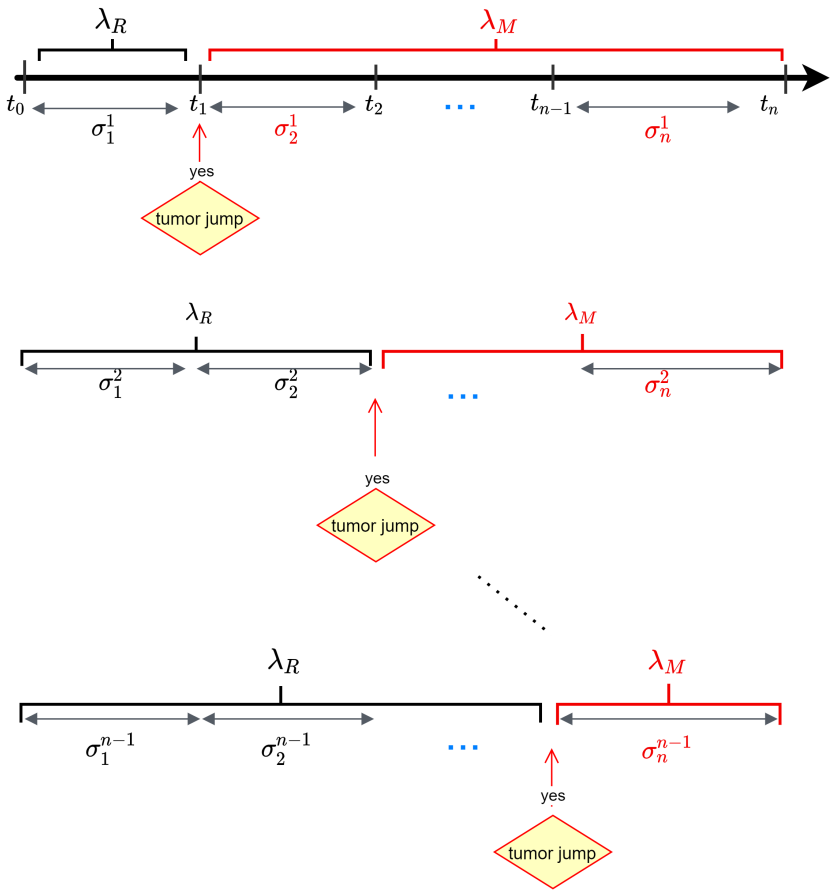

Figure 5.3: **A Visual Representation of Policy II.**

With these two myopic approaches, we aim to show the effect of considering tumor stage jump in the design of chemotherapy-treatment scheduling.

5.2.2 Nonlinear Stochastic Optimization Model

In this section, we present a *Nonlinear Stochastic Optimization (NSO)* model for different scenarios of the stage jump during the cancer chemotherapy treatment. Unlike the two aforementioned myopic approaches, we now formulate the optimization problem as a function of drug delivery rate variables that are stage-dependent by incorporating the tumor jump probabilities.

The proposed *NSO* is as follows:

$$\underset{\sigma_i, i=1,\ldots,n}{\text{minimize}} \quad J[\vec{\sigma}] = E[N(T)] \tag{5.5}$$

$$\text{subject to} \quad \frac{dN^j(t)}{dt} = -\bar{\lambda} N^j(t) ln\left[\frac{N^j(t)}{\theta}\right] - \frac{k_1 \sigma_i}{\gamma \Delta t + \sigma_i} N^j(t), \tag{5.6}$$

$$N(0) = N_0^j, \qquad j = 0, 1, ..., n \tag{5.7}$$

$$E[N(\xi_{l+1})] \leq \eta E[N(\xi_l)], \quad l = 0, 1, 2, \cdots, M \tag{5.8}$$

$$0 \leq v(t) \leq v_{max}, \qquad \forall t \in [0, T] \tag{5.9}$$

$$\int_0^T v(t)dt \leq v_{cum}, \tag{5.10}$$

$\vec{\sigma}$, defined as in Eq. (4.7), is the decision variable and $N(t), \forall t \in [0, T]$, is a state variable. Due to stochastic staging, $N(t_i)$ is now a stochastic process, which makes solution of the above problem quite challenging. We present the *NSO* problem with the objective of minimizing the expected tumor population Eq. (5.5) at the end of chemotherapy treatment, subject to the tumor kinetic equation Eq. (5.6) which incorporates the stochastic staging, and the other constraints: the maximum toxicity Eq. (5.9) and the cumulative toxicity Eq. (5.10) constraints. The tumor burden constraint, Eq. (5.8), is given as an expected value since the probability of stage jump is considered during the treatment checkpoints. We observe that, whether for static or dynamic drug delivery control, the optimal policy for the above problem can be derived (optimally and/or approximately) for special cases of the problem, where the number of possible stage change histories are tractable, e.g. when there are only two stages.

5.3 Results and Discussions

This section summarizes the findings and contributions made by evaluating the effect of probabilistic stage jumps on the drug delivery schedule for chemotherapy treatment. We then compare the solution of policies and the stochastic optimization model to their deterministic counterparts, in terms of expected final tumor sizes and probability of having no jump at the end of the treatment.

Previous research showed that the tumor growth rate (λ) can be increased by the range of $[1, 8]$ fold [Frazier et al., 2000] after the jump of the tumor has been assumed. Therefore, the tumor growth rate at the metastases stages has been arbitrarily set to 2.25 fold of the tumor growth rate at the regional stage. That means the tumor growth rate for the metastases stage is set to $\lambda_M = 0.03375$ when $\lambda_R = 0.015$ for the regional stage for all the proposed models in this chapter. The rest of the parameters' values are the same as presented in the earlier chapters.

5.3.1 Drug Delivery Rate Schedules and Tumor Size Changes

5.3.1.1 Policy I and Policy II

Fig. 5.4a and Fig. 5.5a show the optimal schedule of seven different scenarios ($n = 7$) depending on where the probabilistic stage jump occurs based on Policy I and Policy II, respectively. These figures present seven different treatment plans due to the seven different scenarios that are focused on minimizing the final tumor size. On the graphs, the "no jump" column shows the deterministic-problem solution and the rest of the columns represent the situation where stage jump is involved in design of the treatment. The column "jump at t_6" is the same as in the deterministic design (that has not considered the stage jump) in Fig. 5.4a since the delivery schedule was taken from the deterministic model up to point t_6, as indicated in describing the policy. Recall that drug delivery rates at the treatment times have been assigned based on the limitations of drug toxicity and tumor reduction before the jump happens. Overall, the optimal schedules based on these two policies are the same, except for the scenarios that the probability of stage jump at t_5 and t_6 after the first 4 months of the treatment. Relevantly, Fig. 5.4b and Fig. 5.5b demonstrate the corresponding number of tumor populations based on the obtained optimal drug delivery rates in Fig. 5.4a and Fig. 5.5a, respectively.

To compare the results of the policies, the expected final tumor size is calculated based on Eq. (5.3) by utilizing Eq. (5.1). Table 5.2 clearly shows that the same results are achieved with both policies for the current parameter settings.

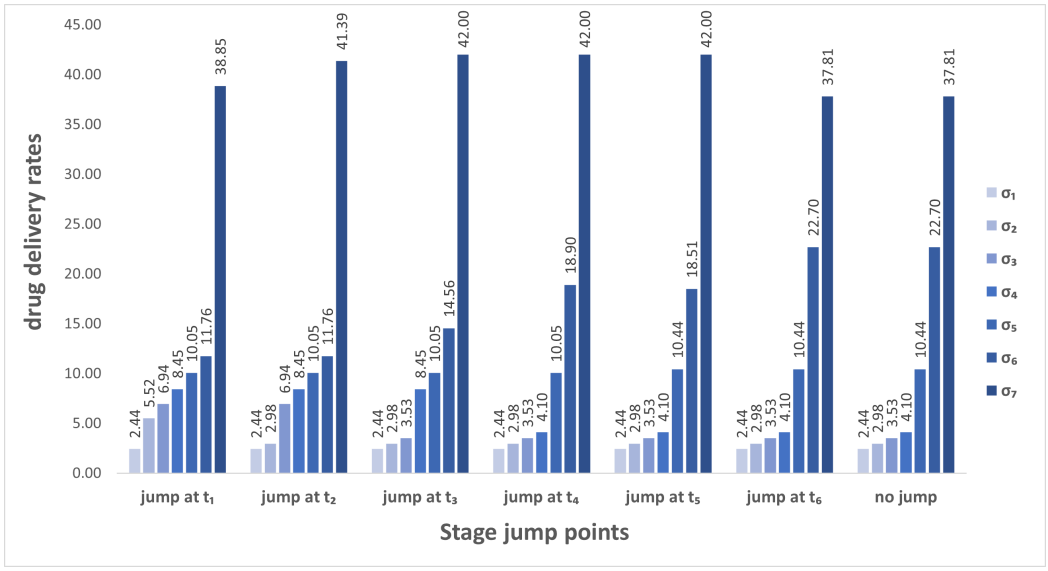

(a)

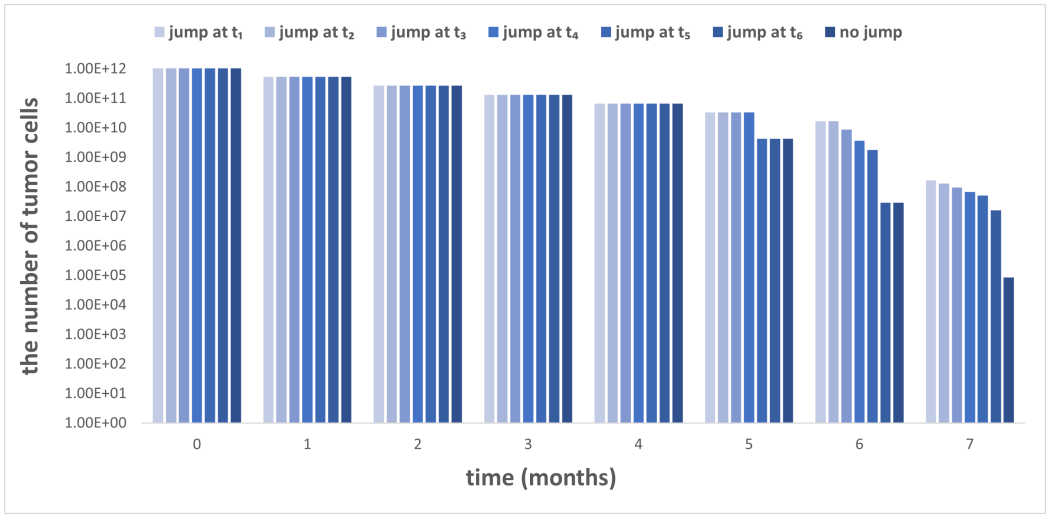

(b)

Figure 5.4: a) **Drug Delivery Rate Schedules and** b) **Tumor Size Change for Policy I.**

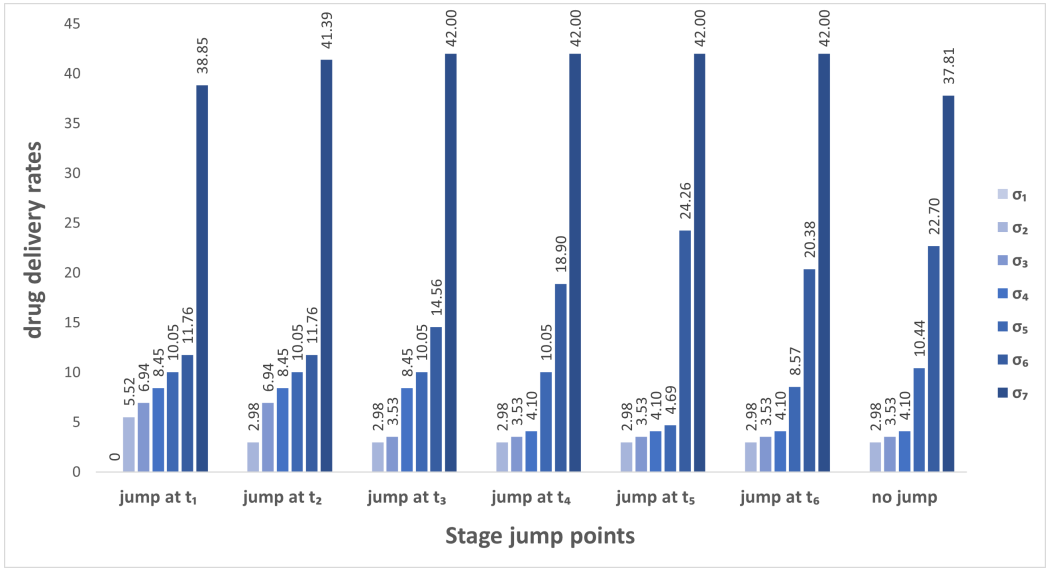

(a)

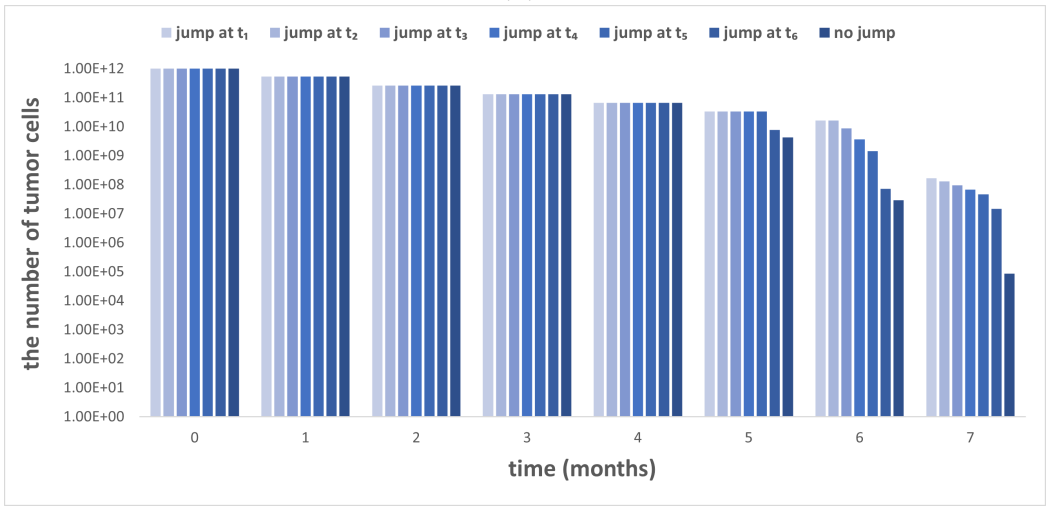

(b)

Figure 5.5: a) **Drug Delivery Rate Schedules and** b) **Tumor Size Change for Policy II.**

Table 5.2: Comparison of Solution Approaches

	Expected Final Tumor Size
Policy I	$4.9171E+07$
Policy II	$4.9152E+07$
Stochastic Optimization	$2.6174E+07$

5.3.1.2 Stochastic Optimization Model

Fig. 5.6a and Fig. 5.6b show the optimal drug delivery schedule and the change in the expected tumor size at each time point, respectively. The expected tumor size has been decreased by 53% compared to the proposed sequential optimization models as seen in Table 5.2. Moreover, in contrast to the optimal solution of the deterministic model discussed in the previous chapter, the optimal solution of the stochastic optimization model has a different structure. That is because the optimal drug delivery rate for $[t_0, t_1]$ decreases the tumor size at t_1 a more than 50%, which is the limit of the problem. This happens since the probability of a stage jump after the first treatment is higher than at the subsequent treatment times, up to the final treatment point.

5.3.2 Comparison of Stage Transition Probabilities

We compared the final expected tumor size for the sequential optimization models and the stochastic optimization model. We reported in Table 5.2 that the stochastic optimization model yields a better result. Additionally, the stage transition probability is another important characteristic of the models for comparison purpose. In sequential optimization models, the probability of a stage jump at particular time points is calculated by utilizing the number of tumor cells obtained from the deterministic model [Eq. (4.1) - Eq. (4.5)]; while the probability of stage jump at other time points is calculated by solving the stochastic optimization model [Eq. (5.5) - Eq. (5.10)].

Table 5.3 presents the likelihood that a tumor jump occurs at the specific time point for both sequential and stochastic optimization models. For instance, the probability of a tumor jump at t_1 is 20% and 18% in both methods, respectively; while the probability of having no tumor jump during treatment is 65% and 74% when $n = 7$.

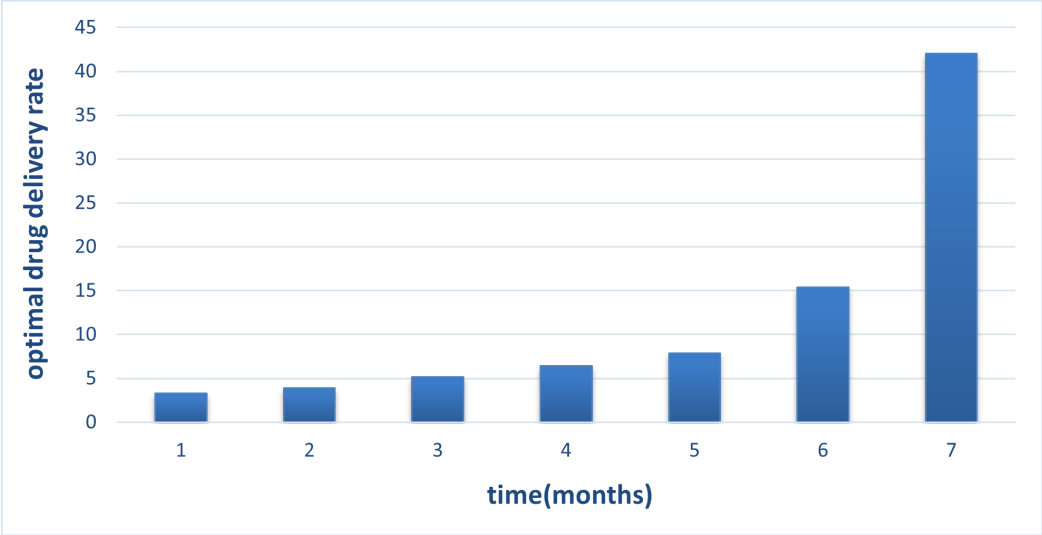

(a)

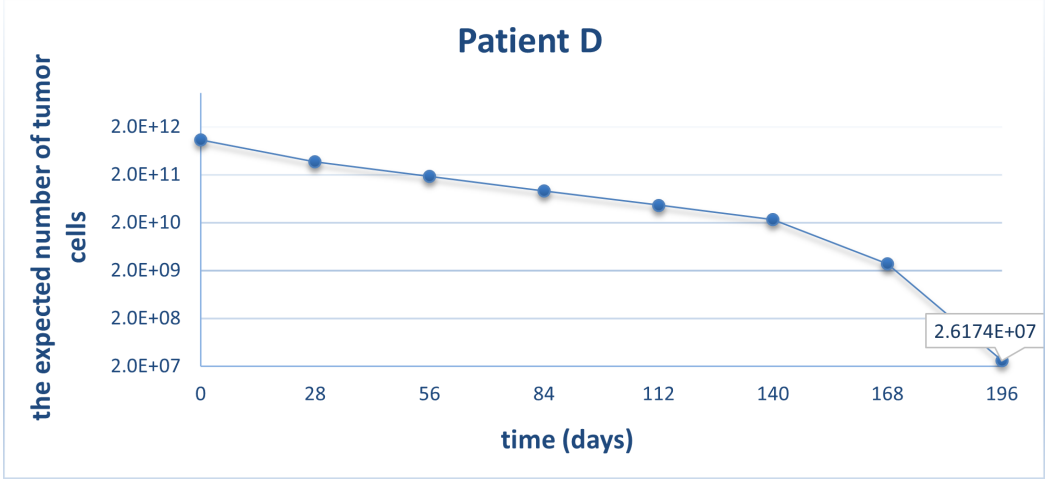

(b)

Figure 5.6: a) **Optimal Drug Delivery Rate and** b) **Tumor Size Change for NSO.**

Table 5.3: Calculation of Transition Probabilities from S_R to S_M

Jump Point	Policy I & Policy II	Stochastic Optimization
ps_1	0.2022	0.1815
ps_2	0.0806	0.0528
ps_3	0.0362	0.0180
ps_4	0.0172	0.0056
ps_5	0.0059	0.0016
ps_6	0.0004	0.0003
ps_7	0.6574	0.7402

5.3.3 Expected Drug Delivery Rate

We now consider another way to improve the results for Policy I and Policy II. Since we generate seven different schedules for seven different scenarios for both policies, the expected drug delivery rates for all the scenarios (e.g. probability of stage jump at $t_i, i = 1, ...n,$) will be sufficient and logical to compare with the other proposed models. First of all, to find the average/expected drug delivery rate for each time interval, the probability of stage jump at each treatment point should be calculated by using Eq. (5.1). Here, N_i is taken from the deterministic model results. Then, $ps_j, j = 1, ..., n$, the likelihood of stage jump scenarios at each time, is found by utilizing $p_i, i = 1, ..., n$. Finally, the expected drug delivery rates are calculated by the multiplication of the drug delivery rate at each time with the likelihood of each stage jump as in the following:

$$\sigma_i = \sum_{j=1}^{n} ps_j \sigma_i^j, \qquad \forall i \in 1, ..., n, \quad n \in \mathbb{R} \tag{5.11}$$

where the superscripts show the tumor stage jump point.

Table 5.4 presents the expected drug delivery doses, while Table 5.5 shows the probability of stage jump scenarios at each time point for all proposed models. Moreover, the number of iterations presents the expected drug delivery rate based on the different probabilities of stage jump. For example, 1.0 under Policy I indicates that the average drug dose was calculated by $ps_j, j = 1, ..., n$ in Table 5.3 by using Eq. (5.11) and σ_i^j from the seven optimal drug dose sets presented in the previous chapter. By using this new expected drug delivery rate set, we calculated the set of new-stage jump probabilities $(ps_j, j = 1, ..., n)$ presented in Table 5.5. Then, the drug delivery rate in 1.1 is obtained based on these stage

probabilities. The same logic was applied while finding the expected drug delivery rate sets based on the different stage jump scenarios for Policy II as well.

Table 5.4: Expected Drug Delivery Rates for Policy I & Policy II and Optimal Drug Delivery Doses for Deterministic & Stochastic Models.

		Deterministic Model	Policy I			Policy II			Stochastic Model
The Number of Iterations			**1.0**	**1.1**	**1.2**	**2.0**	**2.1**	**2.2**	
Drug Delivery Rates at the Treatment Points	σ_1	2.4353	2.4352	2.4353	2.4353	2.4352	2.4353	2.4353	3.2759
	σ_2	2.9777	3.4913	3.4913	3.4913	3.4913	3.4913	3.4913	3.9191
	σ_3	3.5337	4.4964	4.4784	4.4784	4.4965	4.4785	4.4785	5.1306
	σ_4	4.1035	5.4890	5.4241	5.4243	5.4890	5.4242	5.4244	6.4349
	σ_5	10.4411	10.3096	10.3186	10.3185	10.2746	10.3035	10.3030	7.8550
	σ_6	22.6954	19.2176	19.3988	19.3977	19.2505	19.4125	19.4117	15.3845
	σ_7	37.8133	38.5600	38.4528	38.4539	38.5625	38.4548	38.4558	42.0000

It is important to highlight that the results for Policy I and Policy II in Table 5.4 have been obtained without solving the optimization problems, i.e. the solution sets have no constraint limits. Namely, these results are obtained by utilizing Eq. (5.11).

The results of these two myopic policies are then compared with the deterministic model under the stochastic environment in Table 5.5. That means the expected final tumor size is calculated based on the optimal drug schedule obtained by the deterministic model. Therefore, the probability of having no stage jumps based on the drug delivery rate schedules for Policy I & Policy II (68%), and Stochastic optimization (74%) are substantially better than the deterministic model's solution (65%). These results underline the importance of considering the probability of stage jump while designing the treatment. Moreover, the final expected tumor size of the stochastic model is much better than for the deterministic model, and indicates the necessity of involving the probability of stage jump.

Table 5.5: Probability of Stage Jumps for All Models

		Deterministic Model	Policy I			Policy II			Stochastic Model
The Number of Iterations			**p1.0**	**p1.1**	**p1.2**	**p2.0**	**p2.1**	**p2.2**	
Probability of Scenarios	ps_1	0.2022	0.2022	0.2022	0.2022	0.2022	0.2022	0.2022	0.1815
	ps_2	0.0806	0.0753	0.0753	0.0753	0.0753	0.0753	0.0753	0.0528
	ps_3	0.0362	0.0266	0.0267	0.0267	0.0266	0.0267	0.0267	0.0180
	ps_4	0.0172	0.0092	0.0093	0.0093	0.0092	0.0093	0.0093	0.0056
	ps_5	0.0059	0.0025	0.0026	0.0026	0.0025	0.0026	0.0026	0.0016
	ps_6	0.0004	0.0002	0.0002	0.0002	0.0002	0.0002	0.0002	0.0003
	ps_7	0.6574	0.6840	0.6837	0.6837	0.6840	0.6837	0.6837	0.7402
Expected Tumor Size		2.9668E+07	3.1238E+07	3.1240E+07	3.1239E+07	3.1197E+07	3.1221E+07	3.1220E+07	2.6174E+07

5.3.4 Verification of the Result with Brute-Force Search for NSO

Algorithm 4 is proposed for enumerating all control variables by a given set of values as in Algorithm 1. Therefore, we omit the input and output parameters of the algorithm and start to demonstrate how the iteration work differently than the previous Brute-Force search in *OCM* by highlighting with the red lines in the algorithm below.

5.3.4.1 Narrowing Grid Brute-Force Search for NSO

As was explained in the previous chapter, this modified Brute-Force approach requires a defined range for decision variables, $\sigma_i, i = 1, ..., n$, based on the previous solution sets so that we can conduct the faster iterations. We test the results for various step size and present the outcomes in Table 5.7. When the step size decreases, the optimality gap compared to the original Brute-Force search lowers to 0.00015% (which is ignorable), and run time decreases notably with this approach. It is observed that run time depends on the chosen decision-variable range obtained by the previous iteration.

Fig. 5.7 presents the convergence of the algorithm to the optimal solution that has been obtained by *Maple*.

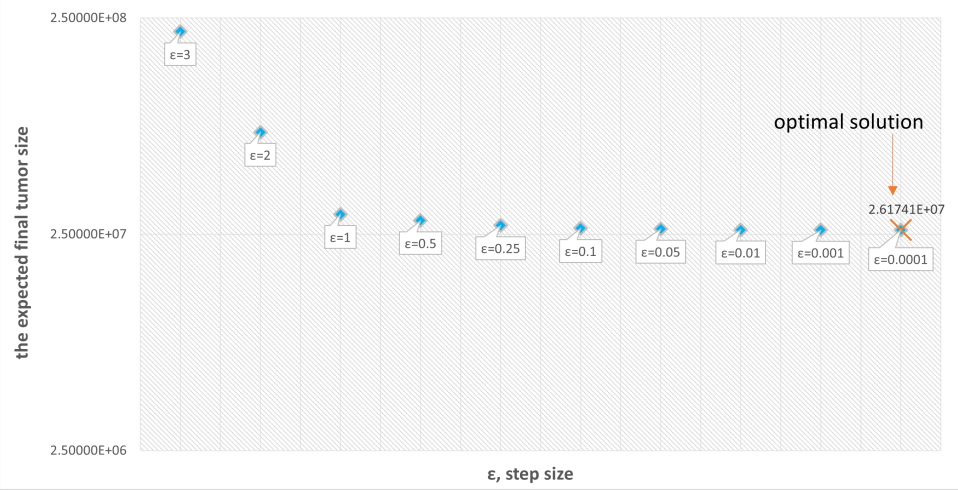

Figure 5.7: **The Convergence of Modified Brute-Force Search to the NSO model.**

ALGORITHM 4: Improvised Brute-Force Search.

```
finaltumor ← E[N_0]
                                                        /* starts the iteration */
for σ_i ← lower value to upper value by ϵ do
    while σ_i ≤ v_max do
        totalv_cum ← Σ_{i=1}^{n} σ_i                    // defines the total vcum
        if totalv_cum = v_cum                           // checks the vcum limit
        then
            for i ← 1 to n do
                for j ← 1 to n do
                    if j ≤ i                            // decides the tumor growth rate
                    then
                        λ_R ← λ̄
                    else
                        λ_M ← λ̄
                    calculate y_i^j in Eq. (4.10)
                    find N_i^j in Eq. (4.8)             // nondimensional transformation
                calculate p_i in Eq. (5.1)              // jump probability
            for i ← 1 to n do
                calculate E[N(t_i)] in Eq. (5.3)
            if E[N_{i+1}] ≤ ηE[N_i]                     // checks tumor reduction limit
            then
                if E[N_n] < finaltumor                  // checks the optimality
                then
                    finaltumor ← E[N_n]
                    σ_i^*                               // gives the best solution
                    feasible ← feasible + 1
                else
                    finaltumor ← finaltumor
                    σ_i                                 // gives the feasible solution
                    feasible ← feasible + 1
            else
                infeasible ← infeasible + 1
        else
            infeasible ← infeasible+1                   // completes the iteration when σ_i = v_max
```

Table 5.6: Results for Brute-Force Search.

Step Size (ϵ)	$E[N(T)]$	**Run Time** (min)	**The Number of Calculations**
14	-	0.048	0
7	-	0.067	462
6	-	0.1	1709
3	$2.16E+08$	8.09	283998
2	$7.41E+07$	131	4225068
1	$3.11E+07$	11535 (8 days)	345972432

Table 5.7: Accelerated Performance Measure in Algorithm 4.

Step Size (ϵ)	$E[N(T)]$	**Run Time** (min)	**The Number of Calculations**
1	$3.09E+07$	0.24	13097
0.05	$2.64E+07$	1.16	66744
0.025	$2.62E+07$	6.49	305409
0.01	$2.62E+07$	24.25	1208976
0.0001	$2.6174E+07$	32.11	358839

5.3.5 Increased Number of Control Variables

In contrast to the *OCM*, we do not analyze the continuous tumor size reduction while increasing the decision variables in *NSO*. The reason is that considering the probability of stage jump in small increments, rather than its monthly effect on the design of the treatment, causes worse results than in the original optimal solution. Moreover, we assume the probability of stage jump at the interval of 28 days, even for increased control variables. By doing that, we can compare the result between different control variables by keeping the constraint the same.

Table 5.8 presents the result of the expected final tumor size for n control variables. The optimal drug schedule for all n is presented in Fig. 5.8. Since we only control the tumor size reduction every four weeks, the optimal solution in each interval is from low to high to achieve the 50% decrease at the treatment point.

Table 5.8: Tumor Cell Population After 7 Months of Therapy Using the Optimal Solutions to the Problem of NSO. n represents the Number of Control Variables.

n	$E[N(T)]$	**Run-Time** (seconds)	Probability of No Jump
7	$2.6174E+07$	3.237	0.7402
14	$2.1413E+07$	4.627	0.7537
28	$2.0294E+07$	68.983	.7599
56	$2.0061E+07$	292.784	0.7606

5.3.6 Sensitivity Analysis of NSO Model on the Drug Delivery Rate Schedule and Tumor Size

5.3.6.1 Sensitivity on the Weighted Transition Probability Function

The first sensitivity analysis that we conduct to understand the behaviour of the drug delivery rates and the tumor population is on the weighted transition probability. We assume the weight of transition probability in Eq. (5.1) as $\mu_s = 1$ for the base-case and consider $\pm 50\,\%$ more weight (i.e., $\mu_s = 0.5$ or 2) for the sensitivity analysis. As seen in Fig. 5.9a and Fig. 5.9b, the optimal drug schedules stabilize the same as in Fig. 5.9c. These modest changes occur to balance the trade-off between cumulative toxicity and tumor reduction constraints. However, their slight changes in the first month of the treatment

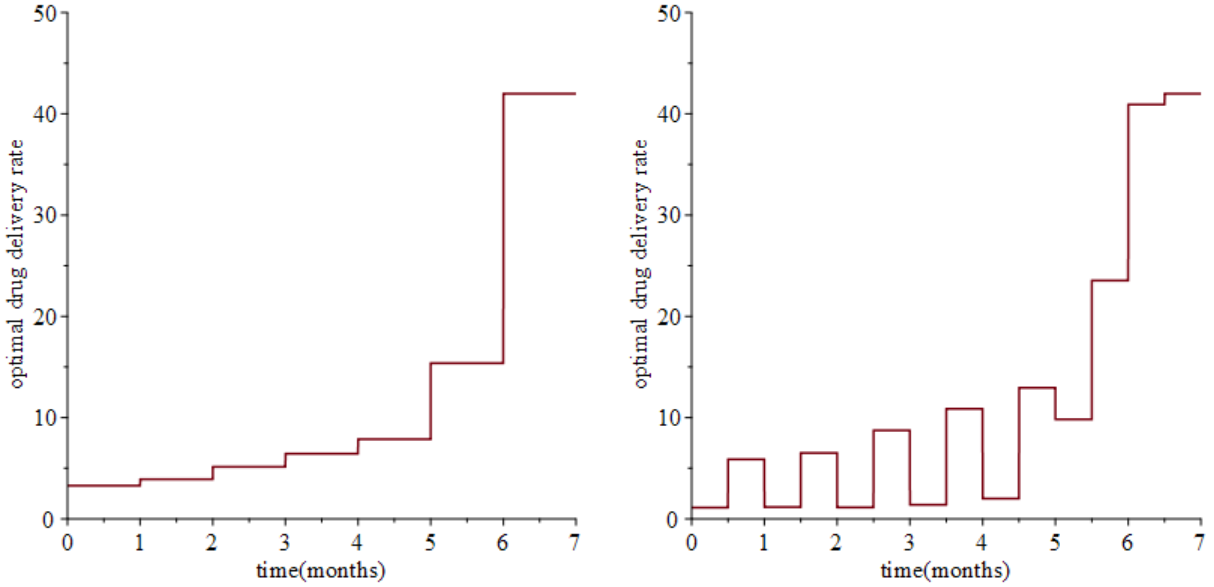

(a) $n = 7$

(b) $n = 14$

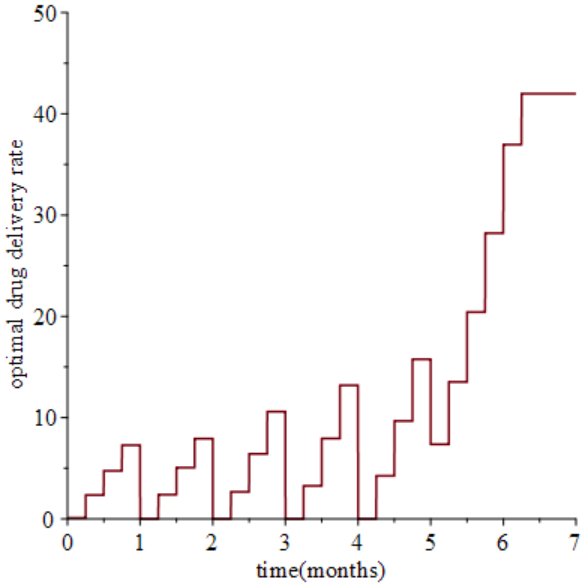

(c) $n = 28$

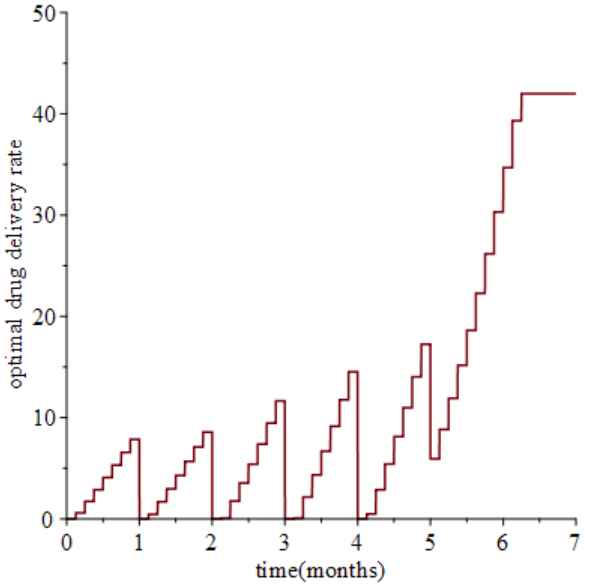

(d) $n = 56$

Figure 5.8: **Optimal Drug Delivery Rates for Increased Number of Decision Variables.**

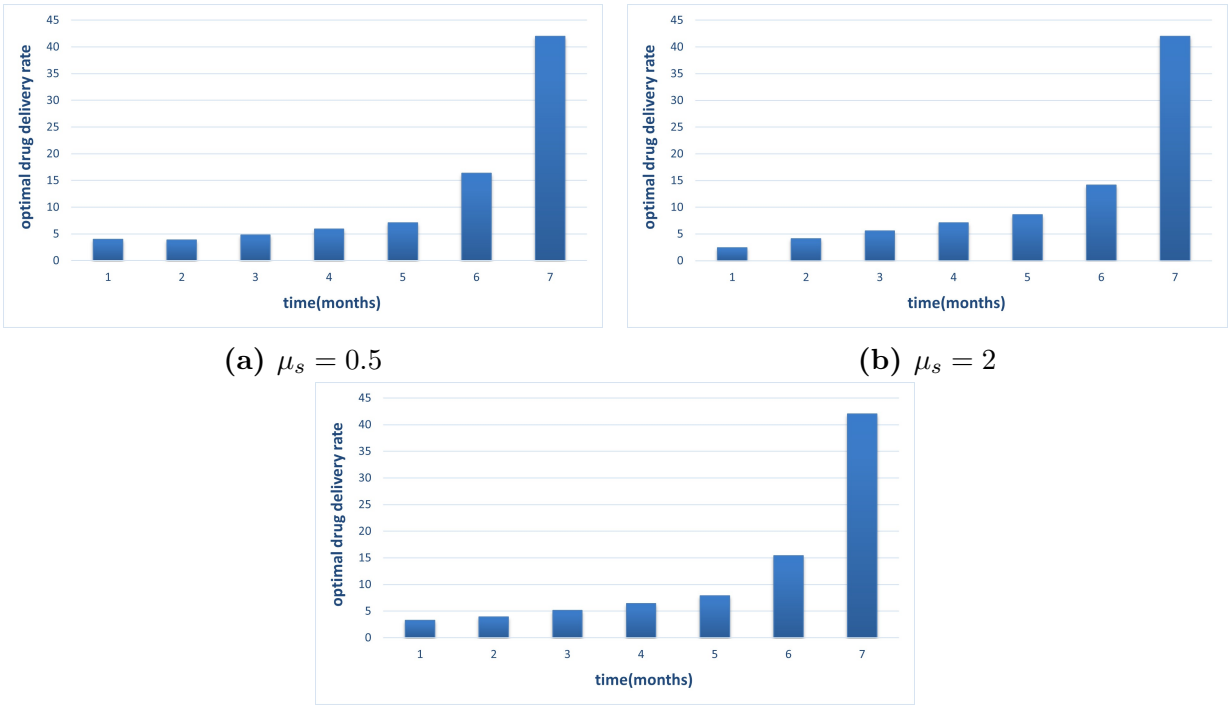

(a) $\mu_s = 0.5$ **(b)** $\mu_s = 2$

(c) $\mu_s = 1$ (base-case)

Figure 5.9: **Optimal Drug Delivery Rates under Linearly Defined Transition Probability Function with Varying Weights.**

schedule affect the final tumor population, e.g. a decrease in Fig. 5.10a or an increase in Fig. 5.10b compared to the base-case in Fig. 5.10c, respectively. This is mainly because the value in the first month of the transition probability is high compared to the rest of the probabilities in the treatment schedule. Once more weight is given to that probability, the tumor growth rate will be high for the rest of the treatment if the tumor stage jump happens that month. This slight increase in value will result in a larger tumor size, while decreasing its value will reduce the final tumor size at the end of the treatment period.

5.3.6.2 Sensitivity on the Cumulative Drug Toxicity Limits

We also conduct sensitivity analysis to see how the tumor population change with toxicity limits as the scheduling decisions are prompt to change.

Fig. 5.11a illustrates that an increased tolerated drug delivery rate limit allows a higher

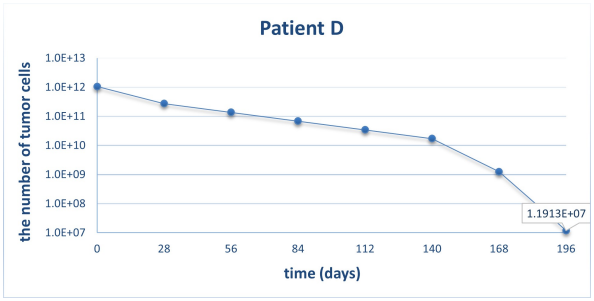

(a) $\mu_s = 0.5$

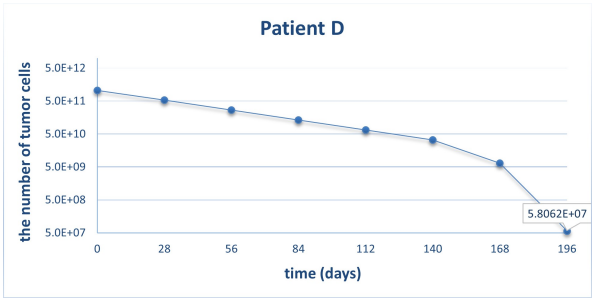

(b) $\mu_s = 2$

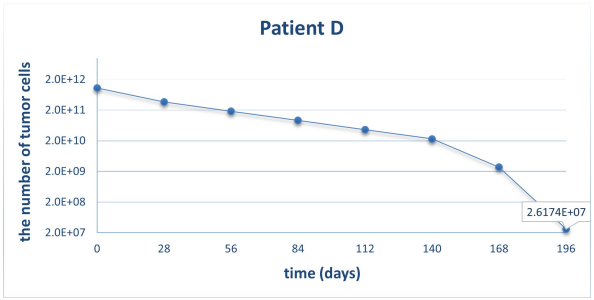

(c) $\mu_s = 1$

Figure 5.10: **Tumor Size Change for Figure 5.9.**

dose in the first month compared to Fig. 5.11b since there is enough drug to reduce the tumor size more than 50% throughout the treatment. However, since the probability of stage jump is high after the first month, the drug delivery rate in the second month is provided carefully considering the need in a future treatment.

Fig. 5.11b demonstrates how drug delivery rate is given gradually to achieve the exact reduction limit of the tumor size for the next treatment point, since the allowable limit of toxicity is lower than Fig. 5.11a. The changes of tumor size based on these given two drug toxicity limits are shown in Fig. 5.11c and Fig. 5.11d.

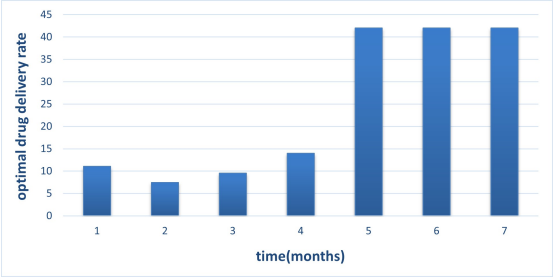

(a) Drug Delivery Rate with $v_{cum} = 5600$

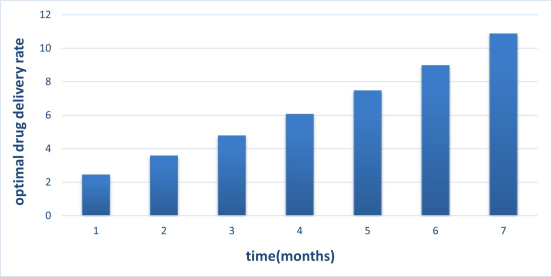

(b) Drug Delivery Rate with $v_{cum} = 1470$

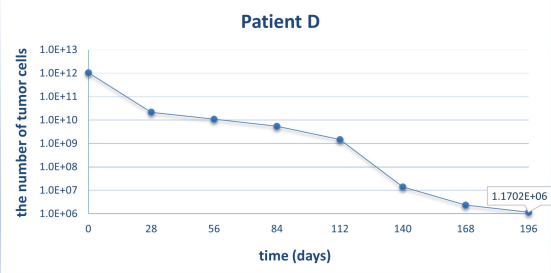

(c) Change of Tumor Size under (5.11a).

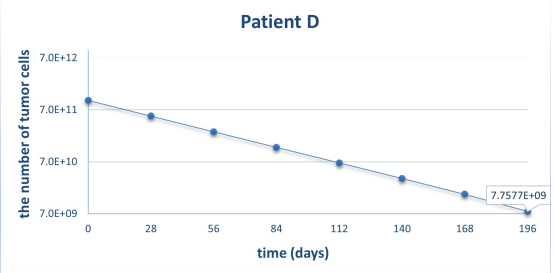

(d) Change of Tumor Size under (5.11b).

Figure 5.11: **Comparison of Optimal Drug Delivery Rate Based on Different Cumulative Toxicity Limits.**

5.3.6.3 Sensitivity on The Tumor Reduction Constraint

Our analysis on tumor reduction constraint shows how the performances alter when the limit of the reduction constraint changes.

Fig. 5.12a represents the drug delivery rate schedule when the tumor reduction limit has increased from 50% to 90%. That means the tumor size reduction for the next treatment time is relaxed. Therefore,after the first month of treatment (since the stage jump

probability is high), the drug delivery dose is low for the subsequent four months, and then increases towards the end, as seen in Fig. 5.12c.

Fig. 5.12b demonstrates the drug delivery rate when the tumor reduction has decreased to 28% from 50%. This means the tumor size reduction is forced to decrease at least 72% for the next treatment time. That lower bound percentage is found while searching for a feasible region of the problem. The expected tumor size change, based on this drug delivery schedule, shown in Fig. 5.12d, is higher than in the optimal solution. That is because the available drug delivery rate is constrained by the cumulative drug limit.

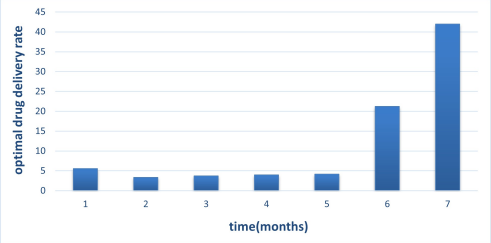

(a) Drug Delivery Rate for an Increased Tumor Size Reduction Limit.

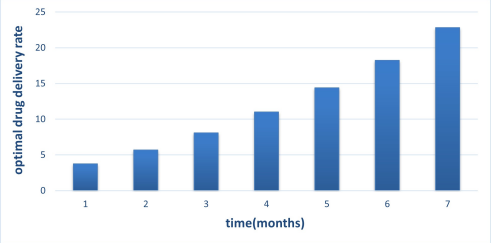

(b) Drug Delivery Rate for an Decreased Tumor Size Reduction Limit.

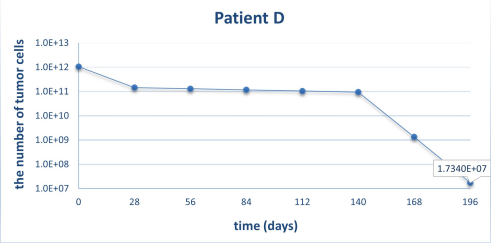

(c) Change of Tumor Size under Fig. 5.12a.

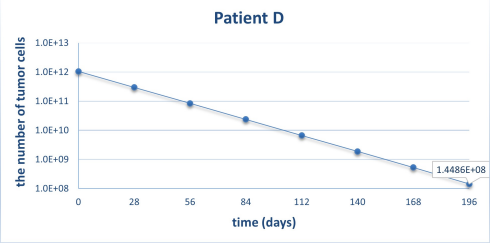

(d) Change of Tumor Size under Fig. 5.12b.

Figure 5.12: **Comparison of Optimal Drug Delivery Rate Based on Different Tumor Size Reduction Limits.**

5.3.6.4 The Effect of Transition Probability Functions on the Drug Delivery Rate Schedule

To analyze the effect of the transition probability function, two other functions are now defined, besides the linear jump probability function that was used in the stochastic optimization model. These functions are synthetic, and used only to compare the behaviour of the problem under different transition probability functions.

1. Linear function:

$$p_i = \mu_1 \left(\frac{\frac{N_{i-1}+N_i}{2}}{\theta} \right), \quad i = 1, 2, ..., n \tag{5.12}$$

2. Convex function:

$$p_i = \mu_2 \left(e^{\frac{N_{i-1}+N_i}{2\theta}-1} \right), \quad i = 1, 2, ..., n \tag{5.13}$$

3. Concave function:

$$p_i = \mu_3 \left(\sqrt{\frac{N_{i-1}+N_i}{2\theta}} \right), \quad i = 1, 2, ..., n \tag{5.14}$$

Initially, the weights of the transition probability functions were calculated by using the same jump probability obtained when the expected final tumor size is computed under the deterministic drug delivery rate schedule. To observe the distribution probabilities, the probabilities at the first and at the last month are taken as equal. Therefore, by taking the value of the jump probability at the first month of treatment which is 0.20216, the weights are found as $\mu_1 = 1, \mu_2 = 0.44896, \mu_3 = 0.44962$, respectively. Nevertheless, the weights are calculated as $\mu_1 = 1, \mu_2 = 0.43, \mu_3 = 0.32$ when the stage jump probability at the last month of the treatment is taken as 0.65743. After establishing the weights, the jump probability in each treatment point is plotted in two different graphs, Fig. 5.13 and Fig. 5.14, for these three functions. As seen in these figures, the result for the convex and linear transition probability functions are quite identical. For the concave function, the result is slightly different. However, the stage jump probability is lower, 54%, at the final treatment point when the probabilities are taken equal, 20%, in the first month of the treatment. On the other hand, the stage jump probability at the first month of the treatment is lower, 14%, if the stage jump probability at the final treatment point is equal, 65%.

5.4 Conclusions

In this chapter, we have designed initially two myopic approaches and then a nonlinear stochastic optimization model to incorporate the probability of stage jump during the treatment plan, since staging is an important indicator to determine the treatment schedule. Our results show that by incorporating the stochastic feature in the optimization model while designing to find an optimal drug schedule, at least 3% and 8% of patients avoided

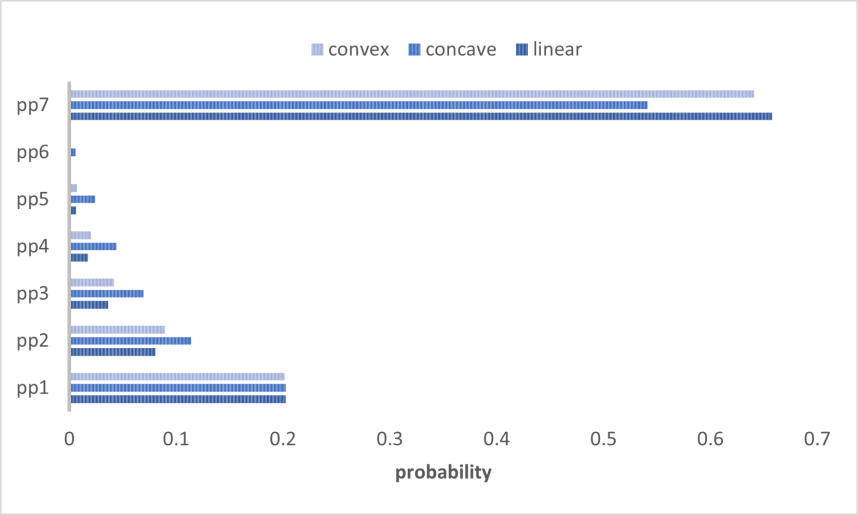

Figure 5.13: **Comparison of Transition Probability Functions while the Jump Probability of the Functions is held the Same in the First Month.**

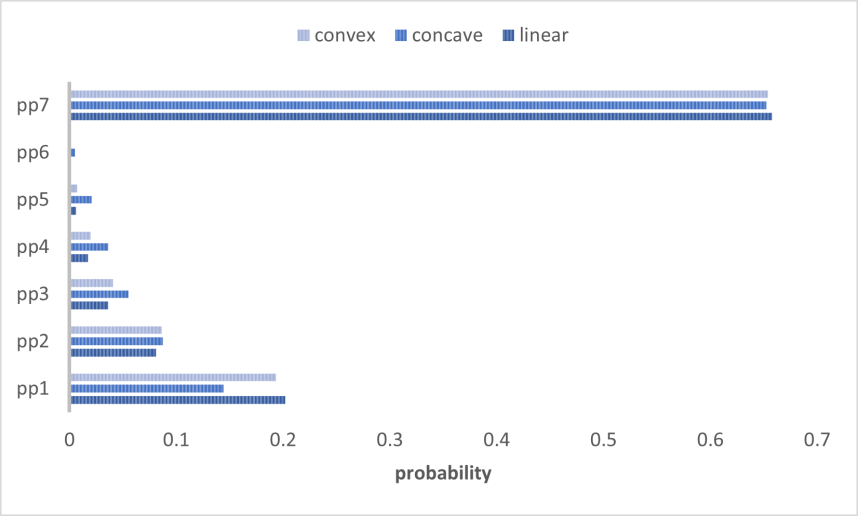

Figure 5.14: **Comparison of Probability Function while the Jump Probability of the Functions are held the Same in the Last Month.**

having a stage jump during the seven months treatment time in the sequential optimization and stochastic optimization models, respectively, compared the deterministic model design in the stochastic environment. The utility of such models is to aid the clinician in the optimization of drug delivery rate schedules for the treatment of cancers in vitro systems.

To verify our solution approach, the Brute-Force search and its modified algorithm were implemented. The results demonstrated their convergence to the optimal solution of the problem. We conducted extensive sensitivity analyses on the constraints limits and weight of the transition probability. Moreover, to analyze the effect of transition probability functions on the optimal drug delivery rate schedule, we proposed two other different probability functions, and showed their effect on the final outcome.

Chapter 6

Simulated Annealing (SA) for Chemotherapy Treatment Planning

In this chapter, we present a metaheuristic approach to design a cancer chemotherapy treatment scheduling defined as a stochastic optimization problem in Chapter 5. The effect of probabilistic staging into the model for a given policy has already been implemented and checked by a total enumeration based approach to solving the stochastic problem for small problem instances. However, as the number of decision variables is increased, the total enumeration approach becomes intractable and inefficient. Moreover, the system of designing an effective chemotherapy treatment schedule might become highly nonlinear, high dimensional and cannot be solved with a computer program when additional factors are implemented to the system. Hence, *Simulated Annealing (SA)* algorithm, randomized search heuristics, is utilized to overcome these obstacles and the results are presented in this chapter.

6.1 Simulated Annealing

Simulated Annealing (SA) is a stochastic optimization method that has been inspired by the process of annealing metals. Physically, annealing involves heating a metal and then slowly cool it down a uniform structure according to a specific schedule. Initially, atoms have the energy to move around and ensure a "random state" when the heating temperature is high enough. Gradually, atoms settle in good spots and establish "thermal equilibrium" when the cooling process is slow enough. Therefore, the objective of physical annealing

is to achieve a low energy state of a metal. SA mimics that process by probabilistically combining random walk and hill climbing algorithms since it picks a "random move" instead of picking the "best move" and allows to find the global extreme for the function that might have local minimums [Spall, 2003].

The first SA algorithm was developed in 1953 [Metropolis et al., 1953]. Then, SA was initially applied to optimization problems as the basis of an optimization technique by Kirkpatrick et al. [1983]. SA method is used in many combinatorial optimization problems including quadratic assignment problem [Misevičius, 2003], graph searching [de Sales Guerra Tsuzuki et al., 2006], healthcare [Knust and Xie, 2019, Rosocha et al., 2015]. This chapter demonstrates the application of the SA method in the chemotherapy treatment scheduling problem.

6.1.1 Outline of Simulated Annealing Process

SA is a probabilistic method that conditionally accepts the worse solution of the problem in the process of finding an approximate global optimum. In Fig. 6.1, the algorithm starts at a random initial point and continues checking if the neighbour solution is better than the current solution. If there is an improvement in the objective function, this new solution is commonly accepted. If the neighbour solution is worse, it is accepted with probability based on how much worse it is and how high the current temperature of the system, since the goal of this process is to escape from possible local minimum points.

The general process of SA is ([Sibalija, 2018], [Bertsimas and Tsitsiklis, 1993]):

Step 1 Regulate the algorithm-specific parameters such as the initial point, stopping criteria (e.g., the final temperature, the total number of algorithm iterations, the difference in objective function), the annealing schedule

Step 2 Starting point: Calculate the objective function based on the given initial point

Step 3 Find a new neighbourhood solution determined by the annealing function and calculate the objective function of this new point

Step 4 Calculate the score, ΔE: the change in the objective function due to the move from the initial point to the new point

Step 5 Decision:

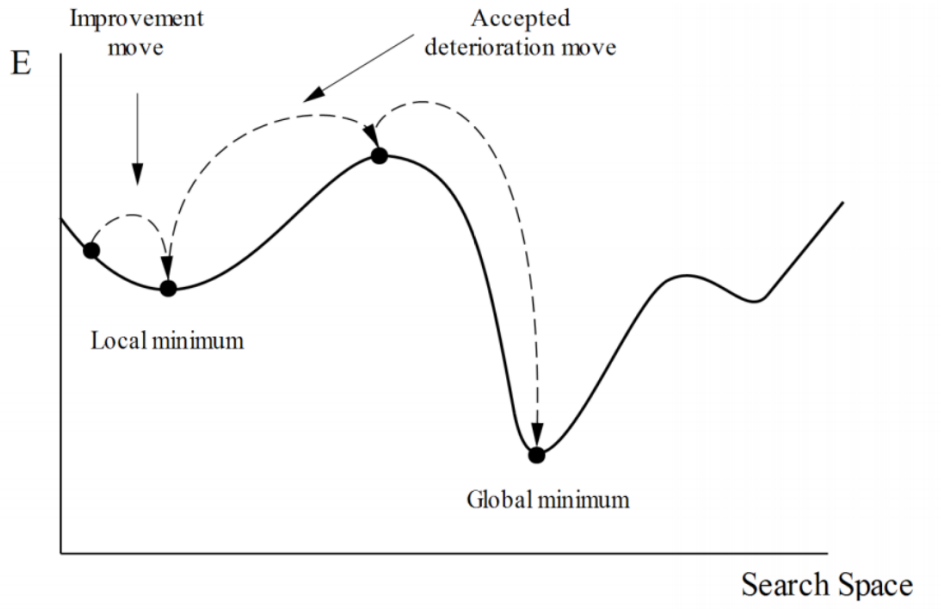

Figure 6.1: **Trajectory of SA Algorithm** [Rosocha et al., 2015].

- If $\Delta E < 0$, accept the new point and use it as the initial point in the next step.
- If $\Delta E > 0$, create a random number, r, in the range (0,1) and then calculate the probability of accepting a new state as:

$$P(\text{accepting the move}) = exp\left(-\frac{\Delta E}{k * T}\right) \tag{6.1}$$

This is called the Metropolis procedure where k-Boltzmann's constant and T stands for temperature [Metropolis et al., 1953]. If $r \leq P(\text{accepting the move})$, then continue. If not, go to **Step 3**.

Step 6 Repeat the process until the number of iterations at a particular temperature has been performed.

Step 7 Update the temperature by lowering the temperature value according to the specified temperature update function [Akella, 2014].

Step 8 The process is terminated if the current temperature is lower than or equal to the specified final temperature and/or the number of algorithm iterations is reached.

A flow chart is presented in Fig. 6.2 to visualize the general approach of the Simulated Annealing algorithm.

6.2 Application of Simulated Annealing in Chemotherapy Treatment Planning

In the implementation of the algorithm for both proposed models, deterministic and stochastic, we start the process first for finding the best initial solution set rather than the randomly generated initial point at the initial temperature which is the common approach in SA.

The initial solution is obtained considering the satisfaction of the tumor reduction constraint. In other words, drug delivery rates have been set to reduce the tumor size by at least 50% for the next treatment point.

Neighbour is structured based on the consideration of the total allowance drug throughout the treatment. In this specific problem, the resources are limited and needed to use

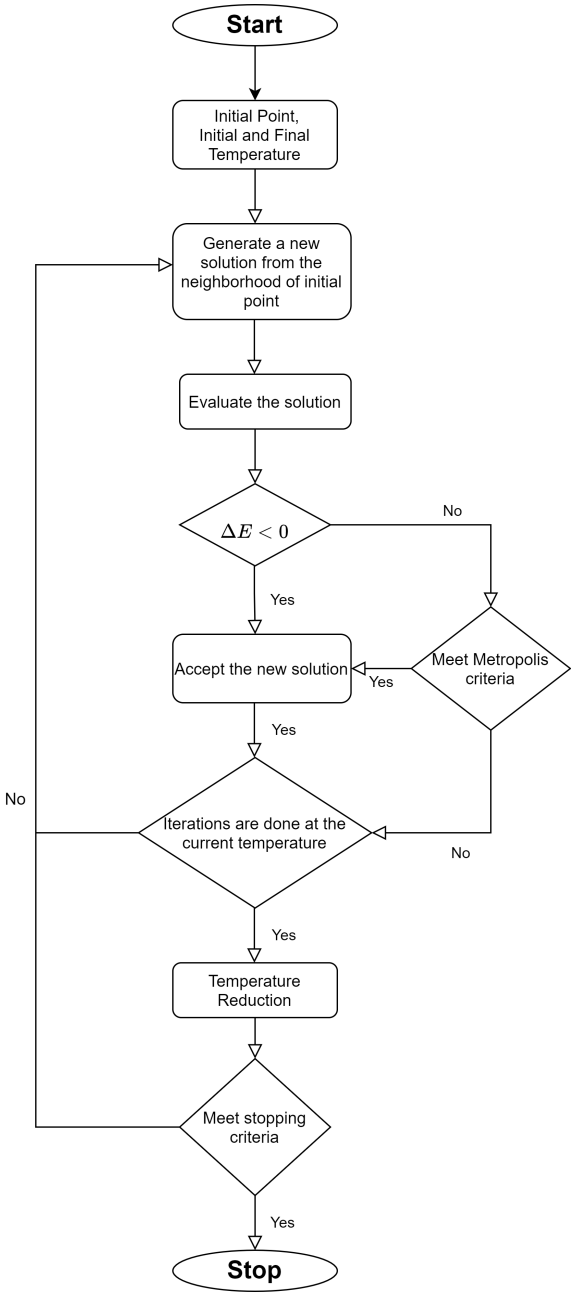

Figure 6.2: **A Flow Chart of the SA Algorithm.**

strategically to find the best solution. For the drug delivery rate schedule, if there is an increase at any of the doses, then another dose at the other treatment time should be decreased or vice versa in terms of protecting the allowable resources. Fig. 6.3 visualizes the notion of drug delivery rate conservation throughout the treatment if a unit has increased, say for σ_1, then one unit has to be decreased for $\sigma_2, \sigma_3, ...,$ or σ_7.

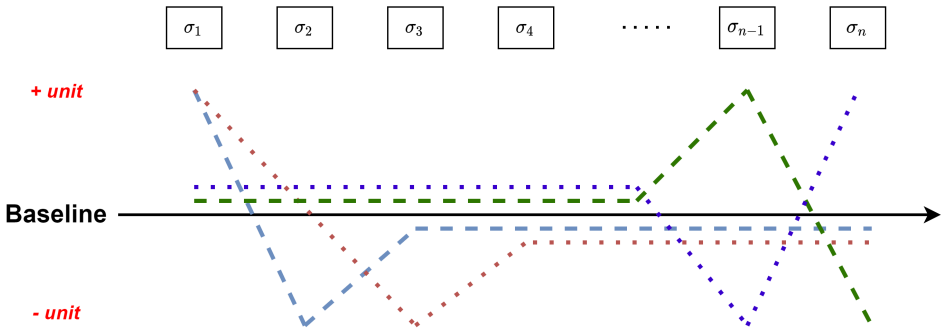

Figure 6.3: **Sample Neighbourhood of Decision Variables Structured as a Network**

6.3 Results and Discussions

We implement SA in both proposed models and discuss our findings in the following sections.

6.3.1 Result for the *OCM*

SA requires some parameters. Fine-tuning values of these parameters are important to approximate the global solution. The most important factor in this procedure is to define the initial temperature and its cooldown factor called the annealing function [Weyland, 2008]. We define the annealing schedule as:

$$\text{cooling schedule}_r = \frac{T_0}{10^{2r-2}}, \qquad r = 1, ..., 6 \tag{6.2}$$

where T_0, the initial value of the temperature is 10000.

Also, we decrease the step size of each run as follows:

$$\epsilon_r = \frac{\epsilon_0}{10^{r-1}}, \qquad r = 1, ..., 6 \tag{6.3}$$

where ϵ_0, the initial step size is 2.

In the implementation of SA for the deterministic model, we have 6 runs that each run consists of ten iterations. In the first run (r), we initialize the process from the initial solution that has been constructed to meet the 50% reduction constraint. Then, in each iteration, we look at the nearest neighbour of the initial solution by increasing and decreasing the control parameter, $\sigma_i, i = 1, ...n$ by ϵ. The solution for the final tumor size in each iteration is accepted even if the nearest neighbour is worse than the previous iteration. We accept the best solution among neighbours in the last run and iteration. After every ten iterations in each run, the temperature is reduced by Eq. (6.2) and ϵ is decreased by Eq. (6.3).

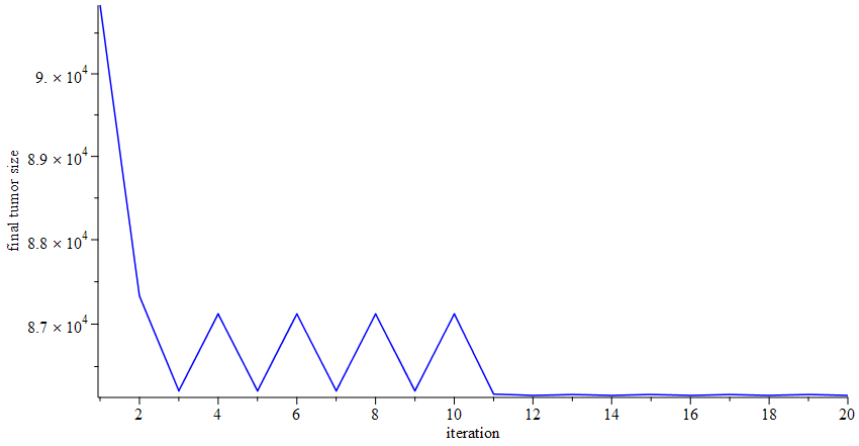

Figure 6.4: **Final Tumor Size Change in Each Iteration.**

Fig. 6.4 demonstrates the final tumor size for the iterations. Although we had six runs, we present only the first 20 iterations, since the solution is getting stuck after 11 iterations and does not provide a significant improvement.

6.3.2 Result for the *NSO*

Similar to the previous section, we first calculate the initial solution to start the SA approach for the proposed stochastic model. We find that the initial solution is already so close to the optimal solution that has been found in Nonlinear Stochastic Optimization.

With the current configurations, regardless of how many iterations we generate, the neighbour search of the initial solution cannot provide a better result and get stuck at the same point. That happens because the problem constraints limit the search and prevent converging any improved results. With this initial solution we have, it is not possible to find a better neighbour solution.

We calculate the final tumor size based on the specific percentage reduction for the first month and then followed by a 50% reduction in the consecutive months and the rest of the drug is allocated the last month and the month before that. In Fig. 6.5, we examine different percentage reductions from 50% to 90% in the first month for the initial solution because the solution of the first month affects the rest of the solution. We find 65% reduction in the first month is optimal that we have found in the stochastic optimization.

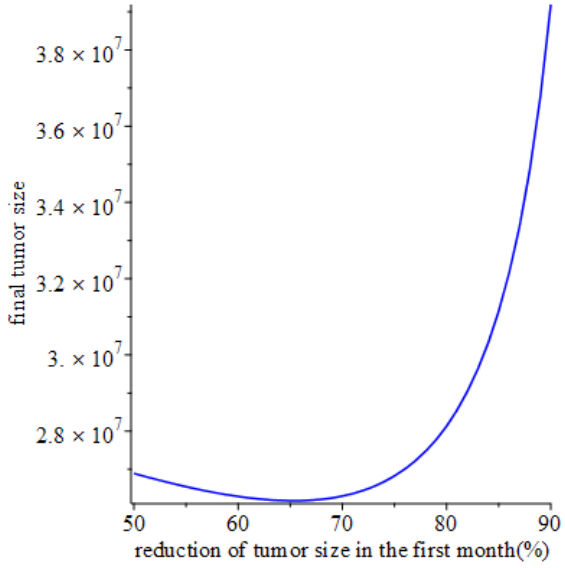

Figure 6.5: **Final Tumor Size Change Based on the Reduction of Tumor Size in the First Month throughout the Whole Iteration.**

To conclude, the solution of SA in the deterministic model improves with the iteration by changing the value of the last three control variables. However, since the initial solution in the stochastic model for SA is close to the optimal solution, the neighbour search is getting stuck in the iterations. We declare that there is more research needed SA for the stochastic model. For example, for the different sets of constraints, we can use the same approach to initialize the SA model from different percentage levels for the first month. Then, we run SA. If there is room for improvement, we can present the result.

Chapter 7

Conclusions and Future Work

7.1 Summary and Conclusions

In this thesis, we have proposed and studied a novel methodology for drug administration decisions under stochastic cancer staging. Results obtained from the comprehensive testing on computer programming satisfy the research hypothesis stipulating that embedding stochastic feature in the deterministic model is crucial for an effective drug delivery rate schedule to treat cancer.

Initially, we have designed a deterministic tumor kinetic model to represent the behaviour of tumor dynamics. We demonstrate that this method is computationally feasible and its power of representation can be validated using a real data from the literature.

Later, an optimal control model has been designed by employing certain restrictions. Since this optimal control model is a nonlinear optimization problem, we have numerically solved it using the control parametrization technique. The result of optimization problem have suggested to keep the initial drug delivery rate low, and then gradually increase with small increments towards the end of treatment. By doing that the optimal drug schedule achieves minimal tumor cells at the end and maintains the allowable drug toxicity level for all treatment time.

Afterwards, we have proposed a stochastic staging mechanism to be incorporated into the proposed optimal control model. The results indicate that considering the probability in stage of cancer significantly changes the structure of the optimal solution and provide a better outcome. By proposing a modified version of Brute-Force search, we emphasize the efficiency of search techniques for large-scale optimization problems and the reduction of time and effort for such activities.

Lastly, we have presented an altered SA algorithm for solving chemotherapy treatment scheduling problem that was formulated as deterministically and stochastically in the previous chapters.

To conclude, our purpose and notable contributions in this study provide a proof-of-concept illustrating that it is possible to extend the classical chemotherapy treatment planning models to be a more realistic model. That extension can be solved efficiently, and provide useful insights for the practitioners.

Our numerical results can be improved by including more realistic terms in the proposed models. Even though the results cannot strongly suggest that standard treatment protocols may not be optimal, every attempt has the potential to improve the quality of treatment for cancer survivors.

7.2 Directions for Further Research

Despite the impact of this research and the steps taken, there are several areas for improvement in our study. More specifically, the following items will be addressed in future research:

A potential future extension of the present research work lies in the direction of considering multi-drug and cell-cycle specific drug administration for the proposed models.

Another potential future research direction as a continuation of this thesis is to conduct a study in the presence of drug resistance.

One of the limitations of this study is to present a SA model that doesn't improve the solution point for the stochastic optimization model due to the restricted constraint limits. Therefore, more research is needed to implement the SA approach for stochastic optimization.

This presented study may provide clinicians substantial insights on chemotherapy scheduling through the identification of biological factors. Therefore, the proposed models can be enriched by a clinical study with a larger number of patients. In the future, we plan to refine the parameters of our model with experimental and clinical data and expect to confer more benefits to real treatments in clinical practice through application or implementation study. Moreover, for the improvement of the OCM, another potential model could be maximizing the survival rate of cancer patients while considering constraints on the final tumor size. However, such an extension would require a significant change in the modeling approach, therefore it is left as future work.

References

Summary Stage 2018 Coding Manual v2.0. *Summary Stage 2018 Coding Manual v2.0*, page 378, 2020.

Mohamed Abdel-Basset, Laila Abdel-Fatah, and Arun Kumar Sangaiah. Chapter 10 - Metaheuristic Algorithms: A Comprehensive Review. In Arun Kumar Sangaiah, Michael Sheng, and Zhiyong Zhang, editors, *Computational Intelligence for Multimedia Big Data on the Cloud with Engineering Applications*, Intelligent Data-Centric Systems, pages 185 – 231. Academic Press, 2018. ISBN 978-0-12-813314-9. doi: 10.1016/B978-0-12-813314-9.00010-4. URL http://www.sciencedirect.com/science/article/pii/B9780128133149000104.

Ismail Abdulrashid, Hakim Ghazzai, Xiaoying Han, and Yehia Massoud. Optimal Control Treatment Analysis for the Predator-Prey Chemotherapy Model. In *2019 31st International Conference on Microelectronics (ICM)*, pages 296–299, Cairo, Egypt, December 2019. IEEE. ISBN 978-1-72814-058-2. doi: 10.1109/ICM48031.2019.9021837. URL https://ieeexplore.ieee.org/document/9021837/.

Zvia Agur, Refael Hassin, and Sigal Levy. Optimizing Chemotherapy Scheduling Using Local Search Heuristics. *Operations Research*, 54(5):829–846, October 2006. ISSN 0030-364X, 1526-5463. doi: 10.1287/opre.1060.0320. URL http://pubsonline.informs.org/doi/abs/10.1287/opre.1060.0320.

Atsuo Akanuma. Parameter analysis of gompertzian function growth model in clinical tumors. *European Journal of Cancer (1965)*, 14(6):681–688, 1978. URL http://www.sciencedirect.com/science/article/pii/0014296478903043.

Premchand Akella. Simulated annealing. page 17, 2014.

Oguzhan Alagoz, Heather Hsu, Andrew J. Schaefer, and Mark S. Roberts. Markov decision processes: A tool for sequential decision making under uncertainty. *Medical decision making : an international journal of the Society for Medical Decision Making*, 30(4): 474–483, 2010. ISSN 0272-989X. doi: 10.1177/0272989X09353194. URL http://www.ncbi.nlm.nih.gov/pmc/articles/PMC3060044/.

M. S. Alam, M. A. Hossain, S. Algoul, M. A. A. Majumader, M. A. Al-Mamun, G. Sexton, and R. Phillips. Multi-objective multi-drug scheduling schemes for cell cycle specific cancer treatment. *Computers & Chemical Engineering*, 58:14–32, November 2013a. ISSN 0098-1354. doi: 10.1016/j.compchemeng.2013.05.021. URL http://www.sciencedirect.com/science/article/pii/S0098135413001853.

Mohammad S. Alam, Saleh Algoul, M. Alamgir Hossain, and M. A. Azim Majumder. Multi-objective Particle Swarm Optimisation for Phase Specific Cancer Drug Scheduling. In Jonathan H. Chan, Yew-Soon Ong, and Sung-Bae Cho, editors, *Computational Systems-Biology and Bioinformatics*, volume 115, pages 180–192. Springer Berlin Heidelberg, Berlin, Heidelberg, 2010. ISBN 978-3-642-16749-2 978-3-642-16750-8. doi: 10.1007/978-3-642-16750-8_16. URL http://link.springer.com/10.1007/978-3-642-16750-8_16. Series Title: Communications in Computer and Information Science.

Nadia Alam, Munira Sultana, M. S. Alam, M. A. Al-Mamun, and M. A. Hossain. Optimal Intermittent Dose Schedules for Chemotherapy Using Genetic Algorithm. *ADCAIJ: Advances in Distributed Computing and Artificial Intelligence Journal*, 2(2):37–52, August 2013b. ISSN 2255-2863. doi: 10.14201/ADCAIJ2013253752. URL https://revistas.usal.es/index.php/2255-2863/article/view/ADCAIJ2013253752. Number: 2.

G. Albano and V. Giorno. A stochastic model in tumor growth. *Journal of Theoretical Biology*, 242(2):329–336, September 2006. ISSN 0022-5193. doi: 10.1016/j.jtbi.2006.03.001.

Mahul B. Amin, Frederick L. Greene, Stephen B. Edge, Carolyn C. Compton, Jeffrey E. Gershenwald, Robert K. Brookland, Laura Meyer, Donna M. Gress, David R. Byrd, and David P. Winchester. The eighth edition AJCC cancer staging manual: Continuing to build a bridge from a population-based to a more "personalized" approach to cancer staging. *CA: A Cancer Journal for Clinicians*, 67(2):93–99, 2017. ISSN 1542-4863. doi: 10.3322/caac.21388. URL http://onlinelibrary.wiley.com/doi/10.3322/caac.21388/abstract.

N Archana, Antony Manoj Fh Benedict, and J Niresh. Chemotherapy drug regimen optimization using deterministic oscillatory search algorithm. 17(6):1135, 2018. ISSN 1596-9827, 1596-5996. doi: 10.4314/tjpr.v17i6.21. URL https://www.ajol.info/index.php/tjpr/article/view/174357.

Francisco Arvelo, Felipe Sojo, and Carlos Cotte. Tumour progression and metastasis. *ecancermedicalscience*, 10, January 2016. ISSN 1754-6605. doi: 10.3332/ecancer.2016.617. URL https://www.ncbi.nlm.nih.gov/pmc/articles/PMC4754119/.

Mehmet U. S. Ayvaci, Oguzhan Alagoz, and Elizabeth S. Burnside. The effect of budgetary restrictions on breast cancer diagnostic decisions. 14(4):600–617, 2012. ISSN 1523-4614. doi: 10.1287/msom.1110.0371. URL https://www.ncbi.nlm.nih.gov/pmc/articles/PMC3767197/.

Alecsandru Ioan Baba and Cornel Câtoi. *TUMOR CELL MORPHOLOGY*. The Publishing House of the Romanian Academy, 2007. URL https://www.ncbi.nlm.nih.gov/books/NBK9553/. Publication Title: Comparative Oncology.

Z Bajzer, M. Marusic, and S. Vuk-Pavlovic. Conceptual frameworks for mathematical modeling of tumor growth dynamics. *Mathematical and Computer Modelling*, 23(6):31 – 46, 1996. ISSN 0895-7177. doi: http://dx.doi.org/10.1016/0895-7177(96)00018-0. URL http://www.sciencedirect.com/science/article/pii/0895717796000180.

Nazila Bazrafshan and M. M. Lotfi. A finite-horizon Markov decision process model for cancer chemotherapy treatment planning: an application to sequential treatment decision making in clinical trials. *Annals of Operations Research*, July 2020. ISSN 1572-9338. doi: 10.1007/s10479-020-03706-5. URL https://doi.org/10.1007/s10479-020-03706-5.

Zahra Beheshti and Siti Mariyam Hj Shamsuddin. A review of population-based meta-heuristic algorithm. page 36, 2013.

Richard Ernest Bellman. *Mathematical Methods in Medicine*. World Scientific Publishing Co., Inc., 1983. ISBN 978-9971-950-21-7.

Sébastien Benzekry. Mathematical and numerical analysis of a model for anti-angiogenic therapy in metastatic cancers. *ESAIM: Mathematical Modelling and Numerical Analysis*, 46(2):207–237, March 2012. ISSN 0764-583X, 1290-3841. doi: 10.1051/m2an/2011041. URL http://www.esaim-m2an.org/10.1051/m2an/2011041.

Sébastien Benzekry. Modeling, mathematical and numerical analysis of anti-cancerous therapies for metastatic cancers. page 251, 2017.

Sébastien Benzekry and Philip Hahnfeldt. Maximum tolerated dose versus metronomic scheduling in the treatment of metastatic cancers. 335:235–244, 2013. ISSN 00225193. doi: 10.1016/j.jtbi.2013.06.036. URL https://linkinghub.elsevier.com/retrieve/pii/S0022519313003196.

Sébastien Benzekry, Clare Lamont, Afshin Beheshti, Amanda Tracz, John M. L. Ebos, Lynn Hlatky, and Philip Hahnfeldt. Classical Mathematical Models for Description and Prediction of Experimental Tumor Growth. *PLoS Computational Biology*, 10(8): e1003800, August 2014. ISSN 1553-7358. doi: 10.1371/journal.pcbi.1003800. URL http://dx.plos.org/10.1371/journal.pcbi.1003800.

Dimitri P. Bertsekas. *Dynamic Programming and Optimal Control*. Athena Scientific, 2nd edition, 2000. ISBN 1886529094.

Dimitris Bertsimas and John Tsitsiklis. Simulated annealing. 8(1):10 – 15, 1993. doi: 10.1214/ss/1177011077. URL https://doi.org/10.1214/ss/1177011077. Publisher: Institute of Mathematical Statistics.

E. P. J. Boer, D. a. M. K. Rasch, and E. M. T. Hendrix. Locally optimal designs in non-linear regression: A case study of the michaelis-menten function. In *Advances in Stochastic Simulation Methods*, Statistics for Industry and Technology, pages 177–188. Birkhäuser, Boston, MA, 2000. ISBN 978-1-4612-7091-1 978-1-4612-1318-5. URL https://link.springer.com/chapter/10.1007/978-1-4612-1318-5_11.

J. M. Boher, J. L. Pujol, J. Grenier, and J. P. Daurès. Markov model and markers of small cell lung cancer: assessing the influence of reversible serum NSE, CYFRA 21-1 and TPS levels on prognosis. 79(9):1419–1427, 1999. ISSN 0007-0920. doi: 10.1038/sj.bjc.6690227.

Freddie Bray and Isabelle Soerjomataram. The Changing Global Burden of Cancer: Transitions in Human Development and Implications for Cancer Prevention and Control. In Hellen Gelband, Prabhat Jha, Rengaswamy Sankaranarayanan, and Susan Horton, editors, *Cancer: Disease Control Priorities, Third Edition (Volume 3)*. The International Bank for Reconstruction and Development / The World Bank, Washington (DC), 2015. ISBN 978-1-4648-0349-9 978-1-4648-0369-7. URL http://www.ncbi.nlm.nih.gov/books/NBK343643/.

Darren R. Brenner, Hannah K. Weir, Alain A. Demers, Larry F. Ellison, Cheryl Louzado, Amanda Shaw, Donna Turner, Ryan R. Woods, and Leah M. Smith. Projected estimates of cancer in Canada in 2020. *CMAJ*, 192(9):E199–E205, March 2020. ISSN 0820-3946,

1488-2329. doi: 10.1503/cmaj.191292. URL https://www.cmaj.ca/content/192/9/E199. Publisher: CMAJ Section: Research.

James Brierley, Brian O'Sullivan, Hisao Asamura, David Byrd, Shao Hui Huang, Anne Lee, Marion Piñeros, Malcolm Mason, Fabio Y. Moraes, Wiebke Rösler, Brian Rous, Julie Torode, J. Han van Krieken, and Mary Gospodarowicz. Global consultation on cancer staging: promoting consistent understanding and use. 16(12): 763–771, 2019. ISSN 1759-4782. doi: 10.1038/s41571-019-0253-x. URL https://www.nature.com/articles/s41571-019-0253-x. Bandiera_abtest: a Cc_license_type: cc_by Cg_type: Nature Research Journals Number: 12 Primary_atype: Reviews Publisher: Nature Publishing Group Subject_term: Cancer models;Cancer screening;Epidemiology;Neoplasm staging;Tumour biomarkers Subject_term_id: cancer-models;cancer-screening;epidemiology;neoplasm-staging;tumour-biomarkers.

C. S. Brock, E. S. Newlands, S. R. Wedge, M. Bower, H. Evans, I. Colquhoun, M. Roddie, M. Glaser, M. H. Brampton, and G. J. Rustin. Phase i trial of temozolomide using an extended continuous oral schedule. 58(19):4363–4367, 1998. ISSN 0008-5472.

G. Büyükdamgaci-Alogan, T. Elele, M. Hayran, M. Erman, and S. Kiliçkap. A decision-analytic model for early stage breast cancer: lumpectomy vs mastectomy. 55(3):222–228, 2008. ISSN 0028-2685.

CCS. Canadian Cancer Statistics 2019. *Health Promotion and Chronic Disease Prevention in Canada*, 39(8/9):255–255, September 2019. ISSN 2368-738X. doi: 10.24095/hpcdp.39.8/9.04. URL https://www.canada.ca/en/public-health/services/reports-publications/health-promotion-chronic-disease-prevention-canada-research-policy-practice/vol-39-no-8-9-2019/notice-canadian-cancer-statistics-2019.html.

Bruce Chabner and Dan L Longo. *Cancer chemotherapy, immunotherapy, and biotherapy: principles and practice*. 2019. ISBN 978-1-4963-7514-8. OCLC: 1035402585.

Chase Cockrell and David E Axelrod. Optimization of Dose Schedules for Chemotherapy of Early Colon Cancer Determined by High-Performance Computer Simulations. *Cancer Informatics*, 18:1176935118822804, January 2019. ISSN 1176-9351. doi: 10.1177/1176935118822804. URL https://doi.org/10.1177/1176935118822804. Publisher: SAGE Publications Ltd STM.

A. J. Coldman and J. H. Goldie. A stochastic model for the origin and treatment of tumors containing drug-resistant cells. *Bulletin of mathematical biology*, 48(3-4):279–292, 1986. URL http://www.sciencedirect.com/science/article/pii/S0092824086900285.

A.J. Coldman and J.H. Goldie. A model for the resistance of tumor cells to cancer chemotherapeutic agents. *Mathematical Biosciences*, 65:291–307, 08 1983.

Andrew J. Coldman and J. M. Murray. Optimal control for a stochastic model of cancer chemotherapy. *Mathematical biosciences*, 168(2):187–200, 2000. URL http://www.sciencedirect.com/science/article/pii/S0025556400000456.

Carolyn C. Compton and Frederick L. Greene. The staging of colorectal cancer: 2004 and beyond. *CA: A Cancer Journal for Clinicians*, 54(6):295–308, 2004. ISSN 1542-4863. doi: 10.3322/canjclin.54.6.295. URL http://onlinelibrary.wiley.com/doi/10.3322/canjclin.54.6.295/abstract.

M. I. S. Costa, J. L. Boldrini, and R. C. Bassanezi. Chemotherapeutic treatments involving drug resistance and level of normal cells as a criterion of toxicity. *Mathematical biosciences*, 125(2):211–228, 1995. URL http://www.sciencedirect.com/science/article/pii/002555649400028X.

L. G De Pillis and A Radunskaya. The dynamics of an optimally controlled tumor model: A case study. 37(11):1221–1244, 2003. ISSN 0895-7177. doi: 10.1016/S0895-7177(03)00133-X. URL http://www.sciencedirect.com/science/article/pii/S089571770300133X.

Marcos de Sales Guerra Tsuzuki, Thiago de Castro Martins, and Fábio Kawaoka Takase. ROBOT PATH PLANNING USING SIMULATED ANNEALING. 39(3):175–180, 2006. ISSN 14746670. doi: 10.3182/20060517-3-FR-2903.00105. URL https://linkinghub.elsevier.com/retrieve/pii/S1474667015358250.

Holger Dette and Stefanie Biedermann. Robust and efficient designs for the michaelis–menten model. *Journal of the American Statistical Association*, 98(463):679–686, 2003. ISSN 0162-1459, 1537-274X. doi: 10.1198/016214503000000585. URL http://www.tandfonline.com/doi/abs/10.1198/016214503000000585.

Carlos Andrés Devia and Giulia Giordano. Optimal duration and planning of switching treatments taking drug toxicity into account: a convex optimisation approach. In *2019 IEEE 58th Conference on Decision and Control (CDC)*, pages 5674–5679, 2019. doi: 10.1109/CDC40024.2019.9028881. ISSN: 2576-2370.

Alberto d'Onofrio, Urszula Ledzewicz, Helmut Maurer, and Heinz Schättler. On optimal delivery of combination therapy for tumors. 222(1):13–26, 2009. ISSN 0025-5564. doi: 10.1016/j.mbs.2009.08.004. URL https://www.sciencedirect.com/science/article/pii/S0025556409001333.

Pinky Dua, Vivek Dua, and Efstratios N. Pistikopoulos. Optimal delivery of chemotherapeutic agents in cancer. 32(1):99–107, 2008. ISSN 00981354. doi: 10.1016/j.compchemeng.2007.07.001. URL https://linkinghub.elsevier.com/retrieve/pii/S0098135407001792.

M. Eisen. *Mathematical Models in Cell Biology and Cancer Chemotherapy*. Lecture Notes in Biomathematics. Springer-Verlag, Berlin Heidelberg, 1979. ISBN 978-3-540-09709-9. doi: 10.1007/978-3-642-93126-0. URL https://www.springer.com/gp/book/9783540097099.

Heiko Enderling and Mark AJ Chaplain. Mathematical modeling of tumor growth and treatment. *Current Pharmaceutical Design*, 20(30):4934–4940, 2014. URL http://www.ingentaconnect.com/content/ben/cpd/2014/00000020/00000030/art00017.

Michael Engelhart, Dirk Lebiedz, and Sebastian Sager. Optimal control for selected cancer chemotherapy ODE models: A view on the potential of optimal schedules and choice of objective function. *Mathematical Biosciences*, 229(1):123–134, January 2011. ISSN 0025-5564. doi: 10.1016/j.mbs.2010.11.007. URL http://www.sciencedirect.com/science/article/pii/S002555641000180X.

Fatih Safa Erenay, Oguzhan Alagoz, and Adnan Said. Optimizing colonoscopy screening for colorectal cancer prevention and surveillance. 16(3):381–400, 2014. ISSN 1523-4614, 1526-5498. doi: 10.1287/msom.2014.0484. URL http://pubsonline.informs.org/doi/abs/10.1287/msom.2014.0484.

Sarah Fleming, Kirk Solo, Xuehua Ke, Waleed Shalaby, and Arlene O. Siefker-Radtke. Use of a dynamic disease progression model to estimate prevalence and prognosis for patients with urothelial carcinoma (UC) in the united states (US). 38(15):e19144–e19144, 2020. ISSN 0732-183X. doi: 10.1200/JCO.2020.38.15_suppl.e19144. URL https://ascopubs.org/doi/10.1200/JCO.2020.38.15_suppl.e19144. Publisher: American Society of Clinical Oncology.

Jasmine Foo, Juliann Chmielecki, William Pao, and Franziska Michor. Effects of pharmacokinetic processes and varied dosing schedules on the dynamics of acquired resistance to erlotinib in EGFR-mutant lung cancer. 7(10):1583–1593, 2012. ISSN 15560864. doi: 10.1097/JTO.0b013e31826146ee. URL https://linkinghub.elsevier.com/retrieve/pii/S1556086415326010.

A. Lindsay Frazier, Graham A. Colditz, Charles S. Fuchs, and Karen M. Kuntz. Cost-effectiveness of Screening for Colorectal Cancer in the General Population. *JAMA*, 284

(15):1954–1961, October 2000. ISSN 0098-7484. doi: 10.1001/jama.284.15.1954. URL https://jamanetwork.com/journals/jama/fullarticle/193186. Publisher: American Medical Association.

Christoph Frei, Thomas Hillen, and Adam Rhodes. A Stochastic Model for Cancer Metastasis: Branching Stochastic Process with Settlement. *bioRxiv*, page 294157, April 2018. doi: 10.1101/294157. URL https://www.biorxiv.org/content/10.1101/294157v1. Publisher: Cold Spring Harbor Laboratory Section: New Results.

Robert A. Gatenby and Philip K. Maini. Mathematical oncology: Cancer summed up. *Nature*, 421(6921):321–321, January 2003. ISSN 1476-4687. doi: 10.1038/421321a. URL https://doi.org/10.1038/421321a.

Robert A. Gatenby, Ariosto S. Silva, Robert J. Gillies, and B. Roy Frieden. Adaptive therapy. 69(11):4894–4903, 2009. ISSN 0008-5472, 1538-7445. doi: 10.1158/0008-5472.CAN-08-3658. URL http://cancerres.aacrjournals.org/lookup/doi/10.1158/0008-5472.CAN-08-3658.

Ritu Gautam, Prableen Kaur, and Manik Sharma. A comprehensive review on nature inspired computing algorithms for the diagnosis of chronic disorders in human beings. *Progress in Artificial Intelligence*, 8(4):401–424, December 2019. ISSN 2192-6352, 2192-6360. doi: 10.1007/s13748-019-00191-1. URL http://link.springer.com/10.1007/s13748-019-00191-1.

Philip Gerlee. The Model Muddle: In Search of Tumor Growth Laws. *Cancer Research*, 73(8):2407–2411, April 2013. ISSN 0008-5472, 1538-7445. doi: 10.1158/0008-5472.CAN-12-4355. URL https://cancerres.aacrjournals.org/content/73/8/2407. Publisher: American Association for Cancer Research Section: Perspectives.

C. J. Goh and K. L. Teo. Control parametrization: A unified approach to optimal control problems with general constraints. *Automatica*, 24(1):3–18, 1988. ISSN 0005-1098. doi: 10.1016/0005-1098(88)90003-9. URL http://www.sciencedirect.com/science/article/pii/0005109888900039.

J. H. Goldie and A. J. Coldman. A mathematic model for relating the drug sensitivity of tumors to their spontaneous mutation rate. *Cancer Treatment Reports*, 63(11):1727–1733, 1979. ISSN 0361-5960.

Benjamin Gompertz. On the nature of the function expressive of the law of human mortality, and on a new mode of determining the value of life contingencies. *Philo-*

sophical transactions of the Royal Society of London, 115:513–583, 1825. URL http://www.jstor.org/stable/107756.

Michael M. Gottesman. Mechanisms of cancer drug resistance. *Annual review of medicine*, 53(1):615–627, 2002. URL http://www.annualreviews.org/doi/abs/10.1146/annurev.med.53.082901.103929.

Richard Gray, Rosie Bradley, Jeremy Braybrooke, Zulian Liu, Richard Peto, Lucy Davies, David Dodwell, Paul McGale, Hongchao Pan, Carolyn Taylor, William Barlow, Judith Bliss, Paolo Bruzzi, David Cameron, George Fountzilas, Sibylle Loibl, John Mackey, Miguel Martin, Lucia Del Mastro, Volker Möbus, Valentina Nekljudova, Sabino De Placido, Sandra Swain, Michael Untch, Kathleen I Pritchard, Jonas Bergh, Larry Norton, Clare Boddington, Julie Burrett, Mike Clarke, Christina Davies, Fran Duane, Vaughan Evans, Lucy Gettins, Jon Godwin, Robert Hills, Sam James, Hui Liu, Elizabeth MacKinnon, Gurdeep Mannu, Theresa McHugh, Philip Morris, Simon Read, Yaochen Wang, Zhe Wang, Peter Fasching, Nadia Harbeck, Pascal Piedbois, Michael Gnant, Guenther Steger, Angelo Di Leo, Stella Dolci, Prue Francis, Denis Larsimont, Jean Marie Nogaret, Catherine Philippson, Martine Piccart, Sabine Linn, Petronella Peer, Vivianne Tjan-Heijnen, Sonja Vliek, John Mackey, Dennis Slamon, John Bartlett, Vivien H Bramwell, Bingshu Chen, Stephen Chia, Karen Gelmon, Paul Goss, Mark Levine, Wendy Parulekar, Joseph Pater, Eileen Rakovitch, Lois Shepherd, Dongsheng Tu, Tim Whelan, Don Berry, Gloria Broadwater, Constance Cirrincione, Hyman Muss, Raymond Weiss, Yi Shan, Yong Fu Shao, Xiang Wang, Binghe Xu, Dong-Bing Zhao, Harry Bartelink, Nina Bijker, Jan Bogaerts, Fatima Cardoso, Tanja Cufer, Jean-Pierre Julien, Philip Poortmans, Emiel Rutgers, Cornelis van de Velde, Eva Carrasco, Miguel Angel Segui, Jens Uwe Blohmer, Serban Costa, Bernd Gerber, Christian Jackisch, Gunter von Minckwitz, Mario Giuliano, Michele De Laurentiis, Christina Bamia, Georgia-Angeliki Koliou, Dimitris Mavroudis, Roger A'Hern, Paul Ellis, Lucy Kilburn, James Morden, John Yarnold, Mohammad Sadoon, Augustinus H Tulusan, Stewart Anderson, Gordon Bass, Joe Costantino, James Dignam, Bernard Fisher, Charles Geyer, Eleftherios P Mamounas, Soon Paik, Carol Redmond, D Lawrence Wickerham, Marco Venturini, Claudia Bighin, Simona Pastorino, Paolo Pronzato, Mario Roberto Sertoli, Theodorus Foukakis, Kathy Albain, Rodrigo Arriagada, Elizabeth Bergsten Nordström, Francesco Boccardo, Etienne Brain, Lisa Carey, Alan Coates, Robert Coleman, Candace Correa, Jack Cuzick, Nancy Davidson, Mitch Dowsett, Marianne Ewertz, John Forbes, Richard Gelber, Aron Goldhirsch, Pamela Goodwin, Daniel Hayes, Catherine Hill, James Ingle, Reshma Jagsi, Wolfgang Janni, Hirofumi Mukai, Yasuo Ohashi, Lori Pierce, Vinod Raina, Peter Ravdin, Daniel Rea, Meredith Regan, John

Robertson, Joseph Sparano, Andrew Tutt, Giuseppe Viale, Nicholas Wilcken, Norman Wolmark, Wiliam Wood, and Milvia Zambetti. Increasing the dose intensity of chemotherapy by more frequent administration or sequential scheduling: a patient-level meta-analysis of 37 298 women with early breast cancer in 26 randomised trials. 393 (10179):1440–1452, 2019. ISSN 01406736. doi: 10.1016/S0140-6736(18)33137-4. URL https://linkinghub.elsevier.com/retrieve/pii/S0140673618331374.

Donna M. Gress, Stephen B. Edge, Frederick L. Greene, Mary Kay Washington, Elliot A. Asare, James D. Brierley, David R. Byrd, Carolyn C. Compton, J. Milburn Jessup, David P. Winchester, Mahul B. Amin, and Jeffrey E. Gershenwald. Principles of Cancer Staging. In Mahul B. Amin, Stephen B. Edge, Frederick L. Greene, David R. Byrd, Robert K. Brookland, Mary Kay Washington, Jeffrey E. Gershenwald, Carolyn C. Compton, Kenneth R. Hess, Daniel C. Sullivan, J. Milburn Jessup, James D. Brierley, Lauri E. Gaspar, Richard L. Schilsky, Charles M. Balch, David P. Winchester, Elliot A. Asare, Martin Madera, Donna M. Gress, and Laura R. Meyer, editors, *AJCC Cancer Staging Manual*, pages 3–30. Springer International Publishing, Cham, 2017. ISBN 978-3-319-40617-6 978-3-319-40618-3. doi: 10.1007/978-3-319-40618-3_1. URL http://link.springer.com/10.1007/978-3-319-40618-3_1.

Xiangming Guan. Cancer metastases: challenges and opportunities. *Acta Pharmaceutica Sinica B*, 5(5):402–418, September 2015. ISSN 22113835. doi: 10.1016/j.apsb.2015.07.005. URL https://linkinghub.elsevier.com/retrieve/pii/S2211383515001094.

P. K. Gupta. Chapter 9 - Principles and basic concepts of toxicokinetics. In P. K. Gupta, editor, *Fundamentals of Toxicology*, pages 87 – 107. Academic Press, 2016. ISBN 978-0-12-805426-0. doi: 10.1016/B978-0-12-805426-0.00009-3. URL http://www.sciencedirect.com/science/article/pii/B9780128054260000093.

Douglas Hanahan and Robert A. Weinberg. The hallmarks of cancer. *Cell*, 100(1):57–70, 2000. URL http://www.sciencedirect.com/science/article/pii/S0092867400816839.

Douglas Hanahan and Robert A. Weinberg. Hallmarks of Cancer: The Next Generation. *Cell*, 144(5):646–674, March 2011. ISSN 00928674. doi: 10.1016/j.cell.2011.02.013. URL http://linkinghub.elsevier.com/retrieve/pii/S0092867411001279.

Niklas Hartung, Séverine Mollard, Dominique Barbolosi, Assia Benabdallah, Guillemette Chapuisat, Gerard Henry, Sarah Giacometti, Athanassios Iliadis, Joseph Ciccolini, Christian Faivre, and Florence Hubert. Mathematical Modeling of Tumor Growth and Metastatic Spreading: Validation in Tumor-Bearing Mice. *Cancer Research*, 74(22):

6397–6407, November 2014. ISSN 0008-5472, 1538-7445. doi: 10.1158/0008-5472.CAN-14-0721. URL https://cancerres.aacrjournals.org/content/74/22/6397. Publisher: American Association for Cancer Research Section: Integrated Systems and Technologies.

Seyed Hossein Hassanpour and Mohammadamin Dehghani. Review of cancer from perspective of molecular. *Journal of Cancer Research and Practice*, 4(4):127–129, December 2017. ISSN 2311-3006. doi: 10.1016/j.jcrpr.2017.07.001. URL http://www.sciencedirect.com/science/article/pii/S2311300617300125.

Volker Haustein and Udo Schumacher. A dynamic model for tumour growth and metastasis formation. *Journal of Clinical Bioinformatics*, 2:11, 2012. ISSN 2043-9113. doi: 10.1186/2043-9113-2-11. URL https://doi.org/10.1186/2043-9113-2-11.

Xiran He, Yang Du, Zhijie Wang, Xin Wang, Jianchun Duan, Rui Wan, Jiachen Xu, Pei Zhang, Di Wang, Yanhua Tian, Jiefei Han, Kailun Fei, Hua Bai, Jie Tian, and Jie Wang. Upfront dose-reduced chemotherapy synergizes with immunotherapy to optimize chemoimmunotherapy in squamous cell lung carcinoma. 8(2):e000807, 2020. ISSN 2051-1426. doi: 10.1136/jitc-2020-000807. URL https://jitc.bmj.com/content/8/2/e000807. Publisher: BMJ Specialist Journals Section: Clinical/translational cancer immunotherapy.

T. Helleday. Chemotherapy-induced toxicity—a secondary effect caused by released DNA? *Annals of Oncology*, 28(9):2054 – 2055, 2017. ISSN 0923-7534. doi: https://doi.org/10.1093/annonc/mdx349. URL http://www.sciencedirect.com/science/article/pii/S0923753419352688.

Gloria H. Heppner. Tumor Heterogeneity. *Cancer Research*, 44(6):2259–2265, June 1984. ISSN 0008-5472, 1538-7445. URL https://cancerres.aacrjournals.org/content/44/6/2259. Publisher: American Association for Cancer Research Section: Perspectives in Cancer Research.

Farid Heydarpoor, Seyed Mehdi Karbassi, Narges Bidabadi, and Mohammad Javad Ebadi. Solving multi-objective functions for cancer treatment by using metaheuristic algorithms. page 16, 2020.

Kenneth J. Himmelstein and Kenneth B. Bischoff. Models of ARA-c chemotherapy of l1210 leukemia in mice. *Journal of Pharmacokinetics and Pharmacodynamics*, 1(1):69–81, 1973. URL http://www.springerlink.com/index/g72llmkk86277551.pdf.

N H Holford and L B Sheiner. Pharmacokinetic and pharmacodynamic modeling in vivo. *Critical Reviews in Bioengineering*, 5 4:273–322, 1981.

Genevieve Housman, Shannon Byler, Sarah Heerboth, Karolina Lapinska, Mckenna Longacre, Nicole Snyder, and Sibaji Sarkar. Drug resistance in cancer: An overview. *Cancers*, 6(3):1769–1792, 2014. ISSN 2072-6694. doi: 10.3390/cancers6031769. URL http://www.ncbi.nlm.nih.gov/pmc/articles/PMC4190567/.

Kashif Hussain, Mohd Najib Mohd Salleh, Shi Cheng, and Yuhui Shi. Metaheuristic research: a comprehensive survey. *Artificial Intelligence Review*, 52(4):2191–2233, December 2019. ISSN 0269-2821, 1573-7462. doi: 10.1007/s10462-017-9605-z. URL http://link.springer.com/10.1007/s10462-017-9605-z.

Farhad Imani, Zihang Qiu, and Hui Yang. Markov Decision Process Modeling for Multistage Optimization of Intervention and Treatment Strategies in Breast Cancer. In *2020 42nd Annual International Conference of the IEEE Engineering in Medicine Biology Society (EMBC)*, pages 5394–5397, July 2020. doi: 10.1109/EMBC44109.2020.9175905. ISSN: 1558-4615.

Sheikh M. A. Iqbal, Imadeldin Mahgoub, E. Du, Mary Ann Leavitt, and Waseem Asghar. Advances in healthcare wearable devices. 5(1):1–14, 2021. ISSN 2397-4621. doi: 10.1038/s41528-021-00107-x. URL https://www.nature.com/articles/s41528-021-00107-x. Bandiera_abtest: a Cc_license_type: cc_by Cg_type: Nature Research Journals Number: 1 Primary_atype: Reviews Publisher: Nature Publishing Group Subject_term: Biomedical materials;Biosensors;Electrical and electronic engineering Subject_term_id: biomedical-materials;biosensors;electrical-and-electronic-engineering.

Donald E. Kirk. *Optimal control theory : An Introduction*. Dover Publications, April 2004. ISBN 0486434842. URL http://www.amazon.com/exec/obidos/redirect?tag=citeulike07-20&path=ASIN/0486434842.

S. Kirkpatrick, C. D. Gelatt, and M. P. Vecchi. Optimization by Simulated Annealing. *Science*, 220(4598):671–680, 1983. ISSN 0036-8075. doi: 10.1126/science.220.4598.671. URL https://science.sciencemag.org/content/220/4598/671. Publisher: American Association for the Advancement of Science _eprint: https://science.sciencemag.org/content/220/4598/671.full.pdf.

Frederik Knust and Lin Xie. Simulated annealing approach to nurse rostering benchmark and real-world instances. 272(1):187–216, 2019. ISSN 1572-9338. doi: 10.1007/s10479-017-2546-8. URL https://doi.org/10.1007/s10479-017-2546-8.

M. Kohandel, S. Sivaloganathan, and A. Oza. Mathematical modeling of ovarian cancer treatments: Sequencing of surgery and chemotherapy. *Journal of Theoretical Biology*, 242(1):62–68, September 2006. ISSN 00225193. doi: 10.1016/j.jtbi.2006.02.001. URL http://linkinghub.elsevier.com/retrieve/pii/S0022519306000579.

Natalia Komarova. Stochastic modeling of drug resistance in cancer. *Journal of Theoretical Biology*, 239(3):351–366, April 2006. ISSN 00225193. doi: 10.1016/j.jtbi.2005.08.003. URL http://linkinghub.elsevier.com/retrieve/pii/S0022519305003346.

Minjoung Monica Koo, Ruth Swann, Sean McPhail, Gary A Abel, Lucy Elliss-Brookes, Greg P Rubin, and Georgios Lyratzopoulos. Presenting symptoms of cancer and stage at diagnosis: evidence from a cross-sectional, population-based study. 21(1):73–79, 2020. ISSN 1470-2045. doi: 10.1016/S1470-2045(19)30595-9. URL https://www.ncbi.nlm.nih.gov/pmc/articles/PMC6941215/.

Emilia Kozłowska, Rafał Suwiński, Monika Giglok, Andrzej Świerniak, and Marek Kimmel. Mathematical model predicts response to chemotherapy in advanced non-resectable non-small cell lung cancer patients treated with platinum-based doublet. 16(10):e1008234, 2020. ISSN 1553-7358. doi: 10.1371/journal.pcbi.1008234. URL https://journals.plos.org/ploscompbiol/article?id=10.1371/journal.pcbi.1008234. Publisher: Public Library of Science.

Davide La Torre, Herb Kunze, Manuel Ruiz-Galan, Tufail Malik, and Simone Marsiglio. Optimal control: Theory and application to science, engineering, and social sciences. *Abstract and Applied Analysis*, 2015:1–2, 2015. ISSN 1085-3375, 1687-0409. doi: 10.1155/2015/890527. URL http://www.hindawi.com/journals/aaa/2015/890527/.

Sigurdur Ólafsson. Chapter 21 Metaheuristics. In *Handbooks in Operations Research and Management Science*, volume 13, pages 633–654. Elsevier, 2006. ISBN 978-0-444-51428-8. doi: 10.1016/S0927-0507(06)13021-2. URL https://linkinghub.elsevier.com/retrieve/pii/S0927050706130212.

Anna Kane Laird. Dynamics of tumour growth. 18(3):490–502, 1964. ISSN 0007-0920. URL https://www.ncbi.nlm.nih.gov/pmc/articles/PMC2071101/.

Anna Kane Laird. Dynamics of tumour growth: comparison of growth rates and extrapolation of growth curve to one cell. *British Journal of Cancer*, 19(2):278, 1965. URL https://www.ncbi.nlm.nih.gov/pmc/articles/PMC2071357/.

Robert R. Langley and Isaiah J. Fidler. Tumor Cell-Organ Microenvironment Interactions in the Pathogenesis of Cancer Metastasis. *Endocrine Reviews*, 28(3):297–321, May 2007.

ISSN 0163-769X. doi: 10.1210/er.2006-0027. URL https://academic.oup.com/edrv/article/28/3/297/2354976. Publisher: Oxford Academic.

A. Lazar. Heuristic Knowledge Discovery for Archaeological Data Using Genetic Algorithms and Rough Sets. 2002.

R. Li, K.L. Teo, K.H. Wong, and G.R. Duan. Control parameterization enhancing transform for optimal control of switched systems. *Mathematical and Computer Modelling*, 43(11-12):1393–1403, June 2006. ISSN 08957177. doi: 10.1016/j.mcm.2005.08.012. URL http://linkinghub.elsevier.com/retrieve/pii/S0895717705004966.

Qun Lin, Ryan Loxton, and Kok Lay Teo. The control parameterization method for nonlinear optimal control: A survey. *Journal of Industrial and Management Optimization*, 10(1):275–309, October 2013. ISSN 1547-5816. doi: 10.3934/jimo.2014.10.275. URL http://www.aimsciences.org/journals/displayArticlesnew.jsp?paperID=9084.

L. A. Liotta. Tumor invasion and metastases: role of the basement membrane. Warner-Lambert Parke-Davis Award lecture. *The American Journal of Pathology*, 117(3):339–348, December 1984. ISSN 0002-9440. URL https://www.ncbi.nlm.nih.gov/pmc/articles/PMC1900581/.

HANNELORE Lisei and DAVID Julitz. A stochastic model for the growth of Cancer tumors. *Studia Univ."Babes-Bolay", Math*, 53:39–56, 2008. URL https://www.researchgate.net/profile/Hannelore_Lisei/publication/242101511_A_stochastic_model_for_the_growth_of_Cancer_tumors/links/00b49528f53206ad4b000000.pdf.

Elisabeth Åvall Lundqvist, Keiichi Fujiwara, and Muhieddine Seoud. Principles of chemotherapy. *International Journal of Gynecology & Obstetrics*, 131:S146–S149, October 2015. ISSN 00207292. doi: 10.1016/j.ijgo.2015.06.011. URL http://doi.wiley.com/10.1016/j.ijgo.2015.06.011.

Kelsey Maass and Minsun Kim. A Markov decision process approach to optimizing cancer therapy using multiple modalities. *Mathematical Medicine and Biology: A Journal of the IMA*, 37(1):22–39, February 2020. ISSN 1477-8599, 1477-8602. doi: 10.1093/imammb/dqz004. URL http://arxiv.org/abs/1706.09481. arXiv: 1706.09481.

Hiroshi Maeda and Mahin Khatami. Analyses of repeated failures in cancer therapy for solid tumors: poor tumor-selective drug delivery, low therapeutic efficacy and unsustainable costs. *Clinical and Translational Medicine*, 7, March 2018. ISSN 2001-

1326. doi: 10.1186/s40169-018-0185-6. URL https://www.ncbi.nlm.nih.gov/pmc/articles/PMC5852245/.

Behzad Mansoori, Ali Mohammadi, Sadaf Davudian, Solmaz Shirjang, and Behzad Baradaran. The Different Mechanisms of Cancer Drug Resistance: A Brief Review. *Advanced Pharmaceutical Bulletin*, 7(3):339–348, September 2017. ISSN 2228-5881. doi: 10.15171/apb.2017.041. URL https://www.ncbi.nlm.nih.gov/pmc/articles/PMC5651054/.

R Martin and K L Teo. *Optimal Control of Drug Administration in Cancer Chemotherapy*. WORLD SCIENTIFIC, 1993. ISBN 978-981-02-1428-9 978-981-283-254-2. doi: 10.1142/2048. URL http://www.worldscientific.com/worldscibooks/10.1142/2048.

R. B. Martin, M. E. Fisher, R. F. Minchin, and K. L. Teo. Low-intensity combination chemotherapy maximizes host survival time for tumors containing drug-resistant cells. *Mathematical Biosciences*, 110(2):221–252, 1992a. ISSN 00255564. doi: 10.1016/0025-5564(92)90039-Y.

R. B. Martin, M. E. Fisher, R. F. Minchin, and K. L. Teo. Optimal control of tumor size used to maximize survival time when cells are resistant to chemotherapy. *Mathematical Biosciences*, 110(2):201–219, 1992b. ISSN 00255564. doi: 10.1016/0025-5564(92)90038-X.

R.B. Martin. Optimal Control Drug Scheduling of Cancer Chemotherapy *. *Automatica*, 28(6):1113–1123, 1992.

R.B. Martin, M.E. Fisher, R.F. Minchin, and K.L. Teo. A mathematical model of cancer chemotherapy with an optimal selection of parameters. *Mathematical Biosciences*, 99(2):205–230, 1990. ISSN 00255564. doi: 10.1016/0025-5564(90)90005-J. URL http://www.sciencedirect.com/science/article/pii/002555649090005J.

S. McPhail, S. Johnson, D. Greenberg, M. Peake, and B. Rous. Stage at diagnosis and early mortality from cancer in England. *British Journal of Cancer*, 112(1):S108–S115, March 2015. ISSN 1532-1827. doi: 10.1038/bjc.2015.49. URL https://www.nature.com/articles/bjc201549. Number: 1 Publisher: Nature Publishing Group.

Nicholas Metropolis, Arianna W. Rosenbluth, Marshall N. Rosenbluth, Augusta H. Teller, and Edward Teller. Equation of State Calculations by Fast Computing Machines. *The Journal of Chemical Physics*, 21(6):1087–1092, June 1953. ISSN 0021-9606, 1089-7690. doi: 10.1063/1.1699114. URL http://aip.scitation.org/doi/10.1063/1.1699114.

Leonor Michaelis and Maud Leonora Menten. *Die kinetik der invertinwirkung*. Universitätsbibliothek Johann Christian Senckenberg, 2007. URL http://path.upmc.edu/divisions/chp/PDF/Michaelis-Menten_Kinetik.pdf.

Alfonsas Misevičius. A modified simulated annealing algorithm for the quadratic assignment problem. 14(4):497–514, 2003. ISSN 0868-4952, 1822-8844. doi: 10.15388/Informatica.2003.037. URL https://informatica.vu.lt/doi/10.15388/Informatica.2003.037.

H. Moore. How to mathematically optimize drug regimens using optimal control. *Journal of Pharmacokinetics and Pharmacodynamics*, 45(1):127–137, 2018. doi: 10.1007/s10928-018-9568-y.

Hamed Moradi, Gholamreza Vossoughi, and Hassan Salarieh. Optimal robust control of drug delivery in cancer chemotherapy: A comparison between three control approaches. *Computer Methods and Programs in Biomedicine*, 112(1):69–83, 2013. ISSN 01692607. doi: 10.1016/j.cmpb.2013.06.020. URL http://linkinghub.elsevier.com/retrieve/pii/S0169260713002198.

Graeme Morgan, Robyn Ward, and Michael Barton. The contribution of cytotoxic chemotherapy to 5-year survival in adult malignancies. *Clinical Oncology*, 16(8):549–560, 2004. ISSN 09366555. doi: 10.1016/j.clon.2004.06.007. URL http://linkinghub.elsevier.com/retrieve/pii/S0936655504002225.

Hope Murphy, Hana Jaafari, and Hana M. Dobrovolny. Differences in predictions of ODE models of tumor growth: a cautionary example. *BMC Cancer*, 16(1), December 2016. ISSN 1471-2407. doi: 10.1186/s12885-016-2164-x. URL http://www.biomedcentral.com/1471-2407/16/163.

J. M. Murray. Optimal control for a cancer chemotherapy problem with general growth and loss functions. *Mathematical Biosciences*, 98(2):273–287, March 1990. ISSN 0025-5564. doi: 10.1016/0025-5564(90)90129-m.

J. M. Murray. The optimal scheduling of two drugs with simple resistance for a problem in cancer chemotherapy. *Mathematical Medicine and Biology: A Journal of the IMA*, 14 (4):283–303, 1997. URL https://academic.oup.com/imammb/article-abstract/14/4/283/655359.

Richard E. Neapolitan and Kumarss Naimipour. *Foundations of Algorithms Using C++ Pseudocode (2nd Ed.)*. Jones and Bartlett Publishers, Inc., USA, 1997. ISBN 0763706205.

Paul K. Newton, Jeremy Mason, Kelly Bethel, Lyudmila A. Bazhenova, Jorge Nieva, and Peter Kuhn. A Stochastic Markov Chain Model to Describe Lung Cancer Growth and Metastasis. *PLOS ONE*, 7(4):e34637, April 2012. ISSN 1932-6203. doi: 10.1371/journal.pone.0034637. URL http://journals.plos.org/plosone/article?id=10.1371/journal.pone.0034637.

L. Norton, R. Simon, H. D. Brereton, and A. E. Bogden. Predicting the course of gompertzian growth. *Nature*, 264(5586):542–545, 1976. ISSN 0028-0836.

M E R O'Brien, A Borthwick, A Rigg, A Leary, L Assersohn, K Last, S Tan, S Milan, D Tait, and I E Smith. Mortality within 30 days of chemotherapy: a clinical governance benchmarking issue for oncology patients. *British Journal of Cancer*, 95(12):1632–1636, December 2006. ISSN 0007-0920. doi: 10.1038/sj.bjc.6603498. URL https://www.ncbi.nlm.nih.gov/pmc/articles/PMC2360753/.

Akira Ohnishi, Yusuke Namekawa, and Tokuro Fukui. Universality in COVID-19 spread in view of the gompertz function. 2020(12), 2020. ISSN 2050-3911. doi: 10.1093/ptep/ptaa148. URL https://doi.org/10.1093/ptep/ptaa148.

W. J. Padgett and C. P. Tsokos. A stochastic model for chemotherapy: computer simulation. *Mathematical Biosciences*, 9:119–133, January 1970. ISSN 0025-5564. doi: 10.1016/0025-5564(70)90097-0. URL http://www.sciencedirect.com/science/article/pii/0025556470900970.

Tirupathi Rao Padi, K. Rao, and Padmalatha K. STOCHASTIC MODELS FOR OPTIMAL DRUG ADMINISTRATION IN CANCER CHEMOTHERAPY. *International Journal of Engineering Science and Technology*, 2:859–865, 2010.

Regina Padmanabhan, Nader Meskin, and Ala-Eddin Al Moustafa. Control Strategies for Cancer Therapy. In Regina Padmanabhan, Nader Meskin, and Ala-Eddin Al Moustafa, editors, *Mathematical Models of Cancer and Different Therapies: Unified Framework*, Series in BioEngineering, pages 215–247. Springer, Singapore, 2021. ISBN 9789811586408. doi: 10.1007/978-981-15-8640-8_10. URL https://doi.org/10.1007/978-981-15-8640-8_10.

Ray Page and Chris Takimoto. Principles of chemotherapy. *Cancer Management: A Multidisciplinary Approach Medical, Surgical & Radiation Oncology. Editors: R Pazdur, LR Coia, WJ Hoskins, LD Wagman. PRR, New York*, pages 21–38, 2004. URL http://www.thymic.org/uploads/reference_sub/03chemoprinc.pdf.

Michael O. Palumbo, Petr Kavan, Wilson H. Miller, Lawrence Panasci, Sarit Assouline, Nathalie Johnson, Victor Cohen, Francois Patenaude, Michael Pollak, R. Thomas Jagoe, and Gerald Batist. Systemic cancer therapy: achievements and challenges that lie ahead. *Frontiers in Pharmacology*, 4, May 2013. ISSN 1663-9812. doi: 10.3389/fphar.2013.00057. URL https://www.ncbi.nlm.nih.gov/pmc/articles/PMC3646247/.

John Carl Panetta. A mathematical model of drug resistance: heterogeneous tumors. 147(1):41–61, 1998. URL http://www.sciencedirect.com/science/article/pii/S0025556497000801.

John Carl Panetta and K. Renee Fister. Optimal Control Applied to Cell-Cycle-Specific Cancer Chemotherapy. *SIAM Journal on Applied Mathematics*, 60(3):1059–1072, January 2000. ISSN 0036-1399, 1095-712X. doi: 10.1137/S0036139998338509. URL http://epubs.siam.org/doi/10.1137/S0036139998338509.

John Carl Panetta and K. Renee Fister. Optimal control applied to competing chemotherapeutic cell-kill strategies. *SIAM Journal on Applied Mathematics*, 63(6):1954–1971, 2003. ISSN 0036-1399, 1095-712X. doi: 10.1137/S0036139902413489. URL http://epubs.siam.org/doi/10.1137/S0036139902413489.

Nuventra Pharma Parkway. Steady-State Concentration Importance in Drug Development, January 2020. URL https://www.nuventra.com/resources/blog/what-is-steady-state-concentration/. Section: Pharmacokinetics & Pharmacodynamics.

Aisha Patel and Howard (Jack) West. What does my stage of cancer mean? 6(8):1308–1308, 2020. ISSN 2374-2437. doi: 10.1001/jamaoncol.2020.1592. URL https://doi.org/10.1001/jamaoncol.2020.1592.

F. L. Pereira, C. E. Pedreira, and J. B. de Sousa. A new optimization based approach to experimental combination chemotherapy. 6(4):257–268, 1995. ISSN 0921-3775.

S.T.R. Pinho, H.I. Freedman, and F. Nani. A chemotherapy model for the treatment of cancer with metastasis. *Mathematical and Computer Modelling*, 36(7-8):773–803, November 2002. ISSN 08957177. doi: 10.1016/S0895-7177(02)00227-3. URL https://linkinghub.elsevier.com/retrieve/pii/S0895717702002273.

Ian H. Plenderleith. Treating the treatment: Toxicity of cancer chemotherapy. *Canadian Family Physician*, 36:1827–1830, 1990. ISSN 0008-350X. URL http://www.ncbi.nlm.nih.gov/pmc/articles/PMC2280515/.

Warren B. Powell. *Approximate Dynamic Programming: Solving the Curses of Dimensionality (Wiley Series in Probability and Statistics)*. Wiley-Interscience, USA, 2007. ISBN 0470171553.

Martin L Puterman. Markov decision processes. *Handbooks in operations research and management science*, 2:331–434, 1990.

P. Rao, J. Jayabharathiraj, and R. Vardhan. Stochastic Optimization Models for Cancer Chemotherapy. *British Journal of Applied Science & Technology*, 4(28):4097–4108, January 2014. ISSN 22310843. doi: 10.9734/BJAST/2014/6445. URL http://www.sciencedomain.org/abstract.php?iid=617&id=5&aid=5566.

Tirupati Rao and K.Srinivasa Rao. TWO STAGE STOCHASTIC MODEL FOR CANCER CELLGROWTH. *Indian Journal of MAthematics and Mathematical Sciences*, 2:17, 2006.

Ambili Remesh. Tackling the Problems of Tumour Chemotherapy by Optimal Drug Scheduling. *JOURNAL OF CLINICAL AND DIAGNOSTIC RESEARCH*, 2013. ISSN 2249782X. doi: 10.7860/JCDR/2013/6223.3144. URL http://www.jcdr.net/article_fulltext.asp?issn=0973-709x&year=2013&month=July&volume=7&issue=7&page=1404-1407&id=3144.

B Ribba, N H Holford, P Magni, I Trocóniz, I Gueorguieva, P Girard, C Sarr, M Elishmereni, C Kloft, and L E Friberg. A Review of Mixed-Effects Models of Tumor Growth and Effects of Anticancer Drug Treatment Used in Population Analysis. *CPT Pharmacometrics Syst. Pharmacol.*, 3(5):e113, May 2014. ISSN 2163-8306. doi: 10.1038/psp.2014.12. URL http://doi.wiley.com/10.1038/psp.2014.12.

Fabiano L. Ribeiro. An attempt to unify some population growth models from first principles. *Revista Brasileira de Ensino de Física*, 39(1), 2017. ISSN 1806-1117. doi: 10.1590/1806-9126-rbef-2016-0118. URL http://www.scielo.br/scielo.php?script=sci_arttext&pid=S1806-11172017000100411&lng=en&tlng=en.

Clara Rojas and Juan Belmonte-Beitia. Optimal control problems for differential equations applied to tumor growth: state of the art. *Applied Mathematics and Nonlinear Sciences*, 3(2):375–402, July 2018. ISSN 2444-8656. doi: 10.21042/AMNS.2018.2.00029. URL https://content.sciendo.com/view/journals/amns/3/2/article-p375.xml.

Gerd Rosenkranz. Growth models with stochastic differential equations. an example from tumor immunology. *Mathematical biosciences*, 75(2):175–186, 1985. URL http://www.sciencedirect.com/science/article/pii/0025556485900367.

Ladislav Rosocha, Silvia Vernerova, and Robert Verner. MEDICAL STAFF SCHEDULING USING SIMULATED ANNEALING. 19(1):1–8, 2015. ISSN 1338-984X, 1335-1745. doi: 10.12776/qip.v19i1.405. URL http://www.qip-journal.eu/index.php/QIP/article/view/405.

Stuart J. Russell and Peter Norvig. *Artificial intelligence: a modern approach*. Prentice Hall series in artificial intelligence. Prentice Hall, Englewood Cliffs, N.J, 1995. ISBN 978-0-13-103805-9.

Metin Uymaz Salamci and Stephen Paul Banks. SDRE optimal control of drug administration in cancer. 18(5):715–729, 2010. doi: 10.3906/elk-1001-411.

Hoda Sbeity. Review of Optimization Methods for Cancer Chemotherapy Treatment Planning. *Journal of Computer Science & Systems Biology*, 8(1):74–95, 2015. ISSN 09747230. doi: 10.4172/jcsb.1000173. URL http://www.omicsonline.org/open-access/review-of-optimization-methods-for-cancer-chemotherapy-treatment-planning-jcsb.1000173.php?aid=36787.

Andrew J. Schaefer, Matthew D. Bailey, Steven M. Shechter, and Mark S. Roberts. Modeling medical treatment using markov decision processes. In *Operations research and health care*, pages 593–612. Springer, 2005. URL http://link.springer.com/chapter/10.1007/1-4020-8066-2_23.

Heinz Schaettler and Urszula Ledzewicz. *Optimal Control Problems for Mathematical Models of Cancer Treatments*. Springer, 2014. ISBN 978-1-4939-2971-9.

Alan Scheller-Wolf. Markov decision processes. In *Handbook of Healthcare Analytics*, pages 319–336. John Wiley & Sons, Ltd, 2018. ISBN 978-1-119-30097-7. doi: 10.1002/9781119300977.ch14. URL https://onlinelibrary.wiley.com/doi/abs/10.1002/9781119300977.ch14. Section: 14 _eprint: https://onlinelibrary.wiley.com/doi/pdf/10.1002/9781119300977.ch14.

Heinz Schättler and Urszula Ledzewicz. *Optimal Control for Mathematical Models of Cancer Therapies*, volume 42 of *Interdisciplinary Applied Mathematics*. Springer New York, New York, NY, 2015. ISBN 978-1-4939-2971-9 978-1-4939-2972-6. doi: 10.1007/978-1-4939-2972-6. URL http://link.springer.com/10.1007/978-1-4939-2972-6.

Jinghua Shi, Oguzhan Alagoz, Fatih Safa Erenay, and Qiang Su. A survey of optimization models on cancer chemotherapy treatment planning. *Annals of Operations Research*, 221 (1):331–356, October 2014. ISSN 0254-5330, 1572-9338. doi: 10.1007/s10479-011-0869-4. URL http://link.springer.com/10.1007/s10479-011-0869-4.

Tatjana Sibalija. *Application of simulated annealing in process optimization: A review*, pages 1–48. 01 2018. ISBN 978-1-53613-674-6.

Rebecca L. Siegel, Kimberly D. Miller, Hannah E. Fuchs, and Ahmedin Jemal. Cancer statistics, 2021. 71(1):7–33, 2021. ISSN 1542-4863. doi: 10.3322/caac.21654. URL https://acsjournals.onlinelibrary.wiley.com/doi/abs/10.3322/caac.21654. _eprint: https://acsjournals.onlinelibrary.wiley.com/doi/pdf/10.3322/caac.21654.

Eman Simbawa. Mechanistic model for cancer growth and response to chemotherapy, 2017. URL https://www.hindawi.com/journals/cmmm/2017/3676295/.

Richard Simon and Larry Norton. The norton–simon hypothesis: designing more effective and less toxic chemotherapeutic regimens. *Nature Clinical Practice Oncology*, 3(8):406–407, 2006. ISSN 1743-4254, 1743-4262. doi: 10.1038/ncponc0560. URL http://www.nature.com/doifinder/10.1038/ncponc0560.

Cem Simsek, Ece Esin, and Suayib Yalcin. Metronomic chemotherapy: A systematic review of the literature and clinical experience, 2019. URL https://www.hindawi.com/journals/jo/2019/5483791/. ISSN: 1687-8450 Pages: e5483791 Publisher: Hindawi Volume: 2019.

H. E. Skipper, F. M. Schabel, and W. S. Wilcox. Experimental Evaluation of Potential Anticancer Agents. XIII. on the Criteria and Kinetics Associated with "Curability" of Experimental Leukemia. *Cancer Chemotherapy Reports*, 35:1–111, 1964. ISSN 0069-0112.

James C. Spall. *Introduction to Stochastic Search and Optimization*. John Wiley & Sons, Inc., USA, 1 edition, 2003. ISBN 0471330523.

J. Sápi, D. A. Drexler, and L. Kovács. Comparison of mathematical tumor growth models. In *2015 IEEE 13th International Symposium on Intelligent Systems and Informatics (SISY)*, pages 323–328, September 2015. doi: 10.1109/SISY.2015.7325403.

Lauren N. Steimle and Brian T. Denton. Markov decision processes for screening and treatment of chronic diseases. In Richard J. Boucherie and Nico M. van Dijk, editors, *Markov Decision Processes in Practice*, volume 248, pages 189–222. Springer International Publishing, 2017. ISBN 978-3-319-47764-0 978-3-319-47766-4. doi: 10.1007/978-3-319-47766-4_6. URL http://link.springer.com/10.1007/978-3-319-47766-4_6. Series Title: International Series in Operations Research & Management Science.

Peter W. Sullivan and Sydney E. Salmon. Kinetics of tumor growth and regression in IgG multiple myeloma. *Journal of Clinical Investigation*, 51(7):1697–1708, July 1972. ISSN 0021-9738. doi: 10.1172/JCI106971. URL http://www.jci.org/articles/view/106971.

G. W. Swan. General applications of optimal control theory in cancer chemotherapy. *Mathematical Medicine and Biology*, 5(4):303–316, 1988. URL http://imammb.oxfordjournals.org/content/5/4/303.short.

G W Swan. Role of optimal control theory in cancer chemotherapy. *Math Biosci*, 101(2): 237–284, 1990. doi: 0025-5564(90)90021-P[pii]. URL http://www.ncbi.nlm.nih.gov/pubmed/2134485.

George W Swan and Thomas L Vincent. Optimal Control Analysis In The Chemotherapy of IgG Multiple Myeloma. *Bulletin of Mathematical Biology,*, 39(3):317–337, 1977.

Andrzej Swierniak, Urszula Ledzewicz, and H Schättler. Optimal control for a class of compartmental models in cancer chemotherapy. 13:357–368, 2003.

Andrzej Swierniak, Jaroslaw Smieja, Andrzej Swierniak, and Jaroslaw Smieja. Analysis and optimization of drug resistant an phase-specific cancer. 2(3):657–670, 2005. ISSN 1551-0018. doi: 10.3934/mbe.2005.2.657. URL http://www.aimspress.com/rticle/doi/10.3934/mbe.2005.2.657.

Tiffany A. Traina and Larry Norton. Log-kill hypothesis. In Manfred Schwab, editor, *Encyclopedia of Cancer*, pages 2074–2075. Springer Berlin Heidelberg, 2011. ISBN 978-3-642-16482-8 978-3-642-16483-5. URL http://link.springer.com/referenceworkentry/10.1007/978-3-642-16483-5_3409.

Tiffany A. Traina and Larry Norton. Norton-simon hypothesis. In Manfred Schwab, editor, *Encyclopedia of Cancer*, pages 3142–3144. Springer Berlin Heidelberg, 2017. ISBN 978-3-662-46874-6 978-3-662-46875-3. URL http://link.springer.com/referenceworkentry/10.1007/978-3-662-46875-3_4130.

Sui Man Tse, Yong Liang, Kwong Sak Leung, Kin Hong Lee, and Tony Shu Kam Mok. A memetic algorithm for multiple-drug cancer chemotherapy schedule optimization. *IEEE Transactions on Systems, Man, and Cybernetics, Part B: Cybernetics*, 37(1):84–91, 2007. ISSN 10834419. doi: 10.1109/TSMCB.2006.883265.

Henry C. Tuckwell. Gompertzian population growth under some deterministic and stochastic jump schedules. *arXiv preprint arXiv:1604.08696*, 2016. URL https://arxiv.org/abs/1604.08696.

University of Washington. Dose-finding (phase 1) study of continuous infusion cladribine, cytarabine and mitoxantrone (CI-CLAM) for adults with relapsed/refractory acute myeloid leukemia or other high-grade myeloid neoplasms treated at UW/SCCA, 2021. URL https://clinicaltrials.gov/ct2/show/NCT04196010. submitted: December 10, 2019.

J. R. Usher. Some mathematical models for cancer chemotherapy. *Computers & Mathematics with Applications*, 28(9):73–80, 1994. URL http://www.sciencedirect.com/science/article/pii/0898122194001790.

Vinay G. Vaidya and Frank J. Alexandro. Evaluation of some mathematical models for tumor growth. *International Journal of Bio-Medical Computing*, 13(1):19–35, January 1982. ISSN 00207101. doi: 10.1016/0020-7101(82)90048-4. URL https://linkinghub.elsevier.com/retrieve/pii/0020710182900484.

M. Villasana and G. Ochoa. Heuristic design of cancer chemotherapies. *IEEE Transactions on Evolutionary Computation*, 8(6):513–521, December 2004. ISSN 1089-778X. doi: 10.1109/TEVC.2004.834154.

Raoul R. Wadhwa and Marco Cascella. Steady State Concentration. In *StatPearls*. StatPearls Publishing, Treasure Island (FL), 2020. URL http://www.ncbi.nlm.nih.gov/books/NBK553132/.

Peilian Wang, Ran Liu, and Zhibin Jiang. Optimization of combination chemotherapy with dose adjustment using a memetic algorithm. *Information Sciences*, 432:63–78, March 2018. ISSN 00200255. doi: 10.1016/j.ins.2017.12.002. URL https://linkinghub.elsevier.com/retrieve/pii/S0020025516319818.

Peilian Wang, Ran Liu, Zhibin Jiang, Yang Yao, and Zan Shen. The Optimization of Combination Chemotherapy Schedules in the Presence of Drug Resistance. *IEEE Transactions on Automation Science and Engineering*, 16(1):165–179, January 2019. ISSN 1558-3783. doi: 10.1109/TASE.2018.2873668. Conference Name: IEEE Transactions on Automation Science and Engineering.

Andrea Weiss and Patrycja Nowak-Sliwinska. Current trends in multidrug optimization: An alley of future successful treatment of complex disorders. 22(3):254–275, 2017.

ISSN 2472-6303. doi: 10.1177/2472630316682338. URL https://doi.org/10.1177/2472630316682338. Publisher: SAGE Publications Inc.

Dennis Weyland. Simulated annealing, its parameter settings and the longest common subsequence problem. In *Proceedings of the 10th annual conference on Genetic and evolutionary computation - GECCO '08*, page 803. ACM Press, 2008. ISBN 978-1-60558-130-9. doi: 10.1145/1389095.1389253. URL http://portal.acm.org/citation.cfm?doid=1389095.1389253.

Charles P. Winsor. The Gompertz Curve as a Growth Curve. *Proceedings of the National Academy of Sciences of the United States of America*, 18(1):1–8, January 1932. ISSN 0027-8424. URL https://www.ncbi.nlm.nih.gov/pmc/articles/PMC1076153/.

Weng Kee Wong, Viatcheslav B. Melas, and Holger Dette. Optimal design for goodness-of-fit of the michaelis-menten enzyme kinetic function. Technical report, Technical Report/Universität Dortmund, SFB 475 Komplexitätsreduktion in Multivariaten Datenstrukturen, 2004. URL https://www.econstor.eu/handle/10419/22536.

Xin-She Yang. Metaheuristic optimization. 6(8):11472, 2011. ISSN 1941-6016. doi: 10.4249/scholarpedia.11472. URL http://www.scholarpedia.org/article/Metaheuristic_Optimization.

J. Zhu, H. Badri, and K. Leder. A Robust Optimization Approach to Cancer Treatment Under Toxicity Uncertainty. *Methods in Molecular Biology*, 1711:297–331, 2018. doi: 10.1007/978-1-4939-7493-1_15.

APPENDICES

Appendix A

Transformation from $N(t)$ to $y(t)$

Proposed tumor kinetic model is presented in the following:

$$\frac{dN(t)}{dt} = -\lambda N(t) ln\left[\frac{N(t)}{\theta}\right] - \frac{k_1 u}{\lambda k_2 + u} N(t), N(0) = N_0 \tag{A.1}$$

We define the nondimensional cancer population as

$$y(t) = \ln\left[\frac{N(t)}{\theta}\right] \tag{A.2}$$

We can obtain $N(t)$ in terms of $y(t)$ as follows:

$$N(t) = \theta e^{y(t)}, \tag{A.3}$$

Then, by taking the differentiation of both sides with respect to t, we can get

$$\dot{N}(t) = \theta e^{y(t)} \dot{y}(t), \tag{A.4}$$

Substituting Eq. (A.3) and Eq. (A.4) into Eq. (A.1), we obtain the following linear differential equation:

$$\dot{y}(t) = -\lambda y(t) - \left(\frac{k_1 u}{\gamma k_2 + u}\right), \tag{A.5}$$

The differential equation in Eq. (A.5) can be solved using integrating factor.

For simplicity, the second term in the right hand side of Eq. (A.5) can be renamed as Q. That makes $Q = \left(\frac{k_1 u}{\gamma k_2 + u}\right)$. Then, the last differential equation can be simply written as:

$$\dot{y}(t) = -\lambda y(t) - Q, \tag{A.6}$$

By taking $\lambda y(t)$ on the left hand side of the Eq. (A.6), we get

$$\dot{y}(t) + \lambda y(t) = -Q, \tag{A.7}$$

This simple ODE can be solved by integrating factor which is found by solving this $e^{\int \lambda dt}$ integration. Its solution is $e^{\lambda t}$. Now, we multiply the each term in Eq. (A.7) by this integrating factor.

$$\begin{aligned}
e^{\lambda t}\frac{dy(t)}{dt} + e^{\lambda t}\lambda y(t) &= -e^{\lambda t}Q \\
\frac{d}{dt}\left[e^{\lambda t}y(t)\right] &= -e^{\lambda t}Q \\
e^{\lambda t}y(t) &= -\int e^{\lambda t}Q dt \\
e^{\lambda t}y(t) &= -\frac{1}{\lambda}e^{\lambda t}Q + c \\
y(t) &= -\frac{1}{\lambda}Q + ce^{-\lambda t} \qquad (A.8) \\
c &= y(t_0) + \frac{1}{\lambda}Q, \quad \text{when t= 0}
\end{aligned}$$

Then write back c into Eq. (A.8)

$$y(t) = -\frac{1}{\lambda}Q + \left(y(t_0) + \frac{1}{\lambda}Q\right)e^{-\lambda t} \tag{A.9}$$

As a result, the solution of Eq. (A.5) is when we write back the value of Q in Eq. (A.9)

$$y(t) = -\frac{1}{\lambda}\left(\frac{k_1 u}{\gamma k_2 + u}\right) + \left[y(t_0) + \frac{1}{\lambda}\left(\frac{k_1 u}{\gamma k_2 + u}\right)\right]e^{-\lambda t}, \tag{A.10}$$

In general, by integrating Eq. (A.5) from t_{i-1} to t_i for $i = 1, 2, \cdots, T$, where T is final treatment time, we can obtain the general solution of this linear differential equation as:

$$y(t_i) = -\frac{1}{\lambda}\left(\frac{k_1 u}{\gamma k_2 + u}\right) + \left[y(t_{i-1}) + \frac{1}{\lambda}\left(\frac{k_1 u}{\gamma k_2 + u}\right)\right] e^{-\lambda \Delta t}, \tag{A.11}$$

Appendix B

Solution of $v(t)$

$$\frac{dv(t)}{dt} = u(t) - \gamma v(t)$$

$$\text{when u(t) = u,} \quad \frac{dv(t)}{dt} = u - \gamma v(t)$$

$$\frac{dv(t)}{dt} + \gamma v(t) = u$$

$$e^{\gamma t}\frac{dv(t)}{dt} + e^{\gamma t}\gamma v(t) = ue^{\gamma t}$$

$$\frac{d}{dt}\left[e^{\gamma t}v(t)\right] = ue^{\gamma t}$$

$$e^{\gamma t}v(t) = \int ue^{\gamma t}dt$$

$$e^{\gamma t}v(t) = \frac{1}{\gamma}ue^{\gamma t} + c$$

$$v(t) = \frac{1}{\gamma}u + ce^{-\gamma t} \quad \text{when t = 0} \tag{B.1}$$

$$c = -\frac{u}{\gamma} \quad \text{at v(0)= 0, Then substitute c in Eq. (B.1),}$$

$$v(t) = \frac{1}{\gamma}u - \frac{u}{\gamma}e^{-\gamma t}$$

$$v(t) = \left(1 - e^{-\gamma t}\right)\frac{u}{\gamma} \tag{B.2}$$

Appendix C

Tumor Reduction Constraint Calculation

$$
\begin{aligned}
N_{t+1} &\leq \eta N_t \\
\theta e^{y_{t+1}} &\leq \eta \theta e^{y_t} \\
e^a \leq e^b, \text{ when } a \leq b & \\
y_{t+1} &\leq \ln(\eta) + y_t \\
y_{t+1} - y_t &\leq \ln(\eta)
\end{aligned}
$$

Appendix D

The Expected Number of Tumor Size Calculation at the End of Each Treatment Period

The expected tumor sizes for the probability of stage jump at each time point are given in the following equations:

$$
\begin{aligned}
E(N_1) &= N_1^7 \\
E(N_2) &= (1-p_1)N_2^7 + p_1 N_2^1 \\
E(N_3) &= (1-p_1)(1-p_2)N_3^7 + (1-p_1)p_2 N_3^2 + p_1 N_3^1 \\
E(N_4) &= (1-p_1)(1-p_2)(1-p_3)N_4^7 + (1-p_1)(1-p_2)p_3 N_4^3 + (1-p_1)(p_2)N_4^2 + p_1 N_4^1 \\
E(N_5) &= (1-p_1)(1-p_2)(1-p_3)(1-p_4)N_5^7 + (1-p_1)(1-p_2)(1-p_3)p_4 N_5^4 \\
&\quad + (1-p_1)(1-p_2)p_3 N_5^3 + (1-p_1)p_2 N_5^2 + p_1 N_5^1 \\
E(N_6) &= (1-p_1)(1-p_2)(1-p_3)(1-p_4)(1-p_5)N_6^7 + (1-p_1)(1-p_2)(1-p_3)(1-p_4)p_5 N_6^5 \\
&\quad + (1-p_1)(1-p_2)(1-p_3)p_4 N_6^4 + (1-p_1)(1-p_2)p_3 N_6^3 + (1-p_1)p_2 N_6^2 + p_1 N_6^1 \\
E(N_7) &= (1-p_1)(1-p_2)(1-p_3)(1-p_4)(1-p_5)(1-p_6)N_7^7 \\
&\quad + (1-p_1)(1-p_2)(1-p_3)(1-p_4)(1-p_5)p_6 N_7^6 \\
&\quad + (1-p_1)(1-p_2)(1-p_3)(1-p_4)p_5 N_7^5 + (1-p_1)(1-p_2)(1-p_3)p_4 N_7^4 \\
&\quad + (1-p_1)(1-p_2)p_3 N_7^3 + (1-p_1)p_2 N_7^2 + p_1 N_7^1
\end{aligned}
$$